Higher-Order Kinematic Error Sensitivity Analysis and Optimum Dimensional Tolerancing of Dyad and Non-Dyad Mechanisms

BY

JOHN RONG MING HO

A THESIS

SUBMITTED TO THE FACULTY OF GRADUATE STUDIES OF THE UNIVERSITY OF MANITOBA

IN PARTIAL FULFILLMENT OF THE REQUIREMENTS FOR THE DEGREE OF

MASTER OF SCIENCE

DEPARTMENT OF MECHANICAL AND INDUSTRIAL ENGINEERING

UNIVERSITY OF MANITOBA

WINNIPEG, MANITOBA, CANADA

THE UNIVERSITY OF MANITOBA

FACULTY OF GRADUATE STUDIES

*****

COPYRIGHT PERMISSION PAGE

HIGHER-ORDER KINEMATIC ERROR SENSITIVITY ANALYSIS AND OPTIMUM DIMENSIONAL TOLERANCING OF DYAD AND NON-DYAD MECHANISMS

BY

JOHN RONG MING HO

A Thesis/Practicum submitted to the Faculty of Graduate Studies of The University of Manitoba in partial fulfillment of the requirements of the degree of

MASTER OF SCIENCE

ABSTRACT

A higher-order kinematic error sensitivity analysis and the synthesis of dimensional tolerance bands for complex planar mechanisms are investigated in this thesis. The initial phase of the research which is reported in *Chapter* 2, involves developing a novel approach for a computer-aided kinematic analysis of dyad and non-dyad mechanisms. The approach includes transforming the original non-dyad mechanism into a series of dyad mechanisms whose solutions are readily computable. This is achieved by disconnecting appropriate link and/or joints, and prescribing dyad drivers for the transformed linkage. An iterative technique is then employed to recover the disconnected links by restoring the affected geometric conditions to their original values. All these steps do not require human intervention as they are generated automatically by the program, aptly entitled as **NDPLAn** (Non-Dyad Planar Linkage Analysis). Two non-dyad mechanisms are solved to demonstrate the procedure, and the programs' accuracies, capabilities and versatilities.

Having developed a method for performing a kinematic analysis of dyad and non-dyad mechanisms, attention is then turned to developing a procedure for synthesizing optimum dimensional tolerances in these complex mechanisms. The method which is based on a mechanical error sensitivity analysis involving displacements, velocities and accelerations, then proceeds to choose the smallest of the maximum input errors associated with these kinematical quantities without exceeding the specified allowable output limits. The work is reported in *Chapters* 3 and 4, with the former focusing on *dyad* mechanisms and the latter on *non-dyad* mechanisms.

In the case of dyad mechanisms, they are treated as consisting of an assemblage of drivers and dyad groups with analytically computed sensitivity coefficients. The details are discussed in *Chapter* 3. This modular approach permits the creation of a general multi-purpose program for design sensitivity analysis and tolerance synthesis of complex linkages. Also, a technique

for the direct identification of the most sensitive error combination without requiring to consider *all* the 2^m possibilities is suggested. This will significantly reduce the computational effort needed to carry out the synthesis of optimum dimensional tolerances in mechanisms. Two linkage examples are solved to demonstrate and assess the accuracy of the method for dyad mechanisms.

In *Chapter* 4, a method is proposed for carrying out a higher-order error sensitivity analysis and optimum dimensional tolerancing of planar non-dyad mechanisms. Unlike the method described in *Chapter* 3 which is applicable to dyad mechanisms only, the method developed in *Chapter* 4 is valid for both dyad and non-dyad mechanisms, and thus, constitutes a more general approach for carrying out the mechanical error sensitivity analysis with optimum dimensional tolerancing. The method is made feasible by the development of a unique analytical procedure for the determination of the position, velocity and acceleration sensitivity coefficients. They are computed via a kinematic analysis of the original and as well as, a supplemental mechanism. The latter is derived from the original mechanism by setting the virtual velocity term to either 0 or ± 1, depending on the particular sensitivity coefficient that is being evaluated. We called this technique the *Method of Virtual Velocity*. Once the sensitivity coefficients have been determined, the process of synthesizing for optimum dimensional tolerancing can be easily carried out. An example involving a 6-bar non-dyad linkage is used to demonstrate the procedure and the results obtained clearly show the method is able to accurately compensate for the prescribed input errors.

ACKNOWLEDGMENT

I would like to acknowledge the encouragement, advice and constructive suggestions from my supervisor Dr. RAY P.S. HAN. I would also like to thank Dr. A.B. Thornton-Trump and Dr. Q. Zhang for carefully reading my thesis.

I wish to thank my classmates, the faculty and staff in the Department of Mechanical and Industrial Engineering for their friendship and help throughout my study at the University of Manitoba.

Finally, most of all, I would like to thank my parents, wife and daughter for their patience and understanding during the period of my study. I would like to apologize to them for being away so much, working constantly in the computer lab.

LIST OF FIGURES

LIST OF TABLES

TABLE OF CONTENTS

CHAPTER 1

Introduction

The performance of moving mechanical systems can be significantly affected by the inherent errors of their input parameters such as joint clearances, and tolerances in link lengths and orientations. These mechanical errors arise from 3 principal sources; excessive design tolerances, poor manufacturing allowances and over time, the accompanying wear and tear of the various parts and joints. When the errors are large, the output motion of the systems not only fails to exhibit the design motion, but is also highly unpredictable. To control this problem, one not only needs to propose a method for the analysis of the mechanical errors but also, to suggest a technique for the synthesis of the dimensional tolerance bands of the input parameters for the specified output motion.

Several approaches have been introduced to handle the problem and they can be classified into two distinct categories; deterministic and stochastic methods. As their names imply, the former deals with known, characterizable variables and the latter, with random variables. The deterministic approach, which includes the traditional analytical and graphical methods is based on the worst-case analysis of individual tolerances, and thus, yields conservative results. This is because the probability of a simultaneous occurrence of these extreme tolerances on each and every link length is negligibly small On the other hand, the stochastic approach being more realistic in nature, can produce good results but the method tends to be difficult and sometimes, impractical to use. With the advent of low-cost, high-speed computers, improved analytical techniques have been suggested and applied with great success to control

the problem. In the next section, a literature survey of the past work in this area of research is presented.

1.1 LITERATURE SURVEY

In an early work, Bruevich (1946) first introduced the position error analysis to improve the output motion of mechanisms. Two years later, Svoboda (1948) presented an analytical procedure for the design of a four-bar linkage. His procedure is based on the computation of the sensitivity coefficients, i.e., partial derivatives of the output displacements with respect to the input parameters, and from them, he determined a linear relationship between the input and the output motions. Hall and Tao (1954) proposed a graphical technique for obtaining the sensitivity coefficients, but it is obvious that the accuracy of the graphical procedure was very poor, and therefore, this method was not widely adopted. Tuttle (1960) developed a method for estimating the average output error based only on the clearance effects, without any consideration of the link dimension tolerances. Hartenberg and Denavit (1964) estimated the mechanical error on the basis of the maximum allowable link dimension tolerance and they showed that the maximum error is given by the sum of the individual errors, a result which was shown to be generally incorrect by Kolhatkar and Yajnik (1970). It was left to Lakshiminaragana and Narayanamurthi (1971) who presented a method for the analysis of mechanical errors by taking into account the effects of tolerance in linkages. With the exception of the graphical technique, all the other error analysis methods are based on differentiating the equations of the input-output displacement relationship and then, solving the resulting linear algebraic equations pertaining to the links and joints.

Using a stochastic evaluation of the mobility band, Garrett and Hall (1969) analyzed the effects of tolerance and clearance in a four-bar linkage. Dhande and Chakraborty (1973) and Chakraborty (1975) developed a stochastic model of the four-bar function generating linkage. Their approach was based on the assumption that the probability of the pin axis of one link lying at any point is the same for all the points inside the race of the adjacent link. In a subsequent publication, Dhande and Chakraborty (1978) applied the stochastic method to

carry out a mechanical error analysis of spatial linkages. Baumgarten and van der Werff (1985) employed probability theory to analyze the effects of manufacturing tolerances on the output performance of constrained kinematic chains. In particular, they applied the method to path generating mechanisms to determine the mean and standard deviation of the vector position of a coupler point. Mallik and Dhande (1987) presented a stochastic model for the analysis and synthesis of mechanical error in a path-generating linkage. In their work, they assumed the tolerances and clearances in hinge joints to be random variables and applied their technique to a planar four-bar mechanism and its associated cognate mechanisms. They also developed a synthesis procedure to allocate tolerances and clearances on different members and joints of a linkage in order to control the output error in the path of the coupler point to within specified limits.

To get optimization results from the mechanical error analysis, Jones and Rooney (1970), Rooney and Rees Jones (1975) applied the definition of residual (variance) and evaluated the partial derivatives of a mechanism constraint function (i.e. the Jacobian) in order to optimize motion generation. Breteler (1979) presented partial derivatives in kinematic optimization. It should be mentioned that performing only the optimization would not guarantee better results for motion and force analyses. It is necessary to consider a sensitivity analysis of the position, velocity and acceleration in order to ensure error stability. For example, Chatterjee and Mallik (1987) applied sensitivity analysis to a four-bar linkage in order to select the best choice from the cognates. Using the symbolic language Macsyma, Fu and co-workers (1987, 1988a, 1988b) presented a method to carry out sensitivity analysis and optimization analysis of the error bands. Fenton, Cleghorn and Fu (1989) presented a method for the allocation of dimensional tolerances for multi-loop planar mechanisms. In a subsequent publication, Cleghorn, Fenton and Fu (1993) discussed optimum tolerancing of planar mechanisms based on an error sensitivity analysis. All the known and published work up to now has focused only on the analysis of the position output error. In order to secure a smoother motion, it is necessary to take into consideration higher order effects from the velocity and acceleration quantities. In this thesis, a new method is developed to obtain not only the position error analysis but also the velocity and acceleration error analyses. To develop this method, it is

necessary to first and foremost, develop a technique that is capable of carrying out a kinematic analysis of complex non-dyad planar mechanisms. This is because kinematic analysis of planar mechanisms is not only the foundation of mechanism design but is also, an inseparable part of the mechanical error analysis. With the rapid advancement of computers and computing technology, several powerful software packages have been developed for mechanism analysis. An in-depth literature review of these developments is presented in the *Introduction* section of *Chapter 2.*

1.2 OBJECTIVES AND SCOPE OF STUDY

A major deficiency of the currently available methods for linkage analysis is that they are highly theoretical in nature and are specific to the type of mechanism being analyzed. One of the objectives of this thesis is to develop a method that is not only practical and easy to implement, but also, must be sufficiently general to model all types of complex planar mechanisms, ranging from dyads to non-dyads. The method must be suitable for carrying out a first-order error analysis, i.e. position related, as well as, higher-order error analysis involving velocities and accelerations. To be useful, it must be able to deal with single and multi-loop linkages. Finally, once the mechanical error analysis is completed, the next step is to develop a method for the synthesis of optimum dimensional tolerance bands for the specified output motion. However, before any of these can be attempted, it is necessary to first develop a procedure to handle the kinematic analysis of both the dyad and non-dyad mechanisms. In summary, the objectives and scope of study of this research can be broadly stated as follows:

- Develop a method for the automatic generation of dyad mechanisms for the kinematic analysis of complex, non-dyad planar mechanisms.
- Develop a method for a higher order mechanical error sensitivity analysis suitable for both dyad and non dyad mechanisms.
- Develop a method for performing an optimum dimensional tolerance synthesis of dyad and non-dyad mechanisms based on the specified output motion.

1.3 THESIS LAYOUT

This thesis consists of five chapters, arranged as follows.

- In Chapter 1, a review and discussion of the literature survey of the known and published research in the area is presented.

- In Chapter 2, a method for the automatic generation of dyad mechanisms for a computer-aided kinematic analysis of complex non-dyad planar mechanisms is introduced.

- In Chapter 3, a method for carrying out a higher-order mechanical error sensitivity analysis and the optimum dimensional tolerancing of planar *dyad* mechanisms is suggested.

- In Chapter 4, the treatment of planar *non-dyad* mechanisms for a higher-order mechanical error sensitivity analysis and the optimum dimensional tolerancing of planar *dyad* mechanisms are proposed.

- In Chapter 5, the conclusions and summary of the work are outlined.

CHAPTER 2

Automatic Generation of Dyad Mechanisms for Computer-Aided Kinematic Analysis of Complex Non-Dyad Planar Mechanisms

2.1 INTRODUCTION

The past two decades have seen an extremely fast pace of development of computers and computer technology, and this has resulted in a growing demand for reliable, efficient, sophisticated and very importantly, user-friendly computer-aided mechanism analysis and design packages. Substantial early developments in this direction include software packages such as IMP (Sheth and Uicker (1972)), ADAMS® (Orlandea (1973)), KIDYAN (Brat and Lederer (1973)), KINSYN III (Rubel and Kaufman (1977)) and DYMAC (Paul (1977)) and LINCAGES© (Erdman and Gustafson (1977)). Recent graphics-driven, user-friendly software have also emerged and these include SYNTRA (Barker (1985)), MICROMECH (William (1986)), KADAM (Vadnagarwala (1988)) and KPLAn (Han and Tsuyuki (1993)). A state-of-the-art review of current mechanism software has recently been published by Erdman (Erdman (1995)). He discussed several popular programs such as ADAMS®, ANALYTIX™ (Fichter, Smith, Todd and Wagner (1992)), DADS® (Haug, Wehage and Barman (1982)) and MINNSKETCH© (Ho, Erdman and Riley (1994)) and demonstrated their capabilities via selected industrial examples. The techniques available for kinematic analysis can be classified into three types: graphical, analytical and numerical. They include for example, the vector loop closure approach (Chace (1964) and Shigley (1969)), complex conjugate exponential method (Smith (1975), Erdman and Sandor (1984)), matrix procedures (Shigley and Uicker

(1980)), dyad and non-dyad modeling (Artobolovski (1977), Suh and Ratcliff (1978), Zhao (1980), Huang (1981)), graph theory (Paul (1960), Crossley (1965), Davies (1968), Raicu (1974), Mruthyunjaya and Raghavan (1984)), and screw theory (Bottema and Roth (1979)). In an attempt to handle complex linkages, some researchers have proposed the use of modular methods to "break-down" a linkage into manageable modules (Kinzel and Chang (1984), Molian (1984) and Smith and Ye (1984)).

The research here attempts to fulfill the desire for a powerful and yet easy to use software by developing a fully automated program that requires minimal human inputs and interventions. A novel approach for the kinematic analysis of complex non-dyad planar mechanisms is presented. It involves transforming the non-dyad mechanism into a series of dyad mechanisms whose solutions are readily computable. By disconnecting appropriate links and prescribing dyad drivers for the transformed linkage, the affected geometric conditions are recovered back to their original values. This idea of disconnected links for kinematic analysis has also been suggested by Wu and Zhang (1988) but their approach is manual and cumbersome, and can solve only the simplest non-dyad linkage. The method presented here is not only fully automated, but could also handle one or more disconnected links, with one or more dyad drivers. The program is named **NDPLAn** (**N**on-**D**yad **P**lanar **L**inkage **An**alysis).

2.2 DECOMPOSITION INTO DYAD MECHANISMS

Considering only planar mechanisms with lower pairs, *Figure* 2.1(a) depicts an 8-link *Assur kinematic chain* (AKC) with joints A, L and H fixed (or their positions are known). As defined for example, in Galletti (1986), an AKC is a closed kinematic chain possessing *zero* mobility and from which, it is not possible to produce another kinematic chain of the same mobility if one or more links are suppressed. The AKC concept can be developed into a very powerful and systematic approach for the kinematic analysis of complex mechanisms. This is because if the position of an AKC link is known, the position of any other links in the AKC can also be determined. For non-dyad mechanisms, the procedure involves suppressing one or more links to transform the chain into a series of dyad mechanisms with finite dof. Then, through a

numerical technique, the positions of all other links are determined by ensuring that the positions of the joints of the removed link produce the *same* distance as the length of the removed link. For example, any one of the three links ①, ③, ⑤ in *Figure* 2.1(a) may be removed to transform the AKC into a series of dyad mechanisms as illustrated in *Figures* 2.1(b), 2.1(c), 2.1(d) respectively. If link ① in *Figure* 2.1(b) is removed from the chain, the following cases of dyad mechanisms corresponding to different input links are obtained.

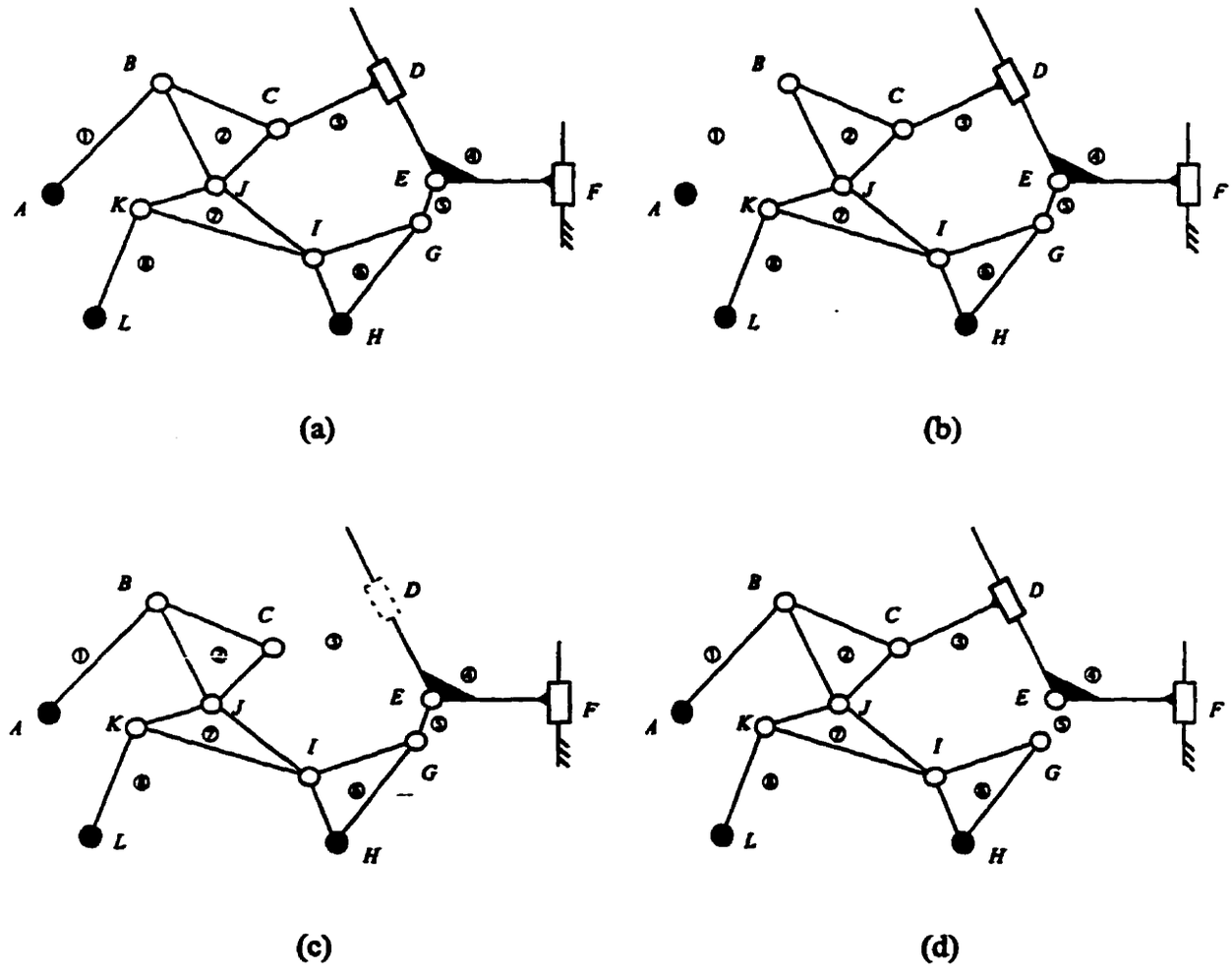

Figure 2.1: Assur kinematic chain (a) and its possible dyad mechanisms (b)-(d) (• position known, o position unknown).

Case A - input ④: dyad ⑤, ⑥; dyad ⑦, ⑧; and dyad ②, ③.

Case B - input ⑥: dyad ⑦, ⑧; dyad ⑤, ④; and dyad ②, ③.

Case C - input ⑧: dyad ⑥, ⑦; dyad ⑤, ④; and dyad ②, ③.

Similarly, if link ③ is removed from the chain as depicted in *Figure* 2.1(c), the transformed dyad mechanisms corresponding to the prescribed input link are:

Case D - input ④: dyad ⑤, ⑥; dyad ⑦, ⑧; and dyad ①, ②.

Case E - input ⑥: dyad ④, ⑤; dyad ⑦, ⑧; and dyad ①, ②.

Case F - input ⑧: dyad ⑥, ⑦; dyad ④, ⑤; and dyad ①, ②.

Finally, if link ⑤ in *Figure* 2.1(d) is removed from the chain, we get the following cases:

Case G - input ⑥: dyad ⑦, ⑧; dyad ①, ②; and dyad ③, ④.

Case H - input ⑧: dyad ⑥, ⑦; dyad ①, ②; and dyad ③, ④.

Any one of the foregoing 8 cases of transformed dyad mechanisms can be used to perform a kinematic analysis of the prescribed AKC. Note that the removal of link ⑧ results in a 2-dof transformed dyad mechanism which requires 2 input variables for solution.

To demonstrate the solution process, we consider Case B with link ① removed as shown in *Figure* 2.1(b). Assuming the input variable is the angle θ, the relationship between the coordinates of joint B and θ is given by,

$$\sqrt{\left(X_A - X_B(\theta)\right)^2 + \left(Y_A - Y_B(\theta)\right)^2} = L_{AB}, \tag{2.1}$$

where L_{AB} is the known length of link ① and (X_A, Y_A), (X_B, Y_B) are the coordinates of joints A and B respectively. It is required to compute in *Equation* (2.1), the value of θ such that the original value of L_{AB} is recovered to within a prescribed tolerance. The most convenient way to solve this nonlinear problem is to do so iteratively via a simplex-based algorithm. An alternative approach based on the method of successive approximation for AKC has been proposed by Huang (1981). So far, the discussion has been confined to the removal of a link to generate the transformed dyad mechanisms. If the removal of a joint is considered, the geometric conditions are slightly more complicated (see for example, Wu and Zhang (1988)). Note that the removal of a joint can generally be simulated by disconnecting two links.

2.3 MN INCIDENCE MATRIX

In the development of an efficient computer program, it is essential that the topology of a kinematic chain be described in a systematic and yet compact manner. A popular way to achieve this efficient storage of topological information is through the use of incidence matrix. Since its introduction in the sixties, the technique has been adopted by many computer-based methods for mechanism analysis. In this paper, the following modifications to the conventional incidence matrix approach is introduced.

(a) The rows and columns of the matrix represent the links and joints respectively. Hence, the total number of rows and columns is given by the total number of links **M** and the total number of joints **N** in the mechanism (the so-called *link-joint* incidence matrix or **MN** matrix for short).

(b) The elements of the incidence matrix are determined by the nature of the link-joint relationship. For instance, a zero entry in the matrix implies that the joint is not connected *directly* to the links being considered, and a non-zero entry denotes otherwise. A revolute joint is represented by 1 and a prismatic joint by 2.

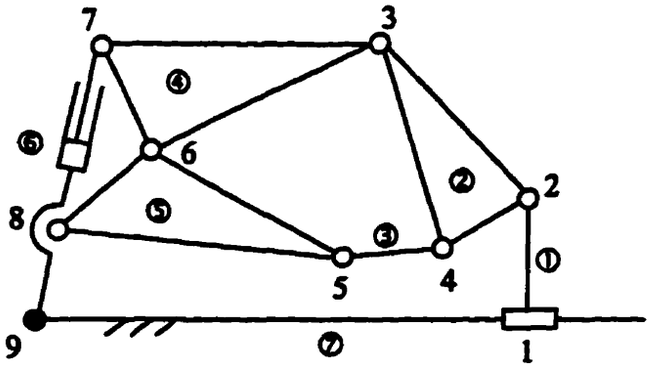

(a) linkage

MN MATRIX

$$\begin{bmatrix} 2 & 1 & 0 & 0 & 0 & 0 & 0 & 0 & 0 \\ 0 & 1 & 1 & 1 & 0 & 0 & 0 & 0 & 0 \\ 0 & 0 & 0 & 1 & 1 & 0 & 0 & 0 & 0 \\ 0 & 0 & 1 & 0 & 0 & 1 & 1 & 0 & 0 \\ 0 & 0 & 0 & 0 & 1 & 1 & 0 & 1 & 0 \\ 0 & 0 & 0 & 0 & 0 & 0 & 1 & 1 & 1 \\ 2 & 0 & 0 & 0 & 0 & 0 & 0 & 0 & 1 \end{bmatrix}$$

(b) prescribed

MM MATRIX

$$\begin{bmatrix} 0 & 1 & 0 & 0 & 0 & 0 & 2 \\ 1 & 0 & 1 & 1 & 0 & 0 & 0 \\ 0 & 1 & 0 & 0 & 1 & 0 & 0 \\ 0 & 1 & 0 & 0 & 1 & 1 & 0 \\ 0 & 0 & 1 & 1 & 0 & 1 & 0 \\ 0 & 0 & 0 & 1 & 1 & 0 & 1 \\ 2 & 0 & 0 & 0 & 0 & 1 & 0 \end{bmatrix}$$

(c) computer-generated

NN MATRIX

$$\begin{bmatrix} 0 & 1 & 0 & 0 & 0 & 0 & 0 & 0 & 1 \\ 1 & 0 & 1 & 1 & 0 & 0 & 0 & 0 & 0 \\ 0 & 1 & 0 & 1 & 0 & 1 & 1 & 0 & 0 \\ 0 & 1 & 1 & 0 & 1 & 0 & 0 & 0 & 0 \\ 0 & 0 & 0 & 1 & 0 & 1 & 0 & 1 & 0 \\ 0 & 0 & 1 & 0 & 1 & 0 & 1 & 1 & 0 \\ 0 & 0 & 1 & 0 & 0 & 1 & 0 & 1 & 1 \\ 0 & 0 & 0 & 0 & 1 & 1 & 1 & 0 & 1 \\ 1 & 0 & 0 & 0 & 0 & 0 & 1 & 1 & 0 \end{bmatrix}$$

(d) computer-generated

Figure 2.2: Linkage (a) and incidence matrices (b)-(d).

For convenient and error-free data handling, the program automatically constructs two other incidence matrices: the conventional link-link incidence matrix (or the MM matrix) and the joint-joint incidence matrix (or the NN matrix) from the prescribed MN matrix. Therefore the MM matrix, depending on the type of link-pairing, would consists of entries 0, 1, 2; and the NN matrix, depending on whether the joints are directly connected or not, would contain entries 0, 1. An example is sketched in *Figure* 2.2(a), with its prescribed MN matrix shown in *Figure* 2.2(b) and the computer-derived MM and NN matrices in *Figures* 2.2(c) and 2.2(d).

2.4 AUTOMATIC GENERATION AND IDENTIFICATION OF BASIC MECHANISM COMPONENTS

The analysis of complex mechanisms can be conveniently and efficiently handled via a modular approach based on their basic mechanism components. This popular technique has been adopted by many general-purpose mechanism analysis programs. The method involves decomposing a mechanism into a series of basic components which are readily analyzable. A systematic identification of the six basic mechanism components for our proposed method is listed in *Table* 2.1. An identification number for each type of mechanism component is shown

Table 2.1: The six basic mechanism components.

Type 1	Type 2	Type 3	Type 4	Type 5	Type 6
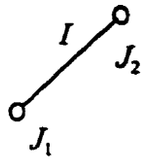	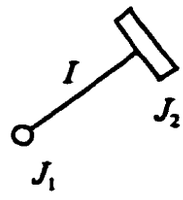	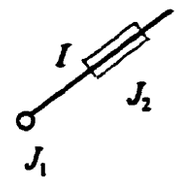	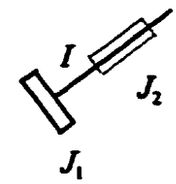	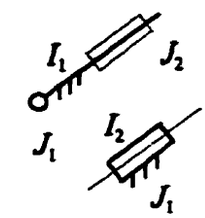	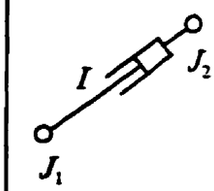
$I\begin{bmatrix} 1 & 1 \end{bmatrix}$	$I\begin{bmatrix} 1 & 2 \end{bmatrix}$	$I\begin{bmatrix} 1 & 2 \end{bmatrix}$	$I\begin{bmatrix} 2 & 2 \end{bmatrix}$	$\begin{matrix} I_1 \\ I_2 \end{matrix}\begin{bmatrix} 1 & 2 \\ 2 & 0 \end{bmatrix}$	$I\begin{bmatrix} 1 & 1 \end{bmatrix}$
$MN(I,J_1)=1$ $MN(I,J_2)=1$	$MN(I,J_1)=1$ $MN(I,J_2)=2$	$MN(I,J_1)=1$ $MN(I,J_2)=2$	$MN(I,J_1)=2$ $MN(I,J_2)=2$	$MN(I,J_2)=\begin{cases}1\\2\end{cases}$ $MN(I,J_2)=\begin{cases}2\\0\end{cases}$	$MN(I,J_1)=1$ $MN(I,J_2)=1$
Link Length Known	Link Length Known	Link Length Unknown	Link Length Unknown	Angle Known J_1 Known	Link Length Unknown

together with its MN matrix and the pertinent geometric information. For example, Type 1 mechanism component is that of a binary link with a known length and its MN matrix listed as shown. Type 2 mechanism component is similar except that it has a slider instead of a revolute joint at J_2, Type 3 mechanism component is a slider of unknown length, and so on, for the remaining mechanism components in the table. Note that for the Type 5 mechanism component, the slide (or the slider) is grounded and thus, the direction of the slider (or slide) and the position of joint J_1 are known. An algorithm describing how the program automatically identifies the six basic mechanism components is sketched in *Figure* 2.3. For simplicity, only that part of the flowchart for a mechanism composed of binary links is displayed. The algorithm starts by determining whether a joint of the binary link is prismatic (P) or revolute (R). It is then routed in accordance to whether geometric information such as

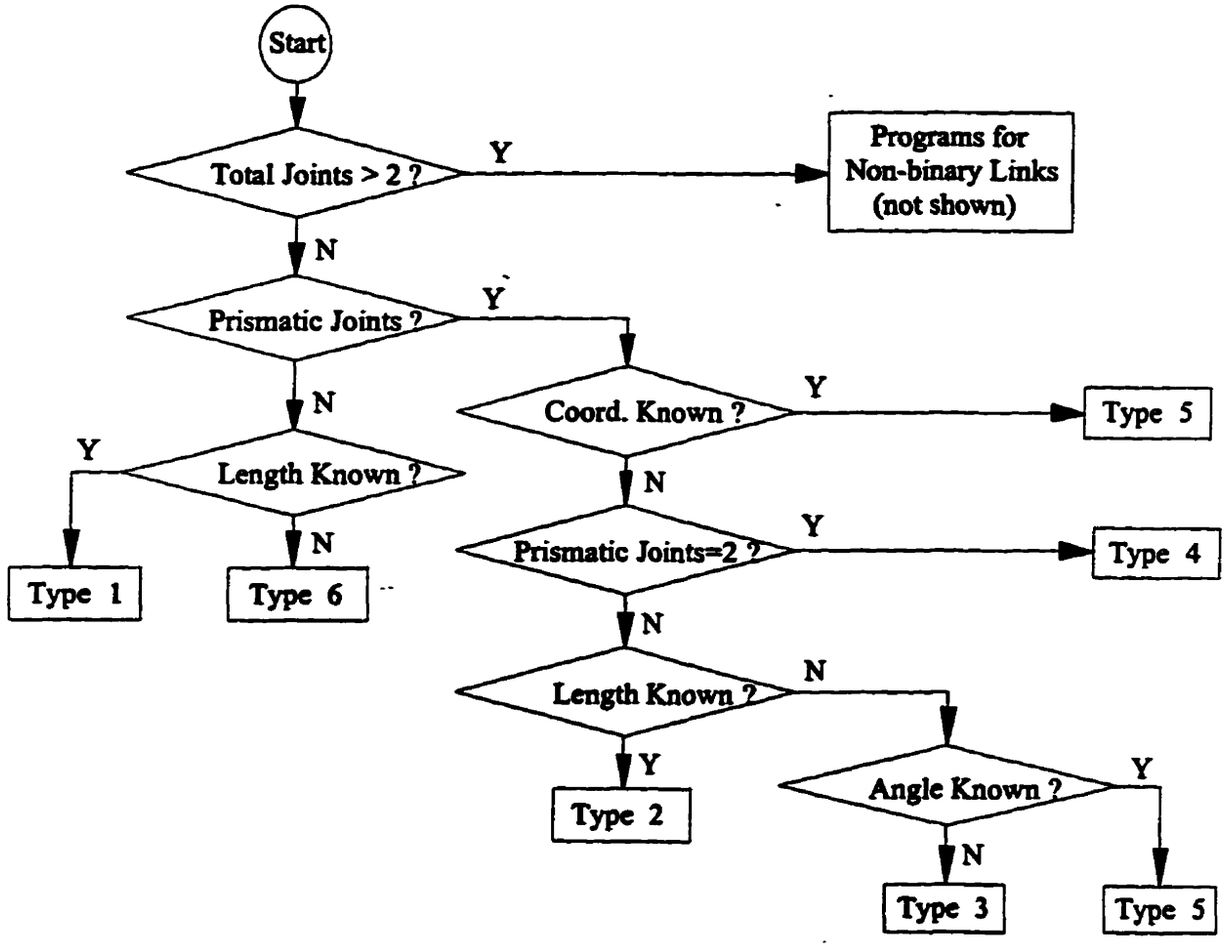

Figure 2.3: Algorithm for choosing the six basic mechanism components.

link-length or angle is known. For example, a basic mechanism component with a non-prismatic joint and an unknown link length must be of Type 6. Once the basic mechanism components have been identified, they can be assembled to form dyad mechanisms. *Table* 2.2 lists the five basic dyad mechanisms that can be generated from planar linkages with lower pairs. In the first category, the RRR dyad group comprises two binary links of Type 1 and hence, given the designation (1)--(1). In the second category, mechanism components of Types 1, 2 and 5 form the RRP dyad group and therefore, identified as either a (1)--(2)--(5) or (5)--(2)--(1) sequence. This method of construction is repeated for the remaining three categories, namely, the RPR, PRP and RPP dyad groups. If the sequence is in a counter-clockwise direction, a positive sign is assigned, otherwise, it is negative.

Table 2.2: Basic dyad mechanisms.

RRR Dyad	RRP Dyad	RPR Dyad	PRP Dyad	RPP Dyad
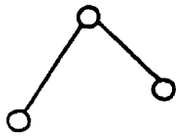	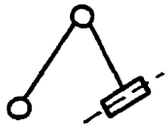	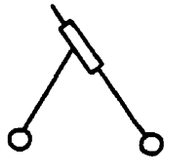	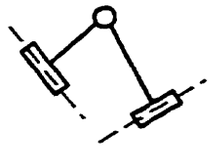	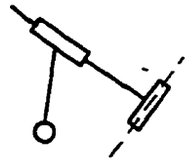
(1) ------ (1)	(1) --- (2) ---(5) (5) --- (2) --- (1)	(2) ------ (3) (3) ------ (2)	(5) ------ (2) --- ---(2) ------(5)	(2) --- (4) --- (5) (5) --- (4) --- (2)

In our proposed method, a kinematic analysis of a non-dyad mechanism is carried out by first transforming it into a series of dyad mechanisms through the removal of one or more links (or equivalently, joints), and then selecting an appropriate dyad driver in the form of either an angular or length input, to drive the dyad mechanism. Since it is possible to arrive at different dyad mechanisms simply by varying the choice of the disconnected link and/or the choice of the dyad driver, there is no unique set of dyad mechanisms associated with a given non-dyad planar

linkage. The final answer, however, must obviously be the same regardless of the choice of the disconnected link and/or dyad driver. For example, consider the 6-bar non-dyad mechanism shown in *Figure* 2.4. The linkage driver is link ① and thus, the position of joint 2 can be easily

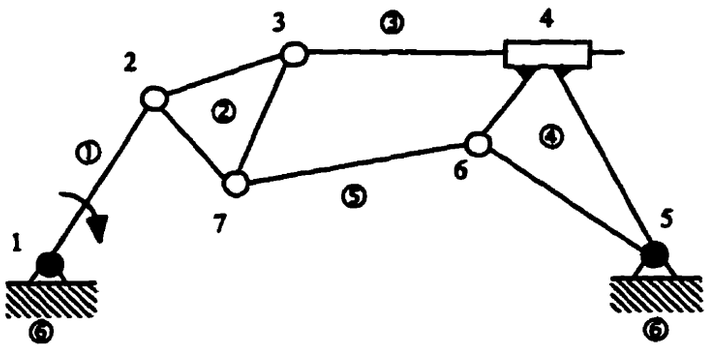

Figure 2.4: Selection of the non-dyad drivers for a 6-link non-dyad mechanism.

determined. With link ① completely solved, the remaining part of the mechanism can be analyzed by decomposing it into a series of dyad mechanisms with appropriate disconnected links and/or dyad drivers. The drivers for the two possible dyad mechanisms are as follow.

(a) Dyad driver is link ②. Choosing links ③ and ④ as the dyad mechanism, and disconnecting link ⑤, then link ④ can be classified as the Type 2 basic mechanism component. It forms an RPR dyad group with link ③. If on the other hand, the dyad mechanism is comprised of links ④ and ⑤, and link ③ is disconnected, then link ⑤ constitutes the Type 1 basic mechanism component and forms an RRR dyad group with link ④.

(b) Dyad driver is link ④. Choosing links ② and ③ as the dyad mechanism, and disconnecting link ⑤, then link ④ constitutes the Type 5 basic mechanism component. It becomes a fixed link (i.e. a frame) for the RRP dyad group composed of links ② and ③. Similarly, if links ② and ⑤ form the dyad mechanism, and link ③ is discarded, then link ⑤ becomes the Type 1 basic mechanism component and forms an RRR dyad group with

link ②.

To illustrate how **NDPLAn** solves the kinematics of the dyad mechanisms, we consider the chain illustrated in *Figure* 2.5. A link I_1 with a known joint J_0 is shown in *Figure* 2.5(a). If the orientation of link I_1 is known, then the location of joint J_1 in *Figure* 2.5(b) can be computed, otherwise, the program proceeds to the adjacent link I_2 with joint J_2 as sketched

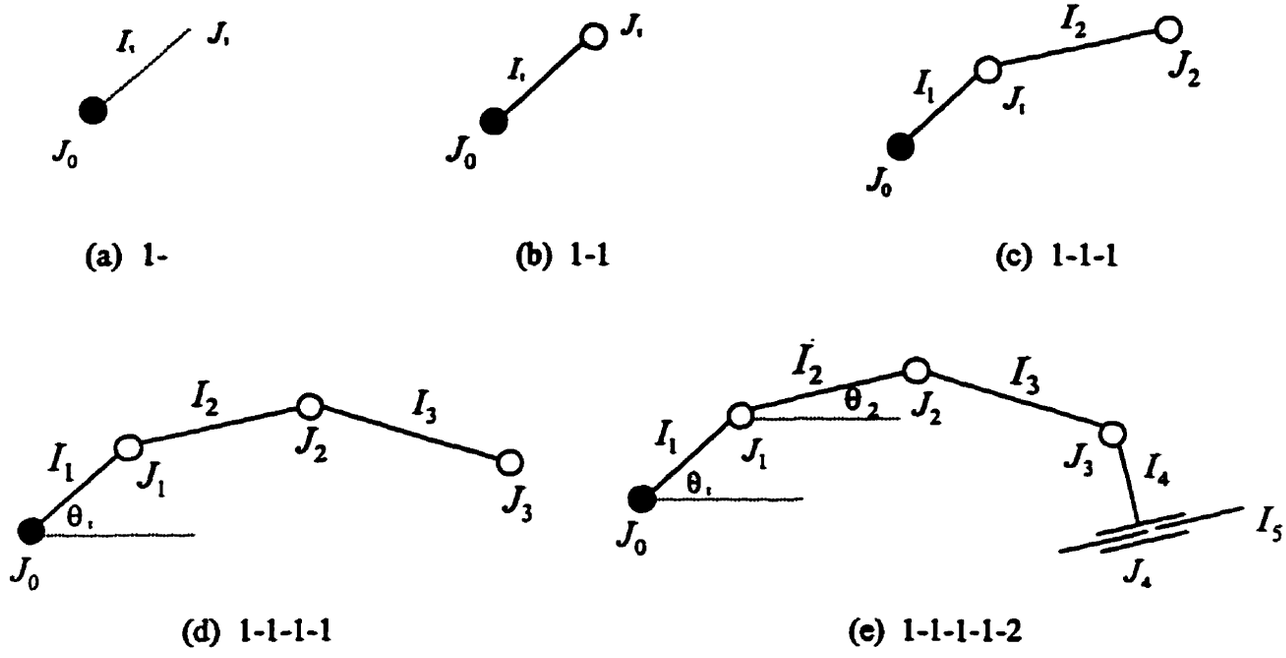

Figure 2.5: Solution process for a dyad mechanism; R-joint (1) and P-joint (2).

In *Figure* 2.5(c). If J_2 is known, then J_1 can be easily evaluated for one of the two possible linkage configurations by prompting the user to input accordingly. On the other hand, if J_2 is unknown, the program proceeds to the next link I_3 and if its joint J_3 is known, then joints J_1 and J_2 can be calculated for an assumed angle θ_1. This is shown in *Figure* 2.5(d). Otherwise, the program proceeds to find the next adjacent link, I_4 in *Figure* 2.5(e). If the orientation of the slider I_5 is known, then for assumed values of θ_1 and θ_2, the joints J_1, J_2, J_3 and J_4 can be calculated. *Figure* 2.6 lists one-half of all possible joint arrangements for a planar

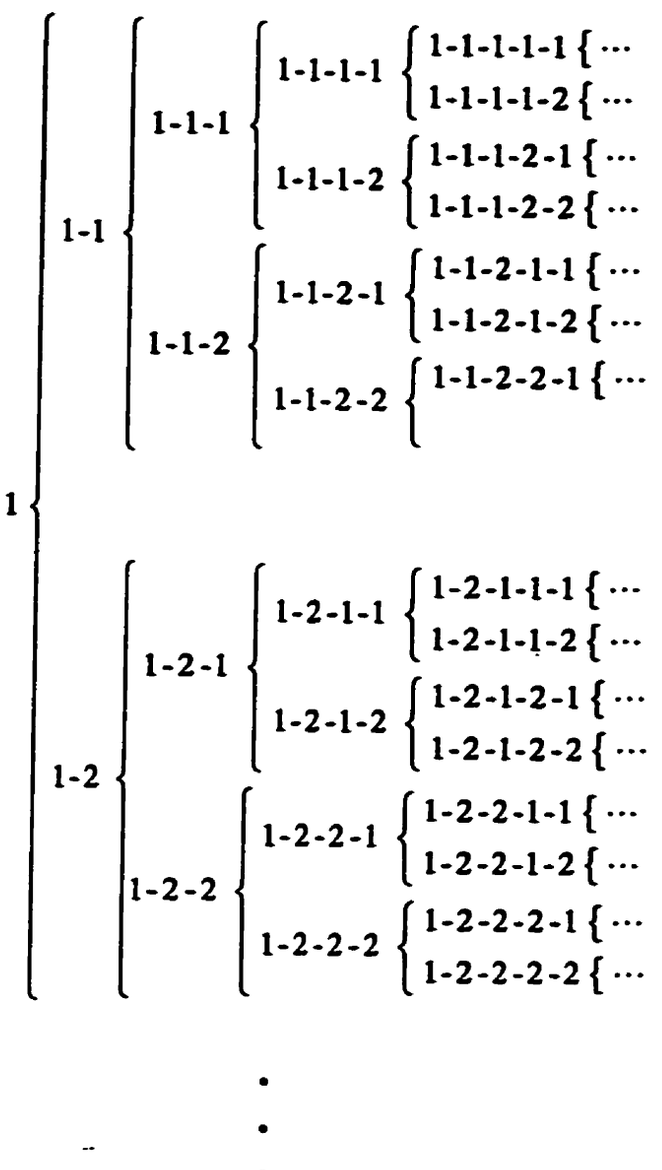

Figure 2.6: **One-half of all possible link arrangements.**

linkage with lower pairing. Starting at the first level with say, an R-joint (1), the program finds a joint which could be either another R-joint, or a P-joint (2) at the second level. That is either a 1-1 sequence or a 1-2 sequence At the third level, we have four sequence possibilities:

1-1-1, 1-1-2, 1-2-1 and 1-2-2. As depicted, the number of possibilities is of the order 2^L where $L = 0,1,2,\cdots$.

Using the definition of the incidence matrix introduced here, it is very easy to establish the relationship between adjacent links and their pairing types. Next, a computer implementation of the foregoing ideas for automatic generation and identification of the basic mechanism components and the subsequent kinematic analysis is described.

2.5 COMPUTER IMPLEMENTATION

The flow chart for the computer implementation is illustrated in *Figure* 2.7. The user inputs the MN matrix and all pertinent geometric data associated with the linkage. Given the MN information of the linkage, **NDPLAn** automatically generates the corresponding MM and NN matrices, together with the basic mechanism components. From the driver link, the program solves for the unknown joint of the link or its unknown length, if the link is a hydraulic cylinder (Type 6 in *Table* 2.1). It then proceeds to search iteratively for all links with only one known joint. Armed with this information, the program constructs either dyad or non-dyad mechanisms in the remaining part of the linkage. If only dyad linkages are present, the solution process is standard and straightforward, and the subroutine dyad is called to perform this operation. On the other hand, if the remaining linkage consists of non-dyad linkages, it will be necessary to disconnect one or more links in order to transform it into a series of dyad mechanisms. To recover the disconnected links, one or more dyad drivers are prescribed, and the unknown positions are then computed via an iterative process by adjusting appropriately, the values of the dyad drivers. A search algorithm based on the simplex method (Fan and Zhang (1982)) is adapted for this purpose. In this way, the lengths of the disconnected links are recovered to their original values, to within a set tolerance. When this process is completed at the location of the linkage driver being considered, kinematic analyses for velocities and accelerations are then carried out. It should be mentioned that for all subsequent locations of the linkage, it is not necessary to either assume disconnected links or prompt user for new approximate input values of the dyad drivers.

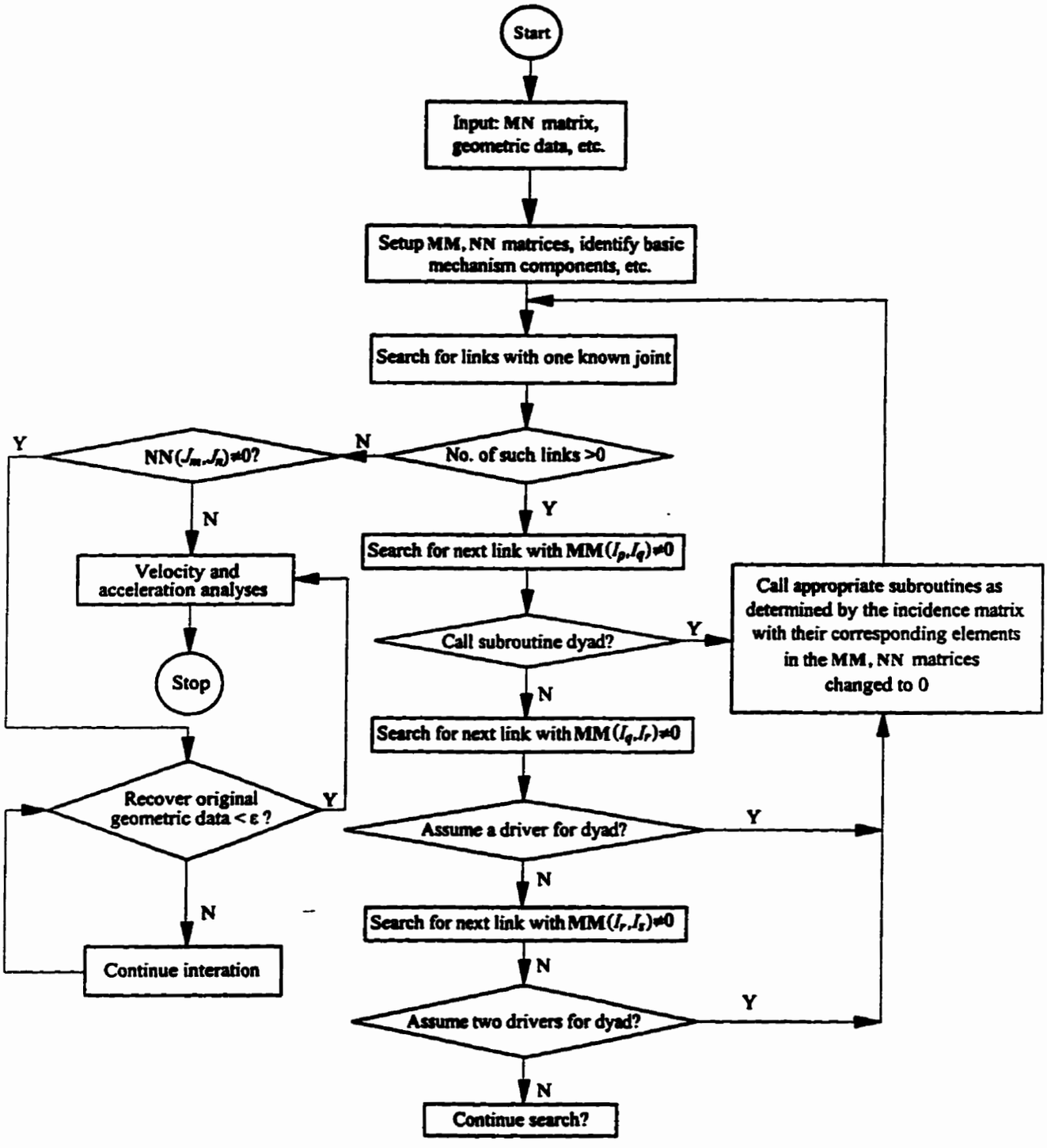

Figure 2.7: Flow-chart for computer implementation.

To illustrate the procedure, the mechanism shown in *Figure* 2.8 is analyzed. The step-by-step procedure is described as follows.

1) *Figure* 2.8(a) - upon inputting the MN incidence matrix and the known geometrical and linkage driver information, the program automatically generates the MM and NN matrices as shown.

2) *Figure* 2.8(b) - the program finds that there are three links ①, ④ and ⑤ containing known joint positions at 1, 6 and 7, respectively (shown as black dots). Since link ① is the linkage driver, joint 2 can be easily calculated via Subroutine RR. Link ① is now completely solved (shown as a darkened line). The MM and NN matrices are also automatically modified by replacing 1 in the affected elements with 0 (as shown by the bold entries in the matrices). Observe that the original MN matrix remains unchanged throughout the process.

3) *Figure* 2.8(c) - from links ②, ④ and ⑤ all of which share the same characteristic of having one known joint, the program determines that there are six paths to calculate the position of the next unknown joint(s). Depending on the choice of the dyad driver for the associated dyad mechanism, the six alternatives (with the dyad driver indicated first) are as follows.

Path 1: links ②--③--④, joints 2--3--4--6

Path 2: links ②--③--⑤, joints 2--3--5--7

Path 3: links ④--③--⑤, joints 6--4--5--7

Path 4: links ④--③--②, joints 6--4--3--2

Path 5: links ⑤--③--②, joints 7--5--3--2

Path 6: links ⑤--③--④, joints 7--5--4--6

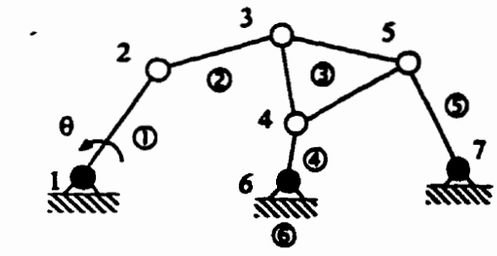

(a)

MN

$$\begin{bmatrix} 1100000 \\ 0110000 \\ 0011100 \\ 0001010 \\ 0000101 \\ 1000011 \end{bmatrix}$$

MM

$$\begin{bmatrix} 010001 \\ 101000 \\ 010110 \\ 001001 \\ 001001 \\ 100110 \end{bmatrix}$$

NN

$$\begin{bmatrix} 0100000 \\ 1010000 \\ 0101100 \\ 0010110 \\ 0011001 \\ 0001000 \\ 0000100 \end{bmatrix}$$

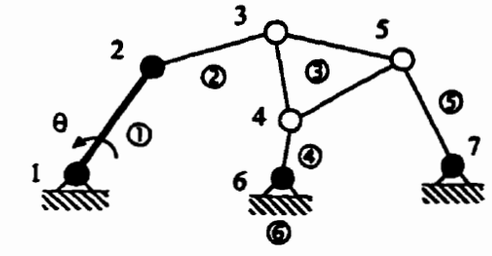

(b)

MN

$$\begin{bmatrix} 1100000 \\ 0110000 \\ 0011100 \\ 0001010 \\ 0000101 \\ 1000011 \end{bmatrix}$$

MM

$$\begin{bmatrix} 000000 \\ 001000 \\ 010110 \\ 001001 \\ 001001 \\ 000110 \end{bmatrix}$$

NN

$$\begin{bmatrix} 0000000 \\ 0010000 \\ 0101100 \\ 0010110 \\ 0011001 \\ 0001000 \\ 0000100 \end{bmatrix}$$

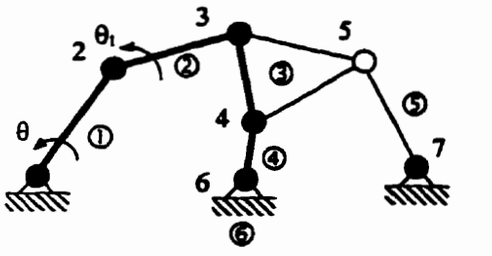

(c)

MN

$$\begin{bmatrix} 1100000 \\ 0110000 \\ 0011100 \\ 0001010 \\ 0000101 \\ 1000011 \end{bmatrix}$$

MM

$$\begin{bmatrix} 000000 \\ 000000 \\ 000010 \\ 000000 \\ 001001 \\ 000010 \end{bmatrix}$$

NN

$$\begin{bmatrix} 0000000 \\ 0000000 \\ 0000100 \\ 0000100 \\ 0011001 \\ 0000000 \\ 0000100 \end{bmatrix}$$

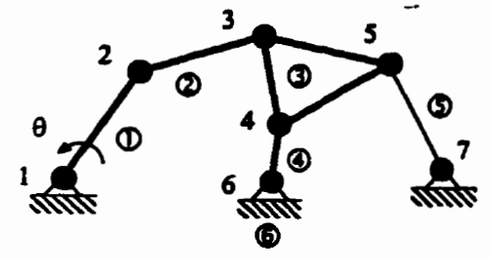

(d)

MN

$$\begin{bmatrix} 1100000 \\ 0110000 \\ 0011100 \\ 0001010 \\ 0000101 \\ 1000011 \end{bmatrix}$$

MM

$$\begin{bmatrix} 000000 \\ 000000 \\ 000000 \\ 000000 \\ 000001 \\ 000010 \end{bmatrix}$$

NN

$$\begin{bmatrix} 0000000 \\ 0000000 \\ 0000000 \\ 0000000 \\ 0000001 \\ 0000000 \\ 0000100 \end{bmatrix}$$

Figure 2.8: Step-by-step solution of a 6-bar mechanism.

Observe that of the six possibilities, only the first three paths 1-3 are independent. Since there is no advantage in this mechanism to choose any particular path, we have programmed for the path with the smallest consecutive joint numbers to be selected. Thus, in this instance, it would be Path 1 via links ②--③--④. For this path, the dyad driver is link ② and the dyad mechanism is formed by links ③ and ④. The program prompts the user to input only once, an approximate value of θ_1 which is consistent with the configuration of the linkage. With this information, **NDPLAn** proceeds to compute joint 3 using Subroutine RR. Joint 4 is then calculated based on solved joints 3 and 6. Since there are 3 revolute joints involved here, Subroutine RRR is called upon for the computation. Once again, the affected elements in the **MM** and **NN** matrices are automatically zeroed as marked in bold. Note that once a particular path is chosen, this path is stored in memory for all subsequent iterations.

4) *Figure* 2.8(d) - at this stage, all joints other than joint 5 in the linkage are known. To solve joint 5, the program employs known joints 3 and 4 in Subroutine RRR. As before, the **MM** and **NN** matrices are modified accordingly, to reflect this situation. When all the joints are solved, the program goes back to the assumed θ_1 and self-corrects the value iteratively as the length of the disconnected link ⑤ is being recovered. Once the length of link ⑤ is obtained to within the prescribed accuracy, the link positions are all fully solved and the velocity and acceleration analyses can then be performed.

NDPLAn currently executes on a PC and has been successfully tested on several non-dyad planar mechanisms with configurations ranging from simple to very complex. The maximum number of links, joints, dyad drivers, disconnected links and dyad mechanisms are constrained only by the available computer memory. Another advantage of the program is that it can handle multi-degrees of freedom linkages (dof) without any undue difficulties.

2.6 NUMERICAL SIMULATIONS

Two non-dyad linkages are analyzed here. The first example involves a 6-link mechanism

with 7-revolute joints. A comparison of its kinematic analysis with results generated by a totally different approach based on the loop closure method is provided, and this second method serves as an assessment of accuracy of the approach. The second example is a more complicated mechanism with 22 links and 31 revolute joints, and its solution clearly demonstrates **NDPLAn**'s capability and versatility.

2.7.1 Example 1: a 6-link mechanism

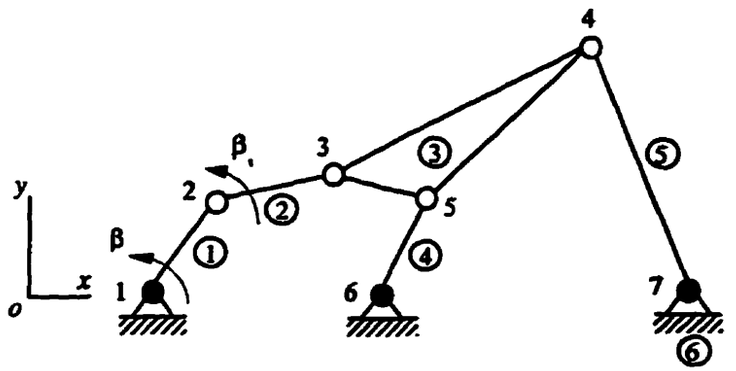

MN MATRIX

$$\begin{bmatrix} 1 & 1 & 0 & 0 & 0 & 0 & 0 \\ 0 & 1 & 1 & 0 & 0 & 0 & 0 \\ 0 & 0 & 1 & 1 & 1 & 0 & 0 \\ 0 & 0 & 0 & 0 & 1 & 1 & 0 \\ 0 & 0 & 0 & 1 & 0 & 0 & 1 \\ 1 & 0 & 0 & 0 & 0 & 1 & 1 \end{bmatrix}$$

Figure 2.9: A 6-link non-dyad mechanism with its MN incidence matrix.

A single-dof 6-link, 7-joint mechanism is shown in *Figure* 2.9 together with its MN incidence matrix. The location of fixed joints and the length of various links are listed in *Table* 2.3. A kinematic analysis of the linkage for displacements, velocities and accelerations is performed as the linkage driver ① is rotated at a constant rate of $\omega = 1$, from $\beta = 0.0^0$ to $\beta = 351^0$, the latter value being the farthest the linkage can turn. During the solving phase a tolerance of 10^{-4} is set for the iterations. To solve the non-dyad linkage, it is necessary to transform it into a dyad mechanism and this is achieved by disconnecting a link and introducing a dyad driver. All these steps are transparent to the user as they are automatically selected by the program. From a visual inspection of the linkage at the starting position of $\beta = 0.0^0$, an initial estimated value of $\beta_1 = -10.0^0$ is prescribed for the dyad driver of the dyad mechanism. The results for

Table 2.3: The 6-link mechanism - joint positions and link lengths.

Known Joint Positions

Joint	x	y
1	1.0	0.0
6	2.0	0.0
7	3.0	0.0

Link Lengths

①: L_{1-2} 0.4	③: L_{3-5} 0.5	⑤: L_{4-7} 1.0
②: L_{2-3} 0.6	③: L_{4-5} 1.2	⑥: L_{1-6} 1.0
③: L_{3-4} 1.6	④: L_{5-6} 0.4	⑥: L_{6-7} 1.0

displacements, velocities and accelerations at three positions; initial, intermediate and final, are summarized in *Table* 2.4. Both the final converged values of β_1 and the RMS length errors of the disconnected link are also depicted. For the purpose of determining the accuracy of the proposed method, angular velocities and accelerations for links ②, ③, ④ and ⑤ are compared with those computed by **KPLAn** which is a program developed using the loop closure method (Han and Tsuyuki (1993)). The results are illustrated in *Figures* 2.10 and 2.11. Excellent agreement between two completely different methods of analysis is obtained for all the links.

Figure 2.12 shows a single-dof 22-link, 31-joint mechanism together with its MN incidence matrix. The complexity of this linkage would present a good challenge to most mechanism analysis programs. The known fixed joints and other geometrical data are tabulated in *Table* 2.5.

Table 2.4: The 6-link mechanism - kinematic results at initial, intermediate and final positions.

Initial Position, $\beta = 0^0$

($\beta_1 = -29.14^0$, RMS Length Error $= 1.95 \times 10^{-5}$)

Joint	x	y	$\dot{x}$	$\dot{y}$	$\ddot{x}$	$\ddot{y}$
1	1.00	0.00	0.00	0.00	0.00	0.00
2	1.40	0.00	0.00	0.40	-0.40	0.00
3	1.90	-0.29	-0.006	0.39	-0.12	0.50
4	2.88	0.99	0.44	0.06	0.43	-0.15
5	2.39	-0.10	0.06	0.23	-0.08	0.24
6	2.00	0.00	0.00	0.00	0.00	0.00
7	3.00	0.00	0.00	0.00	0.00	0.00

Intermediate Position, $\beta = 180^0$

($\beta_1 = 23.69^0$, RMS Length Error $= 2.15 \times 10^{-5}$)

Joint	x	y	$\dot{x}$	$\dot{y}$	$\ddot{x}$	$\ddot{y}$
1	1.00	0.00	0.00	0.00	0.00	0.00
2	0.60	0.00	0.00	-0.40	0.40	0.00
3	1.15	0.24	-0.09	-0.20	0.20	0.25
4	2.60	0.92	-0.15	-0.07	0.27	0.09
5	1.65	0.19	-0.08	-0.15	0.19	0.20
6	2.00	0.00	0.00	0.00	0.00	0.00
7	3.00	0.00	0.00	0.00	0.00	0.00

Final Position, $\beta = 351^0$

($\beta_1 = 74.38^0$, RMS Length Error $= 1.34 \times 10^{-5}$)

Joint	x	y	$\dot{x}$	$\dot{y}$	$\ddot{x}$	$\ddot{y}$
1	1.00	0.00	0.00	0.00	0.00	0.00
2	1.40	-0.06	0.06	0.40	-0.40	0.06
3	1.56	0.52	2.58	-0.31	65.05	-30.03
4	3.08	1.00	2.55	-0.21	59.18	-11.45
5	2.04	0.40	2.58	-0.28	66.48	-24.16
6	2.00	0.00	0.00	0.00	0.00	0.00
7	3.00	0.00	0.00	0.00	0.00	0.00

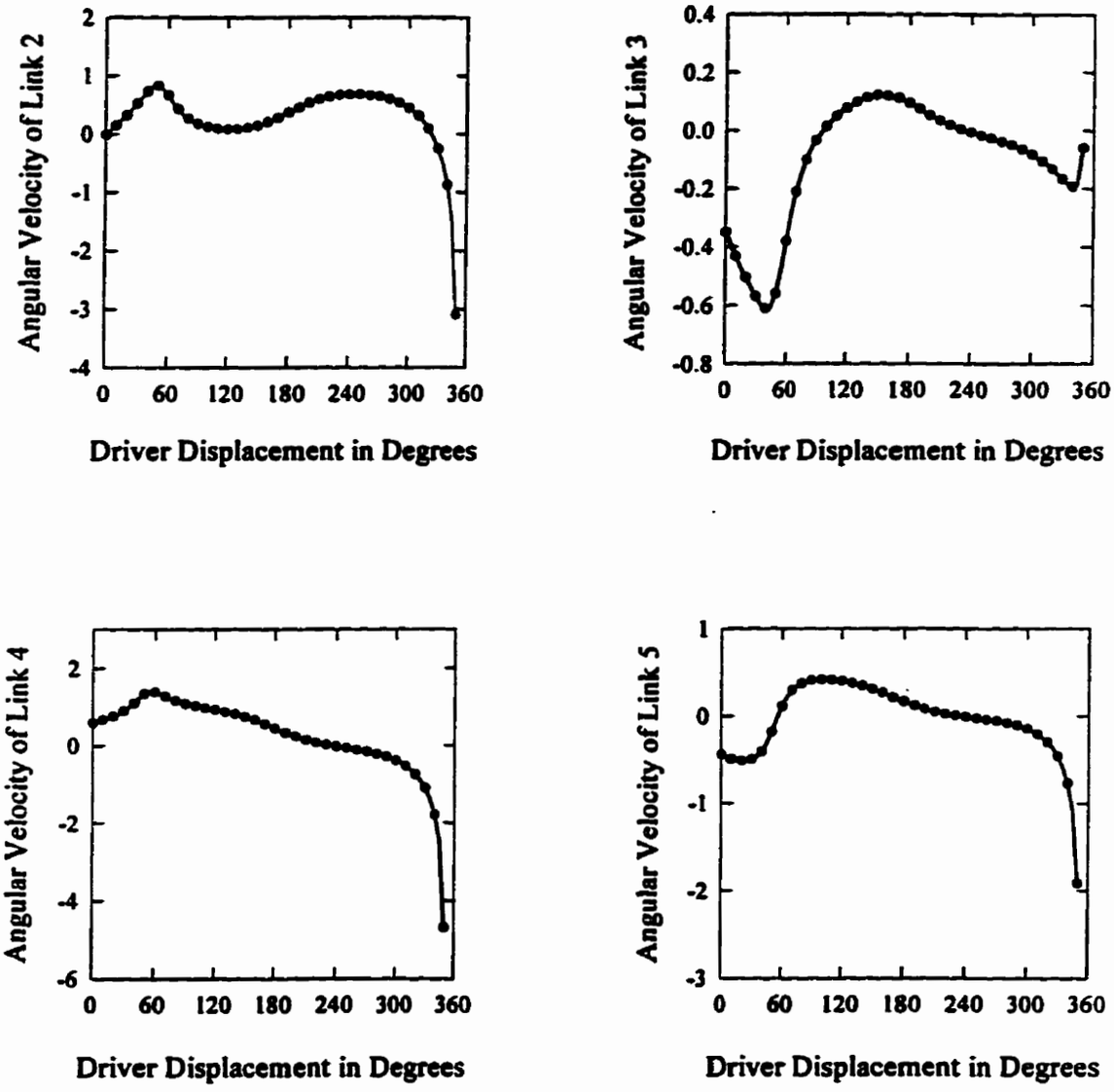

Figure 2.10: Comparison of angular velocities computed by two different methods of analysis (—— **NDPLAn,** ••• **KPLAn**).

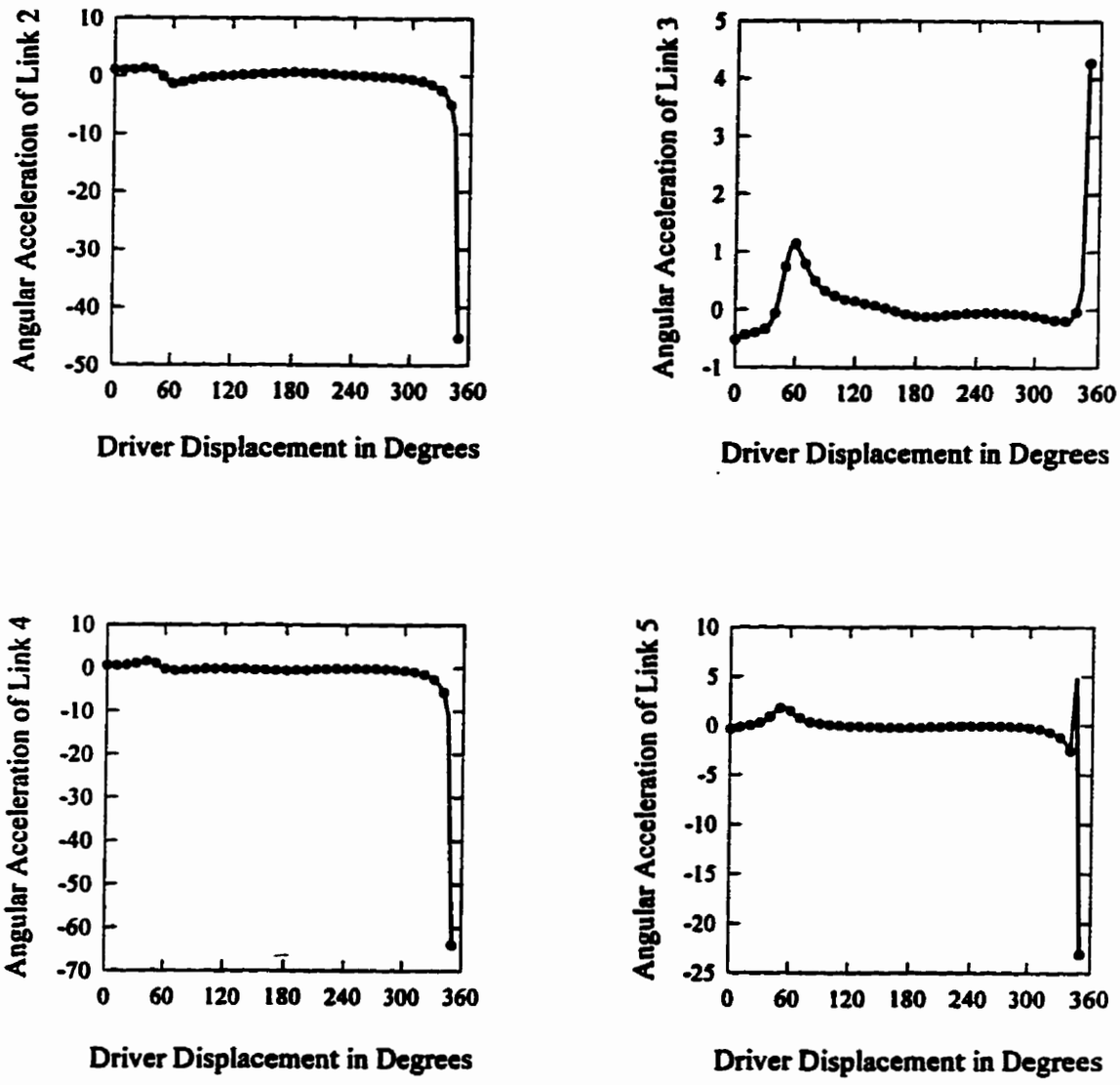

Figure 2.11: Comparison of angular accelerations computed by two different methods of analysis (—— **NDPLAn,** ••• **KPLAn**).

2.7.2 Example 2: a 22-link mechanism

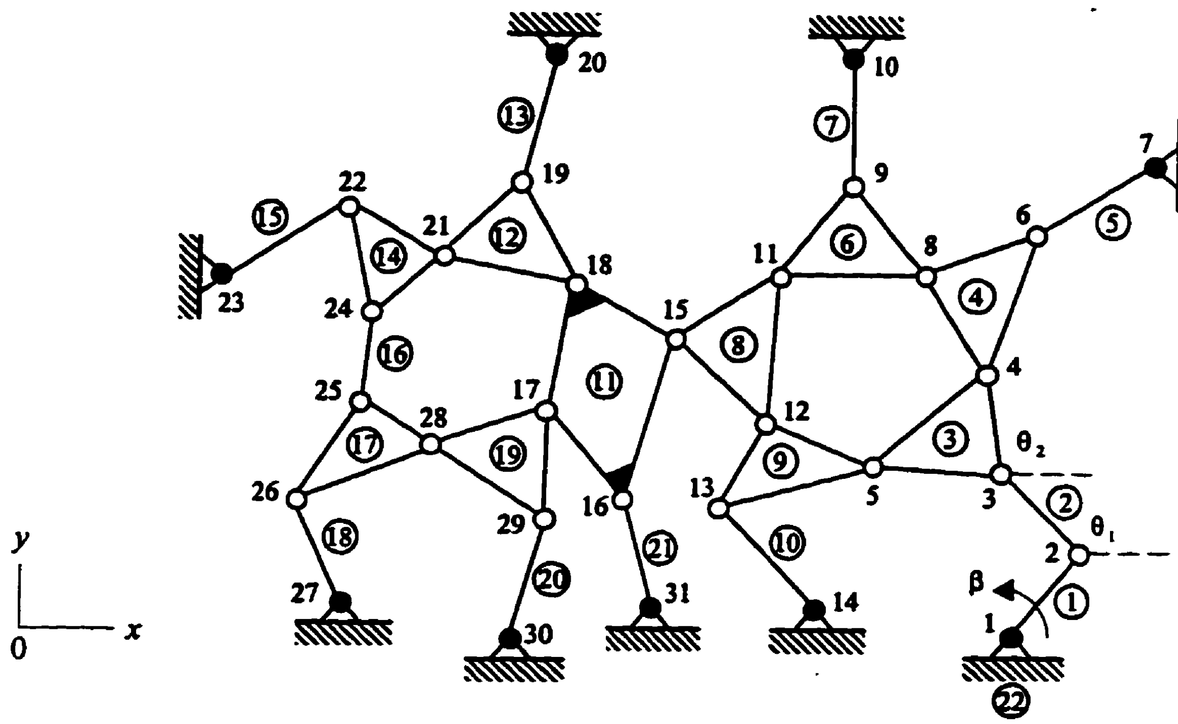

MN MATRIX

1 1 0 0 0 0 0 0 0 0 0 0 0 0 0 0 0 0 0 0 0 0 0 0 0 0 0 0 0 0 0
0 1 1 0 0 0 0 0 0 0 0 0 0 0 0 0 0 0 0 0 0 0 0 0 0 0 0 0 0 0 0
0 0 1 1 1 0 0 0 0 0 0 0 0 0 0 0 0 0 0 0 0 0 0 0 0 0 0 0 0 0 0
0 0 0 1 0 1 0 1 0 0 0 0 0 0 0 0 0 0 0 0 0 0 0 0 0 0 0 0 0 0 0
0 0 0 0 0 1 1 0 0 0 0 0 0 0 0 0 0 0 0 0 0 0 0 0 0 0 0 0 0 0 0
0 0 0 0 0 0 0 1 1 0 1 0 0 0 0 0 0 0 0 0 0 0 0 0 0 0 0 0 0 0 0
0 0 0 0 0 0 0 0 1 1 0 0 0 0 0 0 0 0 0 0 0 0 0 0 0 0 0 0 0 0 0
0 0 0 0 0 0 0 0 0 0 1 1 0 0 1 0 0 0 0 0 0 0 0 0 0 0 0 0 0 0 0
0 0 0 0 0 0 0 0 0 0 0 1 1 0 0 0 0 0 0 0 0 0 0 0 0 0 0 0 0 0 0
0 0 0 0 0 0 0 0 0 0 0 0 1 1 0 0 0 0 0 0 0 0 0 0 0 0 0 0 0 0 0
0 0 0 0 0 0 0 0 0 0 0 0 0 0 1 1 1 1 0 0 0 0 0 0 0 0 0 0 0 0 0
0 0 0 0 0 0 0 0 0 0 0 0 0 0 0 0 0 1 1 0 1 0 0 0 0 0 0 0 0 0 0
0 0 0 0 0 0 0 0 0 0 0 0 0 0 0 0 0 0 1 1 0 0 0 0 0 0 0 0 0 0 0
0 0 0 0 0 0 0 0 0 0 0 0 0 0 0 0 0 0 0 0 1 1 0 1 0 0 0 0 0 0 0
0 0 0 0 0 0 0 0 0 0 0 0 0 0 0 0 0 0 0 0 0 1 1 0 0 0 0 0 0 0 0
0 0 0 0 0 0 0 0 0 0 0 0 0 0 0 0 0 0 0 0 0 0 0 1 1 0 0 0 0 0 0
0 0 0 0 0 0 0 0 0 0 0 0 0 0 0 0 0 0 0 0 0 0 0 0 1 1 0 1 0 0 0
0 0 0 0 0 0 0 0 0 0 0 0 0 0 0 0 0 0 0 0 0 0 0 0 0 1 1 0 0 0 0
0 0 0 0 0 0 0 0 0 0 0 0 0 0 0 0 0 0 0 0 0 0 0 0 0 0 0 1 1 0 0
0 0 0 0 0 0 0 0 0 0 0 0 0 0 0 0 0 0 0 0 0 0 0 0 0 0 0 0 1 1 0
0 0 0 0 0 0 0 0 0 0 0 0 0 0 0 1 0 0 0 0 0 0 0 0 0 0 0 0 0 0 1
1 0 0 0 0 0 1 0 0 1 0 0 0 1 0 0 0 0 0 1 0 0 1 0 0 0 1 0 0 1 1

Figure 2.12: A 22-link non-dyad mechanism with its MN incidence matrix.

It is not immediately obvious if the linkage can rotate at all, however, using **NDPLAn**, we managed to show that it can turn from a minimum value of $\beta = 44.8^0$ to a maximum value of $\beta = 57.2^0$. A constant rate of $\omega = 1$ is imposed on the linkage driver ①. As in the previous

Table 2.5: The 22-link mechanism - joint positions and link lengths.

Known Joint Positions

Joint	x	y	Joint	x	y	Joint	x	y
1	180.0	0.0	14	140.0	10.0	27	30.0	5.0
7	210.0	100.0	20	90.0	125.0	30	80.0	0.0
10	150.0	125.0	23	15.0	90.0	31	110.0	10.0

Link Number and Link Lengths

①: L_{1-2}	28.28	⑥: L_{9-11}	25.00	⑪ : L_{15-18}	25.50	⑮ : L_{22-23}	26.93
②: L_{2-3}	25.00	⑦: L_{9-10}	25.00	⑪ : L_{16-17}	25.00	⑯ : L_{24-25}	20.62
③: L_{3-4}	25.50	⑧: L_{11-12}	30.42	⑪ : L_{16-18}	42.72	⑰ : L_{25-26}	25.00
③: L_{3-5}	25.50	⑧: L_{11-15}	22.36	⑪ : L_{17-18}	25.50	⑰ : L_{25-28}	25.00
③: L_{4-5}	28.28	⑧: L_{12-15}	25.00	⑫ : L_{18-19}	26.93	⑰ : L_{26-28}	35.36
④: L_{4-6}	26.93	⑨: L_{5-12}	26.93	⑫ : L_{18-21}	31.62	⑱ : L_{26-27}	25.50
④: L_{4-8}	25.00	⑨: L_{5-13}	36.40	⑫ : L_{19-21}	25.00	⑲ : L_{17-28}	29.15
④: L_{6-8}	25.50	⑨: L_{12-13}	22.36	⑬ : L_{20-19}	26.93	⑲ : L_{17-29}	25.50
⑤: L_{6-7}	29.15	⑩ : L_{13-14}	28.28	⑭ : L_{21-22}	25.00	⑲ : L_{28-29}	31.62
⑥: L_{8-9}	22.36	⑪ : L_{15-16}	36.40	⑭ : L_{21-24}	21.21	⑳ : L_{29-30}	26.93
⑥: L_{8-11}	25.00	⑪ : L_{15-17}	36.06	⑭ : L_{22-24}	30.41	㉑ : L_{16-31}	25.50

example, the tolerance is set at 10^{-4}. Once again, to transform the non-dyad mechanism into series of dyad mechanisms, the program automatically selects two links for disconnection and also, prescribes two dyad drivers. The results for displacements, velocities and accelerations at the starting and final positions are summarized in Tables 2.6 and 2.7 respectively. Also, the final converged values of the positions θ_1, θ_2 characterizing the two computer-generated dyad drivers and the RMS length errors of the two disconnected links are listed. Table 2.8 depicts angular velocities and accelerations for the various links, corresponding to the starting and final positions.

2.7 CONCLUSIONS

A novel approach for a computer-aided kinematic analysis of complex non-dyad planar mechanisms is developed here. The original non-dyad mechanism is transformed into a series of dyad mechanisms, to permit analysis. This is achieved by disconnecting appropriate links and prescribing dyad drivers to recover the disconnected links. An iterative technique is employed for this purpose. All these steps are transparent to the user as they are automatically generated by **NDPLAn**. The end result is, a powerful and yet simple to use program for the analysis of complex non-dyad planar mechanisms. To demonstrate and assess the accuracies, capabilities and versatilities of the program, two non-dyad mechanisms are solved. Excellent agreement with **KPLAn** is obtained. The method can be easily extended to handle kinematic error analysis, mechanism synthesis and mechanism optimization.

Table 2.6: The 22-link mechanism - kinematic results at the initial position.

Initial Position, $\beta = 44.8^0$ ($\theta_1 = 142.52^0$, $\theta_2 = 100.95^0$, RMS Length Error = 7.41×10^{-5})						
Joint	x	y	$\dot{x}$	$\dot{y}$	$\ddot{x}$	$\ddot{y}$
1	180.00	0.00	0.00	0.00	0.00	0.00
2	200.07	19.93	-19.93	20.07	-20.07	-19.93
3	180.23	35.14	-77.68	-55.25	9681.99	12042.37
4	175.39	60.17	-136.56	-66.65	21146.27	14117.43
5	155.26	40.30	-89.81	-113.99	12175.87	23422.88
6	184.76	85.41	86.31	-149.38	-13010.06	24557.92
7	210.00	100.00	0.00	0.00	0.00	0.00
8	159.89	79.79	36.65	70.17	-3623.39	-7931.86
9	150.33	100.00	-114.83	-1.50	17678.71	757.81
10	150.00	125.00	0.00	0.00	0.00	0.00
11	134.89	80.33	32.58	-117.14	-1662.02	17715.06
12	130.25	50.28	-83.88	-99.15	9410.65	16467.00
13	120.27	30.27	-95.76	-93.22	14976.55	13698.84
14	140.00	10.00	0.00	0.00	0.00	0.00
15	115.02	70.09	-7.09	-40.11	2384.08	10591.60
16	105.21	35.04	-89.33	-17.10	25037.38	4461.45
17	85.13	49.93	-54.40	30.02	15548.36	-8567.27
18	89.99	74.96	4.32	18.61	-613.22	-5569.98
19	80.05	99.98	-21.25	8.45	6763.44	-2669.66
20	90.00	125.00	0.00	0.00	0.00	0.00
21	60.01	85.03	-5.97	-12.02	2382.59	3243.83
22	40.00	100.01	1.06	-2.64	-13.55	33.03
23	15.00	90.00	0.00	0.00	0.00	0.00
24	45.03	70.01	-13.01	-4.99	4792.12	845.78
25	40.20	49.97	-85.23	12.41	23952.76	-3496.06
26	25.13	30.02	-54.71	-10.65	15573.30	2908.75
27	30.00	5.00	0.00	0.00	0.00	0.00
28	60.14	34.90	-62.17	42.94	17547.93	-11875.50
29	90.16	24.94	-67.32	27.42	18860.89	-7893.57
30	80.00	0.00	0.00	0.00	0.00	0.00
31	110.00	10.00	0.00	0.00	0.00	0.00

Table 2.7: The 22-link mechanism - kinematic results at final position.

Final Position, $\beta = 57.2^0$ ($\theta_1 = 135.61^0$, $\theta_2 = 113.37^0$, RMS Length Error = 6.67×10^{-5})						
Joint	x	y	$\dot{x}$	$\dot{y}$	$\ddot{x}$	$\ddot{y}$
1	180.00	0.00	0.00	0.00	0.00	0.00
2	195.32	23.78	-23.77	15.32	-15.32	-23.77
3	177.46	41.26	16.85	56.81	3977.14	3861.20
4	167.34	64.67	-45.12	30.03	-5010.25	-218.06
5	151.97	40.93	17.74	-10.69	4285.94	-6003.79
6	185.01	84.99	11.53	-19.20	6132.79	-10179.29
7	210.00	100.00	0.00	0.00	0.00	0.00
8	159.75	88.49	21.28	51.19	8269.44	3810.65
9	141.55	101.47	-12.13	4.36	4567.47	-1633.83
10	150.00	125.00	0.00	0.00	0.00	0.00
11	137.66	76.78	51.40	-5.63	11862.93	-2613.56
12	126.16	48.62	22.74	6.08	6029.07	-196.18
13	118.02	27.80	9.21	11.37	1342.98	1646.93
14	140.00	10.00	0.00	0.00	0.00	0.00
15	115.95	71.44	45.97	16.48	10777.55	1900.58
16	110.21	35.49	157.43	-1.31	32704.43	-1244.54
17	88.56	47.99	118.68	-68.45	25308.52	-14539.42
18	90.53	73.41	39.86	-62.34	9823.03	-13584.91
19	82.55	99.13	124.86	-35.96	29404.01	-7815.33
20	90.00	125.00	0.00	0.00	0.00	0.00
21	61.42	85.76	80.69	33.88	19504.87	8347.40
22	40.32	99.17	21.48	-59.33	5266.16	-14978.25
23	15.00	90.00	0.00	0.00	0.00	0.00
24	47.63	69.64	151.88	-27.04	37389.75	-6412.20
25	45.02	49.20	149.83	-26.78	30644.65	-5551.99
26	28.48	30.45	111.90	6.69	23477.23	909.21
27	30.00	5.00	0.00	0.00	0.00	0.00
28	63.77	32.65	116.36	-64.70	24183.44	-12719.39
29	93.90	23.06	114.91	-69.25	23478.77	-14930.65
30	80.00	0.00	0.00	0.00	0.00	0.00
31	110.00	10.00	0.00	0.00	0.00	0.00

Table 2.8: The 22-link mechanism - angular velocities and angular accelerations.

Link Number	$\beta = 44.8^0$		$\beta = 57.2^0$	
	Angular Vel.	Angular Accln.	Angular Vel.	Angular Accln.
①	1.00	0.00	1.00	0.00
②	3.80	-619.03	-2.32	-222.76
③	2.35	-456.94	2.65	387.06
④	-8.83	1324.18	-2.79	-555.04
⑤	5.92	-952.59	0.77	407.62
⑥	7.49	-1027.34	2.57	294.36
⑦	-4.59	707.48	-0.52	194.04
⑧	-3.87	366.06	-1.02	-207.63
⑨	-0.59	278.00	-0.65	-225.21
⑩	4.72	-717.25	-0.52	-75.13
⑪	-2.35	644.70	3.10	608.47
⑫	1.02	-294.38	-3.31	-758.05
⑬	-0.85	270.05	4.83	1129.71
⑭	-0.47	160.25	4.42	1092.95
⑮	-0.11	1.33	-2.34	-589.63
⑯	-3.60	952.90	-0.10	-329.84
⑰	1.53	-421.87	-2.02	-385.97
⑱	2.19	-621.38	-4.40	-921.34
⑲	-0.52	132.59	-0.15	-73.39
⑳	2.70	-759.31	-4.98	-1033.06
㉑	3.57	-997.43	-6.18	-1283.14

CHAPTER 3

Higher Order Mechanical Error Sensitivity Analysis and Optimum Dimensional Tolerancing of Planar Dyad Mechanisms

3.1 INTRODUCTION

The output performance of mechanisms depends on clearances in joints and tolerances on link lengths and orientations. Assigning excessive tolerances results in degraded output motions; on the other hand, prescribing extremely tight tolerances is undesirable as it leads to prohibitive manufacturing cost. A realistic approach is to allocate maximum possible tolerances to the various links while at the same time, maintaining mechanical errors to within acceptable limits. Several attempts to analyze mechanical errors and synthesize dimensional tolerance bands of input parameters for specified output motion have been reported (Svoboda 1948, Tuttle 1960, Garrett and Hall 1969, Kolhatkar and Yajnik 1970, Dhande and Chakraborty 1973, Dubowsky, Maatuk and Perreira 1974, Dhande and Chakraborty 1978, Baumgarten and Van Der Werff 1985, Mallik and Dhande 1987, Chatterjee and Mallik 1987, Fenton, Cleghorn and Fu 1989, Cleghorn , Fenton and Fu 1993).

An analytical approach for the error sensitivity analysis and the subsequent optimum dimensional tolerancing of planar dyad mechanisms are presented. It treats planar mechanisms as consisting of an assemblage of drivers and dyad groups. Sensitivity coefficients which relate the output motions to the input parameters via partial derivatives

(similar to the Jacobian matrices of Fenton et al. 1989) for drivers and dyad groups are analytically computed. Expressions for three types of sensitivity coefficients, namely, that of position, velocity and acceleration are presented. Also, a method for the direct identification of the most sensitive error combination from all the 2^m possibilities without any need for calculations is proposed. Thus, the synthesis of optimum dimensional tolerances can be performed with significantly reduced computational effort. The modular approach suggested here permits the creation of a general multi-purpose program for error sensitivity analysis and tolerance synthesis of complex planar dyad linkages. To the best of our knowledge, this is the first time such a procedure has been proposed for handling general planar dyad linkages. Although Fenton et al. (1989) and Cleghorn et al. (1993) have also proposed an analytical treatment for an error-based optimum tolerancing of planar mechanisms, their method is linkage-specific in the sense that it cannot automatically handle general planar linkages. We have also extended the concept to accommodate planar *non*-dyad mechanisms and thereby, cover an even wider category of planar linkages. The method involves a new analytical approach for computing the sensitivity coefficients and the use of disconnected links for the kinematics. The details are described in *Chapter* 4.

3.2 THEORY OF HIGHER-ORDER ERROR SENSITIVITY ANALYSIS

The output variable U describing the displacement of a general linkage characterized by m-input variables θ_j $(j=1, ..., m)$ and n-dimensional parameters q_i $(i=1, ..., n)$ can be written as,

$$U = U(\theta_1, ..., \theta_j, ..., \theta_m, q_1, ..., q_i, ..., q_n). \tag{3.1}$$

Assuming the input variables are prescribed exactly, the output position, velocity and

acceleration errors due to dimensional errors in the linkage can be approximated by the first order terms of a Taylor series expansion as follows,

$$\Delta U = \sum_{i=1}^{n} \frac{\partial U}{\partial q_i} \Delta q_i = \sum_{i=1}^{n} C_{p_i} \Delta q_i , \tag{3.2}$$

$$\Delta \dot{U} = \frac{d(\Delta U)}{dt} = \sum_{i=1}^{n} \left[\sum_{j=1}^{m} \frac{\partial^2 U}{\partial \theta_j \partial q_i} \dot{\theta}_j \right] \Delta q_i = \sum_{i=1}^{n} C_{v_i} \Delta q_i , \tag{3.3}$$

$$\Delta \ddot{U} = \frac{d(\Delta \dot{U})}{dt} = \sum_{i=1}^{n} \left[\sum_{k=1}^{m} \sum_{j=1}^{m} \frac{\partial^3 U}{\partial \theta_j \partial \theta_k \partial q_i} \dot{\theta}_j \dot{\theta}_k + \sum_{j=1}^{m} \frac{\partial^2 U}{\partial \theta_j \partial q_i} \ddot{\theta}_j \right] \Delta q_i = \sum_{i=1}^{n} C_{a_i} \Delta q_i , \tag{3.4}$$

where C_{p_i}, C_{v_i} and C_{a_i} are called respectively the position, velocity and acceleration sensitivity coefficients corresponding to the dimensional error Δq_i. Analytical expressions of the sensitivity coefficients for the RR and PR drivers, the five basic dyad mechanisms first identified in *Table* 2.2 and the various dyad groups are not difficult to obtain and will be presented next. Note that the term dyad group as used here comprises a driver link and at least one of the 5 basic dyad mechanisms. Using this approach, a planar dyad linkage can be represented by a series of the distinct dyad groups and analyzed as such for the mechanical dimensional tolerances.

3.2.1 Determination of the Sensitivity Coefficients for the RR and PR Driver Links

The sensitivity coefficients C_{p_i}, C_{v_i} and C_{a_i} for the RR and PR drivers can be readily generated from geometrical considerations and the results are summarized in *Table* 3.1.

Table 3.1: Sensitivity coefficients for the RR and PR driver links.

Dimensional Error Δq_i	Sensitivity Coefficients $C_{p_i}, C_{v_i}, C_{a_i}$	RR Driver 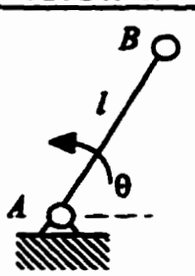	PR Driver 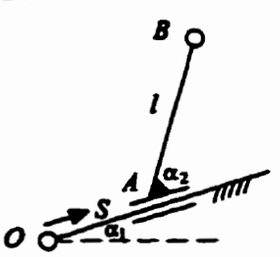
Δl	$C_{pl}^{(x)} = \partial x_B / \partial l$	$\cos\theta$	$\cos(\alpha_1 + \alpha_2)$
	$C_{pl}^{(y)} = \partial y_B / \partial l$	$\sin\theta$	$\sin(\alpha_1 + \alpha_2)$
	$C_{vl}^{(x)} = \partial \dot{x}_B / \partial l$	$-\sin\theta \cdot \dot{\theta}$	0
	$C_{vl}^{(y)} = \partial \dot{y}_B / \partial l$	$\cos\theta \cdot \dot{\theta}$	0
	$C_{al}^{(x)} = \partial \ddot{x}_B / \partial l$	$-\cos\theta \cdot \dot{\theta}^2 - \sin\theta \cdot \ddot{\theta}$	0
	$C_{al}^{(y)} = \partial \ddot{y}_B / \partial l$	$-\sin\theta \cdot \dot{\theta}^2 + \cos\theta \cdot \ddot{\theta}$	0
Δx_A	$C_{px_A}^{(x)} = \partial x_B / \partial x_A$	1	N.A.
	$C_{px_A}^{(y)} = \partial y_B / \partial x_A$	0	N.A.
	$C_{vx_A}^{(x)} = \partial \dot{x}_B / \partial x_A$	0	N.A.
	$C_{vx_A}^{(y)} = \partial \dot{y}_B / \partial x_A$	0	N.A.
	$C_{ax_A}^{(x)} = \partial \ddot{x}_B / \partial x_A$	0	N.A.
	$C_{ax_A}^{(y)} = \partial \ddot{y}_B / \partial x_A$	0	N.A.
Δy_A	$C_{py_A}^{(x)} = \partial x_B / \partial y_A$	0	N.A.
	$C_{py_A}^{(y)} = \partial y_B / \partial y_A$	1	N.A.
	$C_{vy_A}^{(x)} = \partial \dot{x}_B / \partial y_A$	0	N.A.
	$C_{vy_A}^{(y)} = \partial \dot{y}_B / \partial y_A$	0	N.A.
	$C_{ay_A}^{(x)} = \partial \ddot{x}_B / \partial y_A$	0	N.A.
	$C_{ay_A}^{(y)} = \partial \ddot{y}_B / \partial y_A$	0	N.A.
Δx_O	$C_{px_O}^{(x)} = \partial x_B / \partial x_O$	N.A.	1
	$C_{px_O}^{(y)} = \partial y_B / \partial x_O$	N.A.	0
	$C_{vx_O}^{(x)} = \partial \dot{x}_B / \partial x_O$	N.A.	0
	$C_{vx_O}^{(y)} = \partial \dot{y}_B / \partial x_O$	N.A.	0

	$C^{(x)}_{ax_O} = \partial \ddot{x}_B / \partial x_O$	N.A.	0
	$C^{(y)}_{ax_O} = \partial \ddot{y}_B / \partial x_O$	N.A.	0
Δy_O	$C^{(x)}_{py_O} = \partial x_B / \partial y_O$	N.A.	0
	$C^{(y)}_{py_O} = \partial y_B / \partial y_O$	N.A.	1
	$C^{(x)}_{vy_O} = \partial \dot{x}_B / \partial y_O$	N.A.	0
	$C^{(y)}_{vy_O} = \partial \dot{y}_B / \partial y_O$	N.A.	0
	$C^{(x)}_{ay_O} = \partial \ddot{x}_B / \partial y_O$	N.A.	0
	$C^{(y)}_{ay_O} = \partial \ddot{y}_B / \partial y_O$	N.A.	0
$\Delta\alpha_1$	$C^{(x)}_{p\alpha_1} = \partial x_B / \partial \alpha_1$	N.A.	$-s\sin\alpha_1 - l\sin(\alpha_1+\alpha_2)$
	$C^{(y)}_{p\alpha_1} = \partial y_B / \partial \alpha_1$	N.A.	$s\cos\alpha_1 + l\cos(\alpha_1+\alpha_2)$
	$C^{(x)}_{v\alpha_1} = \partial \dot{x}_B / \partial \alpha_1$	N.A.	$-\dot{s}\sin\alpha_1$
	$C^{(y)}_{v\alpha_1} = \partial \dot{y}_B / \partial \alpha_1$	N.A.	$\dot{s}\cos\alpha_1$
	$C^{(x)}_{a\alpha_1} = \partial \ddot{x}_B / \partial \alpha_1$	N.A.	$-\ddot{s}\sin\alpha_1$
	$C^{(y)}_{a\alpha_1} = \partial \ddot{y}_B / \partial \alpha_1$	N.A.	$\ddot{s}\cos\alpha_1$
$\Delta\alpha_2$	$C^{(x)}_{p\alpha_2} = \partial x_B / \partial \alpha_2$	N.A.	$-l\sin(\alpha_1+\alpha_2)$
	$C^{(y)}_{p\alpha_2} = \partial y_B / \partial \alpha_2$	N.A.	$l\cos(\alpha_1+\alpha_2)$
	$C^{(x)}_{v\alpha_2} = \partial \dot{x}_B / \partial \alpha_2$	N.A.	0
	$C^{(y)}_{v\alpha_2} = \partial \dot{y}_B / \partial \alpha_2$	N.A.	0
	$C^{(x)}_{a\alpha_2} = \partial \ddot{x}_B / \partial \alpha_2$	N.A.	0
	$C^{(y)}_{a\alpha_2} = \partial \ddot{y}_B / \partial \alpha_2$	N.A.	0

3.2.2 Determination of the Sensitivity Coefficients for the Five Dyad Mechanisms

Table 3.2 lists the five basic dyad mechanisms that can be generated from planar linkages with lower pairs, together with their dimensional error parameters. Once again, the sensitivity coefficients C_{p_i}, C_{v_i} and C_{a_i} can be derived in a similar fashion as for the driver links, using geometrical considerations. For brevity, only the results for the RRR dyad are given here.

Table 3.2: **Five basic dyad mechanisms together with their dimensional error parameters.**

RRR Dyad	RRP Dyad	RPR Dyad	PRP Dyad	RPP Dyad
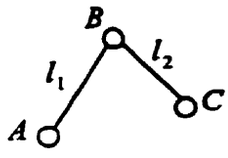	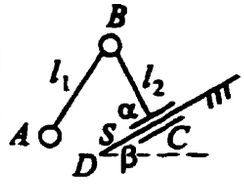	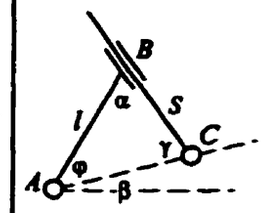	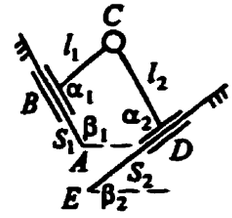	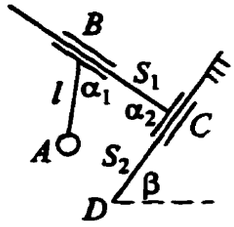
$l_1, l_2,$ x_A, y_A, x_C, y_C	$l_1, l_2, \alpha, \beta,$ x_A, y_A, x_D, y_D	$l, \alpha,$ x_A, y_A, x_C, y_C	$l_1, l_2, \alpha_1, \alpha_2, \beta_1, \beta_2,$ x_A, y_A, x_E, y_E	$l, \alpha_1, \alpha_2, \beta,$ x_A, y_A, x_D, y_D

The results for the dimensional errors of the RRR dyad are listed as follows.

Dimensional Error Δl_1

$$
\begin{aligned}
C_{pl}^{(x)} &= \frac{\partial x_B}{\partial l_1} = \frac{1}{D}\begin{vmatrix} l_1 & (y_B - y_A) \\ 0 & (y_B - y_C) \end{vmatrix}, \quad C_{pl}^{(y)} = \frac{\partial y_B}{\partial l_1} = \frac{1}{D}\begin{vmatrix} (x_B - x_A) & l_1 \\ (x_B - x_C) & 0 \end{vmatrix}, \\
C_{vl}^{(x)} &= \frac{\partial \dot{x}_B}{\partial l_1} = \frac{1}{D}\begin{vmatrix} M_1 & (y_B - y_A) \\ M_2 & (y_B - y_C) \end{vmatrix}, \quad C_{vl}^{(y)} = \frac{\partial \dot{x}_B}{\partial l_1} = \frac{1}{D}\begin{vmatrix} (x_B - x_A) & M_1 \\ (x_B - x_C) & M_2 \end{vmatrix}, \\
C_{al}^{(x)} &= \frac{\partial \ddot{x}_B}{\partial l_1} = \frac{1}{D}\begin{vmatrix} N_1 & (y_B - y_A) \\ N_2 & (y_B - y_C) \end{vmatrix}, \quad C_{al}^{(y)} = \frac{\partial \ddot{y}_B}{\partial l_1} = \frac{1}{D}\begin{vmatrix} (x_B - x_A) & N_1 \\ (x_B - x_C) & N_2 \end{vmatrix},
\end{aligned}
\tag{3.5}
$$

where

$$
D = \begin{vmatrix} (x_B - x_A) & (y_B - y_A) \\ (x_B - x_C) & (y_B - y_C) \end{vmatrix},
$$

$$
\begin{aligned}
M_1 &= (\dot{x}_A - \dot{x}_B)\partial x_B/\partial l_1 + (\dot{y}_A - \dot{y}_B)\partial y_B/\partial l_1, \\
M_2 &= (\dot{x}_C - \dot{x}_B)\partial x_B/\partial l_1 + (\dot{y}_C - \dot{y}_B)\partial y_B/\partial l_1, \\
N_1 &= (\ddot{x}_A - \ddot{x}_B)\partial x_B/\partial l_1 + 2(\dot{x}_A - \dot{x}_B)\partial \dot{x}_B/\partial l_1 + (\ddot{y}_A - \ddot{y}_B)\partial y_B/\partial l_1 + 2(\dot{y}_A - \dot{y}_B)\partial \dot{y}_B/\partial l_1, \\
N_2 &= (\ddot{x}_C - \ddot{x}_B)\partial x_B/\partial l_1 + 2(\dot{x}_C - \dot{x}_B)\partial \dot{x}_B/\partial l_1 + (\ddot{y}_C - \ddot{y}_B)\partial y_B/\partial l_1 + 2(\dot{y}_C - \dot{y}_B)\partial \dot{y}_B/\partial l_1.
\end{aligned}
$$

The results for Δl_2 can be obtained simply by replacing l_1 with l_2.

Dimensional Error Δx_A

$$
\begin{aligned}
C_{px_A}^{(x)} &= \frac{\partial x_B}{\partial x_A} = \frac{1}{D}\begin{vmatrix}(x_B - x_A) & (y_B - y_A)\\ 0 & (y_B - y_C)\end{vmatrix}, & C_{px_A}^{(y)} &= \frac{\partial y_B}{\partial x_A} = \frac{1}{D}\begin{vmatrix}(x_B - x_A) & (x_B - x_A)\\ (x_B - x_C) & 0\end{vmatrix},\\
C_{vx_A}^{(x)} &= \frac{\partial \dot{x}_B}{\partial x_A} = \frac{1}{D}\begin{vmatrix}M_3 & (y_B - y_A)\\ M_4 & (y_B - y_C)\end{vmatrix}, & C_{vx_A}^{(y)} &= \frac{\partial \dot{x}_B}{\partial x_A} = \frac{1}{D}\begin{vmatrix}(x_B - x_A) & M_3\\ (x_B - x_C) & M_4\end{vmatrix},\\
C_{ax_A}^{(x)} &= \frac{\partial \ddot{x}_B}{\partial x_A} = \frac{1}{D}\begin{vmatrix}N_3 & (y_B - y_A)\\ N_4 & (y_B - y_C)\end{vmatrix}, & C_{ax_A}^{(y)} &= \frac{\partial \ddot{y}_B}{\partial x_A} = \frac{1}{D}\begin{vmatrix}(x_B - x_A) & N_3\\ (x_B - x_C) & N_4\end{vmatrix},
\end{aligned}
\tag{3.6}
$$

where

$$
\begin{aligned}
M_3 &= (\dot{x}_B - \dot{x}_A)(1 - \partial x_B/\partial x_A) + (\dot{y}_A - \dot{y}_B)\partial y_B/\partial x_A,\\
M_4 &= (\dot{x}_C - \dot{x}_B)\partial x_B/\partial x_A + (\dot{y}_C - \dot{y}_B)\partial y_B/\partial x_A,\\
N_3 &= (\ddot{x}_A - \ddot{x}_B)(1 - \partial x_B/\partial x_A) + 2(\dot{x}_A - \dot{x}_B)\partial \dot{x}_B/\partial x_A + (\ddot{y}_A - \ddot{y}_B)\partial y_B/\partial x_A + 2(\dot{y}_A - \dot{y}_B)\partial \dot{y}_B/\partial x_A,\\
N_4 &= (\ddot{x}_C - \ddot{x}_B)\partial x_B/\partial x_A + 2(\dot{x}_C - \dot{x}_B)\partial \dot{x}_B/\partial x_A + (\ddot{y}_C - \ddot{y}_B)\partial y_B/\partial x_A + 2(\dot{y}_C - \dot{y}_B)\partial \dot{y}_B/\partial x_A.
\end{aligned}
$$

Dimensional Error Δy_A

$$
\begin{aligned}
C_{py_A}^{(x)} &= \frac{\partial x_B}{\partial y_A} = \frac{1}{D}\begin{vmatrix}(y_B - y_A) & (y_B - y_A)\\ 0 & (y_B - y_C)\end{vmatrix}, & C_{py_A}^{(y)} &= \frac{\partial y_B}{\partial y_A} = \frac{1}{D}\begin{vmatrix}(x_B - x_A) & (y_B - y_A)\\ (x_B - x_C) & 0\end{vmatrix},\\
C_{vy_A}^{(x)} &= \frac{\partial \dot{x}_B}{\partial y_A} = \frac{1}{D}\begin{vmatrix}M_5 & (y_B - y_A)\\ M_6 & (y_B - y_C)\end{vmatrix}, & C_{vy_A}^{(y)} &= \frac{\partial \dot{x}_B}{\partial y_A} = \frac{1}{D}\begin{vmatrix}(x_B - x_A) & M_5\\ (x_B - x_C) & M_6\end{vmatrix},\\
C_{ay_A}^{(x)} &= \frac{\partial \ddot{x}_B}{\partial y_A} = \frac{1}{D}\begin{vmatrix}N_5 & (y_B - y_A)\\ N_6 & (y_B - y_C)\end{vmatrix}, & C_{ay_A}^{(y)} &= \frac{\partial \ddot{y}_B}{\partial y_A} = \frac{1}{D}\begin{vmatrix}(x_B - x_A) & N_5\\ (x_B - x_C) & N_6\end{vmatrix},
\end{aligned}
\tag{3.7}
$$

where

$$
\begin{aligned}
M_5 &= (\dot{x}_A - \dot{x}_B)\partial x_B/\partial y_A - (\dot{y}_A - \dot{y}_B)(1 - \partial y_B/\partial y_A),\\
M_6 &= (\dot{x}_C - \dot{x}_B)\partial x_B/\partial y_A + (\dot{y}_C - \dot{y}_B)\partial y_B/\partial y_A,\\
N_5 &= (\ddot{x}_A - \ddot{x}_B)\partial x_B/\partial y_A + 2(\dot{x}_A - \dot{x}_B)\partial \dot{x}_B/\partial y_A - (\ddot{y}_A - \ddot{y}_B)(1 - \partial y_B/\partial y_A) + 2(\dot{y}_A - \dot{y}_B)\partial \dot{y}_B/\partial y_A,\\
N_6 &= (\ddot{x}_C - \ddot{x}_B)\partial x_B/\partial y_A + 2(\dot{x}_C - \dot{x}_B)\partial \dot{x}_B/\partial y_A + (\ddot{y}_C - \ddot{y}_B)\partial y_B/\partial y_A + 2(\dot{y}_C - \dot{y}_B)\partial \dot{y}_B/\partial y_A.
\end{aligned}
$$

Expressions for dimensional errors $\Delta x_C, \Delta y_C$, etc. are similar to those for $\Delta x_A, \Delta y_A$.

3.2.3 Determination of the Sensitivity Coefficients for the Dyad Groups

Dyad groups consist of one or more driver links and some combinations of the basic dyad mechanisms. Thus, they form the *building blocks* for the construction of the actual planar dyad linkage. This concept of a dyad group is introduced here in order to validate the process of performing the error analysis of a planar dyad linkage by a systematic term-by-term assemblage of the individual error components of the driver links and the five basic dyad mechanisms. Specifically, it explains how the sensitivity coefficients of any points on the linkage with respect to a chosen input parameter can be computed from the individual sensitivity coefficients of the driver links and the basic dyad mechanisms . For brevity, only the R-dyad groups are discussed here. *Figure* 3.1 depicts the three most common R-dyad groups which would enable the construction of almost any R-planar dyad linkages.

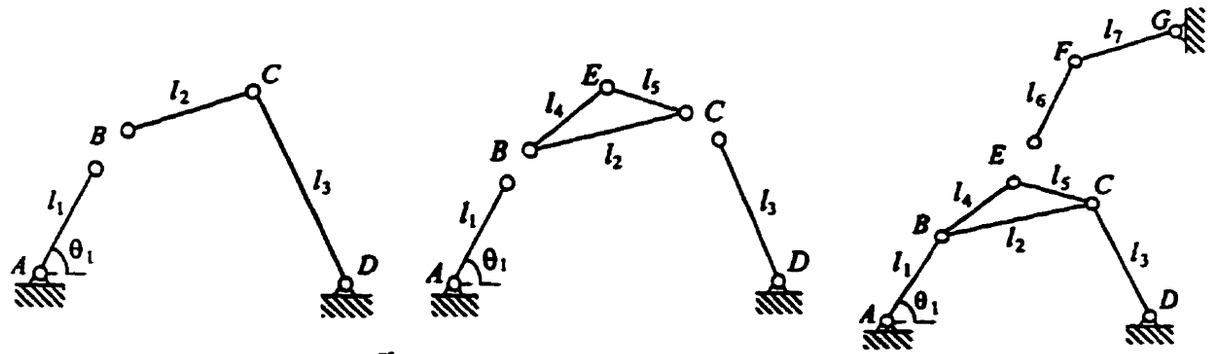

Figure 3.1: Three R-dyad groups.

In order to justify a systematic term-by-term summing of the individual sensitivity coefficients derived in the previous sections, it is necessary to show how the sensitivity coefficients of any point on a link with respect to a selected input parameter (e.g. l_1 of the driver link) is computed. For example, the following sensitivity coefficients are required:

Figure 3.1(a) -$\partial x_C/\partial l_1$; *Figure* 3.1(b)-$\partial x_E/\partial l_1$,$\partial x_E/\partial l_2$,$\partial x_E/\partial l_3$ and *Figure* 3.1(c)-$\partial x_F/\partial l_1$. To determine the first sensitivity coefficient $\partial x_C/\partial l_1$ for the dyad group sketched in *Figure* 3.1(a), the following equations apply:

$$\begin{gathered}\frac{\partial x_C}{\partial l_1}=\frac{\partial x_C}{\partial x_B}\frac{\partial x_B}{\partial l_1},\\ y_B = x_B \tan\theta_1,\\ (x_B-x_C)\left(1-\frac{\partial x_C}{\partial x_B}\right)+(y_B-y_C)\left(\frac{\partial y_B}{\partial x_B}-\frac{\partial y_C}{\partial x_B}\right)=0,\\ (x_D-x_C)\left(0-\frac{\partial x_C}{\partial x_B}\right)+(y_D-y_C)\left(0-\frac{\partial y_C}{\partial x_B}\right)=0.\end{gathered} \tag{3.8}$$

For the dyad group illustrated in *Figure* 3.1(b), the following equations for evaluating $\partial x_E/\partial l_1$ can be used:

$$\begin{gathered}\frac{\partial x_E}{\partial l_1}=\frac{\partial x_E}{\partial x_B}\frac{\partial x_B}{\partial l_1},\\ y_B = x_B \tan\theta_1,\\ (x_B-x_E)\left(1-\frac{\partial x_E}{\partial x_B}\right)+(y_B-y_E)\left(\frac{\partial y_B}{\partial x_B}-\frac{\partial y_E}{\partial x_B}\right)=0,\\ (x_C-x_E)\left(\frac{\partial x_C}{\partial x_B}-\frac{\partial x_E}{\partial x_B}\right)+(y_C-y_E)\left(\frac{\partial y_C}{\partial x_B}-\frac{\partial y_E}{\partial x_B}\right)=0.\end{gathered} \tag{3.9}$$

Note that in *Equation* (3.9), $\partial x_C/\partial x_B$,$\partial y_C/\partial x_B$ can be computed via *Equation* (3.8). Likewise, $\partial x_E/\partial l_2$,$\partial x_E/\partial l_3$ can be determined using an equation similar to *Equation* (3.9). Finally, the equations for evaluating $\partial x_F/\partial l_1$ for the dyad group shown in *Figure* 3.1(c) are listed as follows:

$$\begin{aligned}
\frac{\partial x_F}{\partial l_1} &= \frac{\partial x_F}{\partial x_E}\frac{\partial x_E}{\partial l_1}, \\
\frac{\partial y_E}{\partial x_E} &= \frac{\partial y_E}{\partial x_B}\frac{\partial x_B}{\partial x_E}, \\
(x_E - x_F)\left(1 - \frac{\partial x_F}{\partial x_E}\right) + (y_E - y_F)\left(\frac{\partial y_E}{\partial x_E} - \frac{\partial y_F}{\partial x_E}\right) &= 0, \\
(x_G - x_F)\left(0 - \frac{\partial x_F}{\partial x_E}\right) + (y_G - y_F)\left(0 - \frac{\partial y_F}{\partial x_E}\right) &= 0.
\end{aligned} \tag{3.10}$$

Once again, terms such as $\partial y_E/\partial x_B, \partial x_B/\partial x_E$ can be computed using *Equation* (3.9). All other sensitivity coefficients are either covered by the standard formulas for the driver links and the five basic dyad mechanisms (e.g. $\partial x_B/\partial l_1, \partial x_C/\partial l_2$), or can be easily deduced in a similar fashion as presented here (e.g. $\partial x_C/\partial x_A, \partial x_C/\partial y_A$). Using this approach, the sensitivity coefficients of any point on the planar dyad linkage can be determined by an appropriate combination of the individual sensitivity coefficients derived for the driver links, the basic dyad mechanisms and the dyad groups. The expressions for velocity and acceleration sensitivity coefficients can be derived by taking time derivatives of the position sensitivity coefficients. Angular quantities such as $\psi, \dot{\psi}, \ddot{\psi}$ can be readily computed using relationship $\tan\psi_{MN} = (y_M - y_N)/(x_M - x_N)$. Similar expressions can also be readily derived for the P-dyad groups and all combinations of R and P dyad groups.

3.3 ERROR SENSITIVITY ANALYSIS OF PLANAR DYAD MECHANISMS

Planar dyad mechanisms are modeled as consisting of an assemblage of drivers and dyad groups. This approach permits the handling of complex planar dyad linkages. In the computer implementation, both kinematic and error sensitivity analyses are performed simultaneously for the determination of positions, velocities, accelerations and sensitivity coefficients. Output errors corresponding to position, velocity and acceleration quantities, due to a single or any combinations of input dimensional errors, can then be easily obtained using *Equations* (3.2)-

(3.4). For convenience, these output errors are grouped into 2 types: $\Delta P, \Delta V, \Delta A$ for linear quantities and $\Delta\psi, \Delta\dot{\psi}, \Delta\ddot{\psi}$ for angular quantities. Their expressions are as follows,

$$\Delta P = \begin{Bmatrix} \Delta P_{1x} \\ \Delta P_{1y} \\ \vdots \\ \Delta P_{nx} \\ \Delta P_{ny} \end{Bmatrix} = \begin{bmatrix} c_{p_{1x,1}} & \cdots & c_{p_{1x,n}} \\ c_{p_{1y,1}} & & c_{p_{1y,n}} \\ \vdots & \ddots & \vdots \\ c_{p_{nx,1}} & & c_{p_{nx,n}} \\ c_{p_{ny,1}} & \cdots & c_{p_{ny,n}} \end{bmatrix} \begin{Bmatrix} \Delta q_1 \\ \Delta q_2 \\ \vdots \\ \Delta q_n \end{Bmatrix}, \tag{3.11}$$

$$\Delta V = \begin{Bmatrix} \Delta V_{1x} \\ \Delta V_{1y} \\ \vdots \\ \Delta V_{nx} \\ \Delta V_{ny} \end{Bmatrix} = \begin{bmatrix} c_{v_{1x,1}} & \cdots & c_{v_{1x,n}} \\ c_{v_{1y,1}} & & c_{v_{1y,n}} \\ \vdots & \ddots & \vdots \\ c_{v_{nx,1}} & & c_{v_{nx,n}} \\ c_{v_{ny,1}} & \cdots & c_{v_{ny,n}} \end{bmatrix} \begin{Bmatrix} \Delta q_1 \\ \Delta q_2 \\ \vdots \\ \Delta q_n \end{Bmatrix}, \tag{3.12}$$

$$\Delta A = \begin{Bmatrix} \Delta A_{1x} \\ \Delta A_{1y} \\ \vdots \\ \Delta A_{nx} \\ \Delta A_{ny} \end{Bmatrix} = \begin{bmatrix} c_{a_{1x,1}} & \cdots & c_{a_{1x,n}} \\ c_{a_{1y,1}} & & c_{a_{1y,n}} \\ \vdots & \ddots & \vdots \\ c_{a_{nx,1}} & & c_{a_{nx,n}} \\ c_{a_{ny,1}} & \cdots & c_{a_{ny,n}} \end{bmatrix} \begin{Bmatrix} \Delta q_1 \\ \Delta q_2 \\ \vdots \\ \Delta q_n \end{Bmatrix}, \tag{3.13}$$

$$\Delta\underline{\psi} = \begin{Bmatrix} \Delta\psi_1 \\ \vdots \\ \Delta\psi_n \end{Bmatrix} = \begin{bmatrix} c_{p_{1,1}} & \cdots & c_{p_{1,n}} \\ \vdots & \ddots & \vdots \\ c_{p_{n,1}} & \cdots & c_{p_{n,n}} \end{bmatrix} \begin{Bmatrix} \Delta q_1 \\ \vdots \\ \Delta q_n \end{Bmatrix}, \tag{3.14}$$

$$\Delta\dot{\psi} = \begin{Bmatrix} \Delta\dot{\psi}_1 \\ \vdots \\ \Delta\dot{\psi}_n \end{Bmatrix} = \begin{bmatrix} c_{v_{1,1}} & \cdots & c_{v_{1,n}} \\ \vdots & \ddots & \vdots \\ c_{v_{n,1}} & \cdots & c_{v_{n,n}} \end{bmatrix} \begin{Bmatrix} \Delta q_1 \\ \vdots \\ \Delta q_n \end{Bmatrix}, \tag{3.15}$$

$$\Delta\ddot{\psi} = \begin{Bmatrix} \Delta\ddot{\psi}_1 \\ \vdots \\ \Delta\ddot{\psi}_n \end{Bmatrix} = \begin{bmatrix} c_{a_{1,1}} & \cdots & c_{a_{1,n}} \\ \vdots & \ddots & \vdots \\ c_{a_{n,1}} & \cdots & c_{a_{n,n}} \end{bmatrix} \begin{Bmatrix} \Delta q_1 \\ \vdots \\ \Delta q_n \end{Bmatrix}. \tag{3.16}$$

3.4 SENSITIVITY COEFFICIENTS FOR A FOUR-BAR LINKAGE

To demonstrate and assess the accuracy of the procedure, a 4-bar linkage is analyzed. The linkage together with its nominal link dimensions are shown in *Figure* 3.2. Since it is intended to compare the sensitivity coefficients with those computed by Cleghorn et al. (1993), we have adopted their link dimensions for the 4-bar here. The results for the output angular displacement sensitivity coefficient $C_{pi} = \partial\theta_4/\partial l_i;\ i = 1,\cdots 4$, as the linkage rotates one complete revolution are plotted in *Figure* 3.3(a). As shown, excellent agreement with Cleghorn et al. is seen. The output angular velocity and acceleration sensitivity coefficients as defined by $C_{vi} = \partial^2\theta_4/(\partial t\partial l_i)\dot{\theta}_2, C_{ai} = \partial^3\theta_4/(\partial t^2\partial l_i)\dot{\theta}_2^2 + \partial^2\theta_4/(\partial t\partial l_i)\ddot{\theta}_2;\ i = 1,\cdots 4$, are also

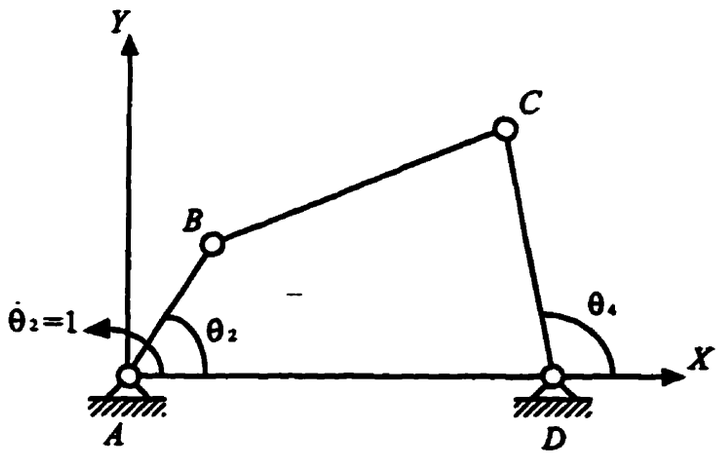

Nominal Dimensions

$l_1 = L_{AD} = 1.00000$
$l_2 = L_{AB} = 0.40000$
$l_3 = L_{BC} = 1.20000$
$l_4 = L_{CD} = 1.03923$

Figure 3.2: A four-bar linkage.

plotted in *Figures* 3.3(b) and (c) respectively, for the 360° rotation. However, since these higher-order quantities were not computed in Cleghorn et al., no comparisons are given for

them. As an additional indication of the correctness of the method we note the following observations. From the superimposed position, velocity and acceleration graphs, we see that extremum positions for C_{pi} are attained when C_{vi} is exactly zero. Likewise, extremum C_{vi} is reached precisely at locations of zero C_{ai}.

As a final check of the proposed technique, the following test is carried out. Once again, we use the link length errors $\Delta l_1 = +0.025, \Delta l_2 = +0.010, \Delta l_3 = +0.030, \Delta l_4 = +0.026$ taken from Cleghorn et al. (1993). Note that for the purpose of performing this test, we assumed only positive errors. The test involves two independent steps. In the first step, the method of virtual velocity is used to calculate the kinematic sensitivity coefficients based on the nominal dimensions of the mechanism and the prescribed dimensional error. From these coefficients, the output position, velocity and acceleration error bands of joint C (or any other point for that matter) are computed using *Equations* (3.11), (3.12) and (3.13). In the second step, we employ the kinematic analysis program **NDPLAn** (in *Chapter* 2) to calculate the position, velocity and acceleration values of joint C directly based on the *actual* (i.e. nominal plus error) link dimensions as input parameters. The results of these two steps are then compared to see if good agreement between them is obtained. *Figure* 3.4 (a), (b) and (c) depicts the position, velocity and acceleration of joint C, respectively. Observe that the results obtained by the two independent approaches agree extremely well, and thus, confirm the accuracy of the proposed method for computing the kinematic sensitivity coefficients.

3.5 SYNTHESIS FOR OPTIMUM DIMENSIONAL TOLERANCES

In design situations, it is common to choose tolerance bands for input parameters based on specified output error limits. Introducing the following expression for notational compactness $\langle \Delta x, \Delta y, \Delta \dot{x}, \Delta \dot{y}, \Delta \ddot{x}, \Delta \ddot{y}, \Delta \psi, \Delta \dot{\psi}, \Delta \ddot{\psi} \rangle^T = \langle \Delta W_1, \Delta W_2, \cdots, \Delta W_8, \Delta W_9, \rangle^T$ this practice is described by

$$\left|(\Delta W_i)_{\max}\right| \geq \left|(\Delta W_i^c)_{\max}\right| = \left(\left|C_{i1}\Delta q_1 + C_{i2}\Delta q_2 + \cdots + C_{in}\Delta q_n\right|\right)_{\max}; \; i = 1,2,\cdots,9; \; n = n_1 + n_2, \quad (3.17)$$

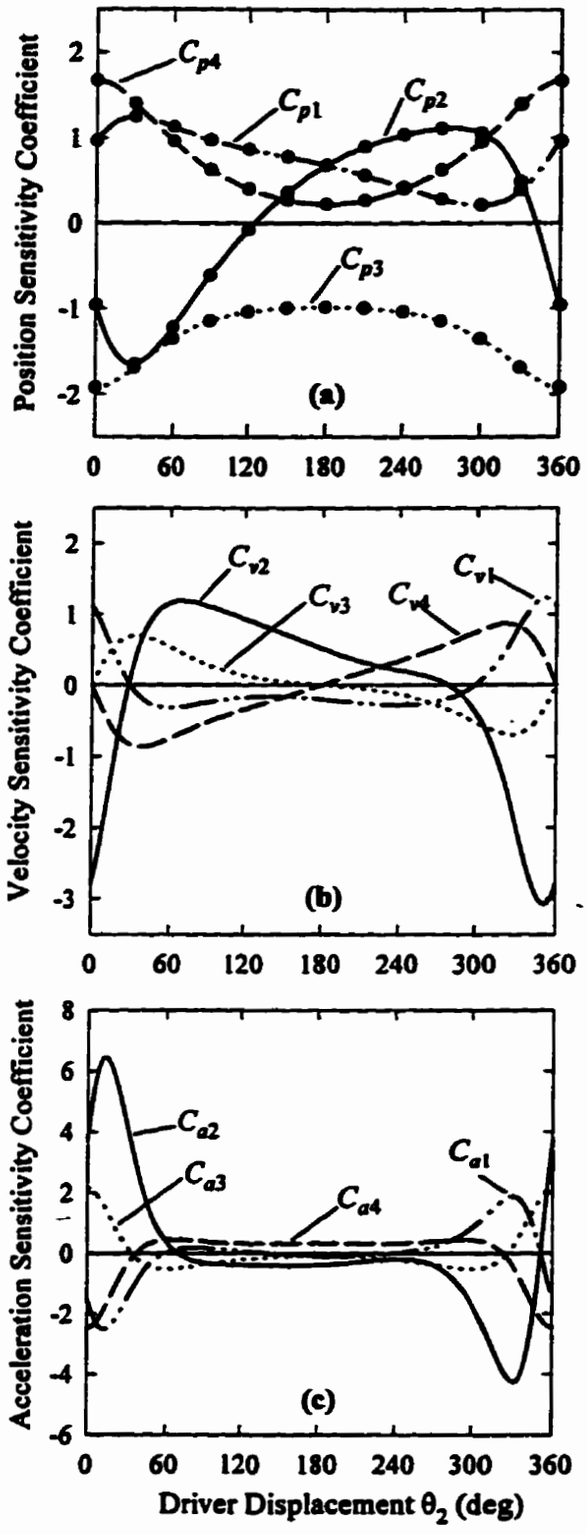

Figure 3.3: Angular displacement, velocity and acceleration sensitivity coefficients for a 4-bar linkage (• •• Cleghorn et al. 1993).

where $(\Delta W_i)_{max}$ is the maximum allowable output error and $(\Delta W_i^c)_{max}$ is the maximum output error for a complete cycle of motion as calculated by *Equations* (3.2)-(3.4). Also, Δq_k is the binary tolerance band corresponding to the input parameter q_k, C_{ik} is the sensitivity coefficient, and n_1, n_2 refer respectively to the number of linear and angular dimensions. Since there are $n\,(=n_1+n_2)$ tolerance bands in each of the ith inequality in *Equation* (3.17), it is necessary to reduce the number of unknown Δq_k to obtain solutions. To achieve this reduction, we adopt the standard practice (see Fenton et al., 1989) of grouping tolerance bands of similar types and then, prescribe within each group, tolerance values that are proportional to a suitably selected error parameter. Assuming only linear and angular quantities, the maximum input error can be computed from

$$\Delta q_i = \begin{cases} k_i \Delta l_0; & i = 1,2,\cdots,n_1 \\ k_i \Delta \alpha_0; & i = (n_1+1),\cdots,n \end{cases}; \tag{3.18}$$

where k_i is a known weighting factor, usually prescribed in proportion to the nominal values of the linear and angular dimensions. For example, for a four-bar linkage with link lengths l_1, l_2, l_3, l_4, the weighting factors could be $k_1 = 1, k_2 = l_2/l_1, k_3 = l_3/l_1, k_4 = l_4/l_1$. Note that in our formulation, Δq_i pertains not only to position, but also to velocity and acceleration, and it is assumed that they are all expressible into the form given by *Equation* (3.18), each with its own distinct $(\Delta l_0, \Delta \alpha_0)$ pair. Substituting *Equation* (3.18) into *Equation* (3.17) yields an implicit inequality for solving the $(\Delta l_0, \Delta \alpha_0)$ pair. That is,

$$\begin{aligned} \left|(\Delta W_i)_{max}\right| \geq \left|(\Delta W_i^c)_{max}\right| &= \left|\left(C_{i1}k_1 + C_{i2}k_2 + \cdots + C_{in_1}k_{n_1}\right)_{max}\right|(\Delta l_0) \\ &+ \left|\left(C_{i(n_1+1)}k_{(n_1+1)} + C_{i(n_1+2)}k_{(n_1+2)} + \cdots + C_{in}k_n\right)_{max}\right|(\Delta \alpha_0); \quad i = 1,2,\cdots,9. \end{aligned} \tag{3.19}$$

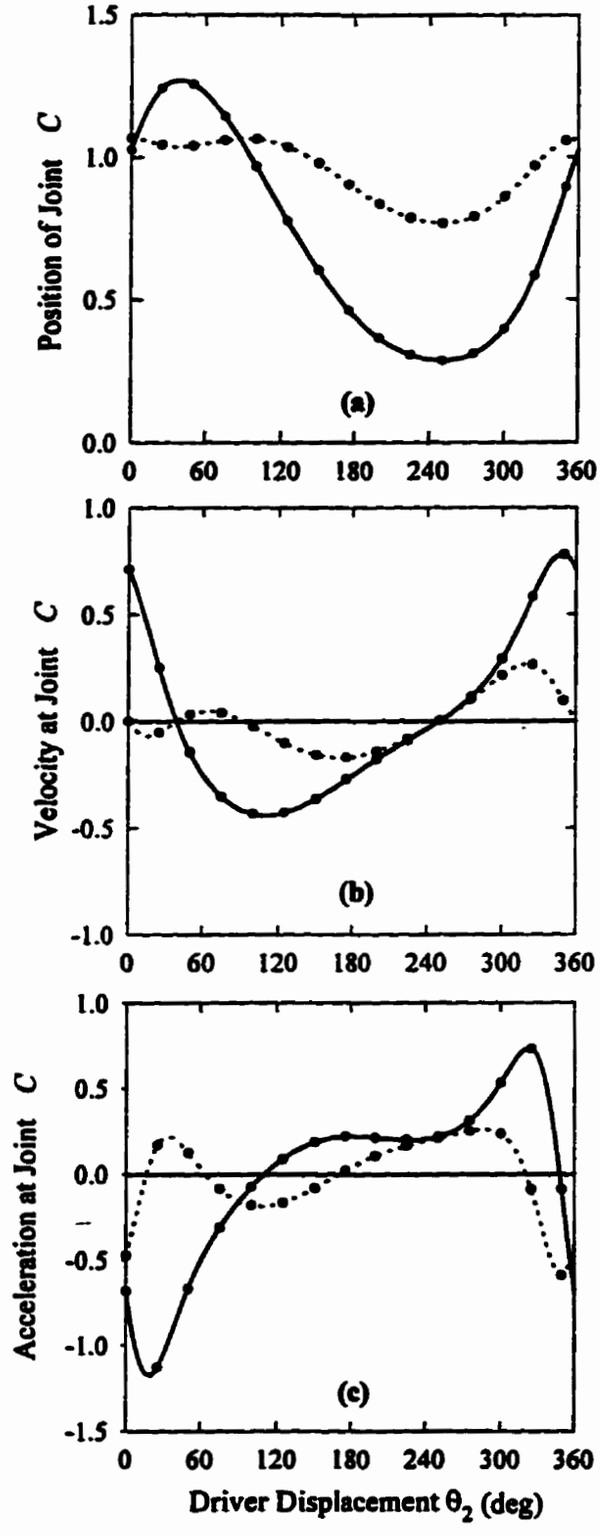

Figure 3.4: Comparison of the position, velocity and acceleration at joint C (——x-component and —— y-component via error analysis, and ●●●NDPLAn).

The *i*th inequality in *Equation* (3.19) is solved for Δl_0 corresponding to a specified value of $\Delta\alpha_0$ such that the resulting solution produces the largest manufacturing tolerance (and hence, the cheapest cost to the manufacturer). Having obtained $(\Delta l_0, \Delta\alpha_0)$, the manufacturing tolerance can be computed using

$$\hat{q}_i = \bar{q}_i \pm \Delta q_i, \tag{3.20}$$

in which $\hat{q}_i, \bar{q}_i$ represent the actual and nominal dimensions respectively. The actual choice of the ± sign in *Equation* (3.20) depends only on the sign of the respective sensitivity coefficient. In using *Equation* (3.20), it is necessary to identify the most sensitive error combination and in the next section, a method which will do so directly without requiring the consideration of *any* of the possible error combinations is described.

3.5.1 Identification of the Most Sensitive Error Combination

The tolerance bands of input parameters are always expressed with binary signs, for example, $\pm\Delta l_1, \pm\Delta x_A, \pm\Delta y_A, \pm\Delta\alpha_1$. It is therefore necessary to consider all combinations of positive and negative input errors in calculating the maximum/minimum output errors. Assuming m input parameters, the total number of such combinations is 2^m. To determine the overall maximum/ minimum output errors for one complete cycle of motion, all 2^m combinations must be analyzed at *every* motion increment. This can make the task computationally very intensive and thereby, significantly slowing the process. For example, a mechanism with $m = 12$ input parameters produces 4,096 combinations and if the mechanism is analyzed at 30^0 interval, there will be a total of just under 50,000 computations for one 360^0 rotation! Researchers have suggested several remedies to address this situation. A popular technique is to do so graphically via an "error" plot over the entire cycle of motion for all the 2^m combinations. Fenton et al. (1989) have proposed an approximate method based on the concept of dynamic programming to solve this problem. Here we would like to put forth the following idea where the most sensitive error combination of all the 2^m possibilities can be identified directly

without any need for calculations. The premise of our idea lies in the requirement that all tolerance bands are specified with binary signs. With this knowledge and noting that the sensitivity coefficients can also be either positive or negative, then the largest output error must be given by that combination where the product of its sensitivity coefficients and the respective tolerance bands is always net positive (or net negative)! Also, since the signs of the sensitivity coefficients are known, then it is a simple matter of adopting these signs when it comes to allocating the dimensional tolerances. To demonstrate this concept, let us consider the 4-bar linkage. Assuming its sensitivity coefficients at a certain position are $+C_{p1}, -C_{p2}, -C_{p3}, +C_{p4}$, and it is required to determine the most sensitive error combination at that position. The total number of combinations for a 4-bar linkage is $2^4 = 16$ and these are listed in *Table* 3.3. From the $(+,-,-,+)$ signs of the sensitivity coefficients, we see from *Table* 3.3 that Combination 7 (9) results in a net positive (net negative) product and hence, when summed together yields the largest (smallest) output error. Therefore, the conclusion is, due to the binary nature of the sign, we can get the maximum by summing terms of the *same* sign, and the minimum by adding terms of the *opposite* sign.

3.5.2 Optimum Dimensional Tolerancing

In this section, we discuss the optimization of the dimensional tolerances based on the proposed error sensitivity analysis. Similar to Fenton et al. (1989), the following objective function is chosen:

$$f(\Delta l_0) = \left(\left|(\Delta \bar{W}_i)_{\max}\right| - \left|(\Delta W_i^a)_{\max}\right|\right)^2 + \left(\left|(\Delta W_i)_{\max}\right| - \left|(\Delta W_i^a)_{\min}\right|\right)^2, \tag{3.21}$$

where $\left|(\Delta W_i^a)_{\max}\right| = \left|(W_i(\hat{q}) - W_i(\bar{q}))_{\max}\right|$ is the actual maximum output error based on the most sensitive error combination and $\left|(\Delta W_i^a)_{\min}\right| = \left|(W_i(\hat{q}) - W_i(\bar{q}))_{\min}\right|$ is the actual minimum output error based on the most sensitive error combination. To carry out the process of optimization, the algorithm depicted in *Figure* 3.5 is employed. A kinematic analysis for position, velocity,

Table 3.3: Tolerance band combinations for a 4-bar linkage.

Combination No.	Δl_1	Δl_2	Δl_3	Δl_4
1	+	+	+	+
2	+	+	+	-
3	+	+	-	+
4	+	-	+	+
5	-	+	+	+
6	+	+	-	-
7	+	-	-	+
8	-	-	+	+
9	-	+	+	-
10	+	-	+	-
11	-	+	-	+
12	+	-	-	-
13	-	+	-	-
14	-	-	+	-
15	-	-	-	+
16	-	-	-	-

acceleration and their corresponding sensitivity coefficients is first performed. Next, the largest of all the most sensitive error combinations for either the complete or part cycle of the

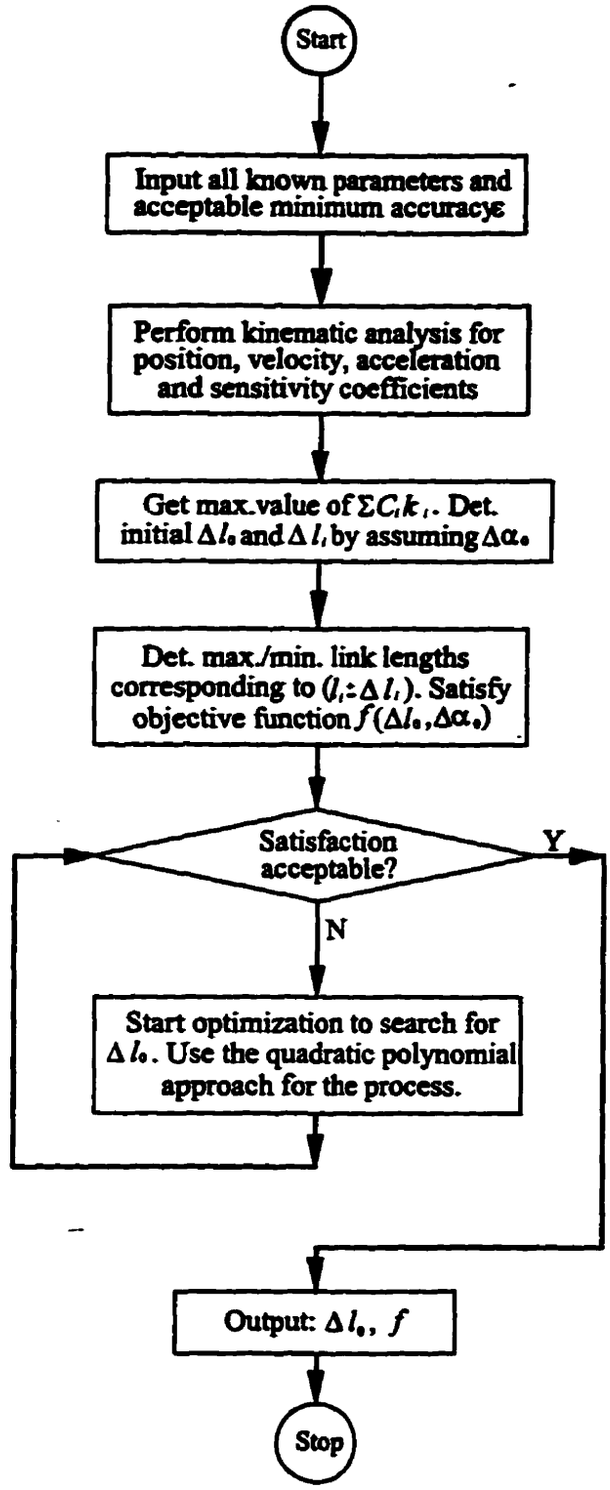

Figure 3.5: Flowchart for tolerance optimization.

motion (depending on the mechanism) is determined so that when substituted into *Equation* (3.19) results in computation of Δl_0 for specified values of $\Delta\alpha_0$. This is used as the *starting* point for the optimization. To generate the actual maximum output error $\left|\left(\Delta W_i^a\right)_{max}\right|$, the sign of Δl_0 is chosen to match the corresponding sign of C_{ij} (net positive) and to obtain the actual minimum output error $\left|\left(\Delta W_i^a\right)_{min}\right|$, the sign of Δl_0 is chosen so that it is opposite to that of the corresponding sign of C_{ij} (net negative). For the first iteration where the nominal values are used, the actual maximum output error is equal to actual minimum output error. After the first iteration, they will not be equal since we took into account only the first term of the Taylor expansion, in calculating the sensitivity coefficients. Finally, a quadratic polynomial search optimization technique (Fan and Zhang (1982)) is used to solve *Equation* (3.21) for $\Delta q_i = \left\langle k_i \Delta l_0, k_i \Delta\alpha_0 \right\rangle^T$ iteratively, until the prescribed accuracy is attained.

3.6 NUMERICAL EXAMPLES

The 4-bar linkage in *Figure* 3.2 is once again used to demonstrate and assess the accuracy of the proposed method of optimum dimensional tolerancing. As an application of the method, a 2-loop, 6-bar linkage is studied. For both linkages, tolerance bands based on the position, velocity and acceleration requirements are computed and from these results, the smallest is chosen for the final mechanism design.

3.6.1 Four Bar Linkage

The following weighting factors $k_1 = 1, k_2 = l_2/l_1 = 0.4, k_3 = l_3/l_1 = 1.2, k_4 = l_4/l_1 = 1.03923$, computed from the link lengths of the 4-bar linkage in *Figure* 3.2, are used to synthesize the dimensional tolerances. Adopting the same numerical value for the maximum allowable output bands corresponding to the position, velocity and acceleration requirements, we have,

$$\begin{aligned} \left|(\Delta\theta_4)_{max}\right| &= 0.02 \text{ rad}, \\ \left|(\Delta\dot{\theta}_4)_{max}\right| &= 0.02 \text{ rad/s}, \\ \left|(\Delta\ddot{\theta}_4)_{max}\right| &= 0.02 \text{ rad/s}^2. \end{aligned} \tag{3.22}$$

To get an idea of which of the 3 requirements in *Equation* (3.22) would govern, a graph of the weighted sensitivity coefficients from the maximum and minimum error combinations is plotted in *Figure* 3.6. Observe that the maximum/minimum weighted sensitivity coefficient pair calculated from the acceleration requirement is the largest and thus, governs in the final design selection

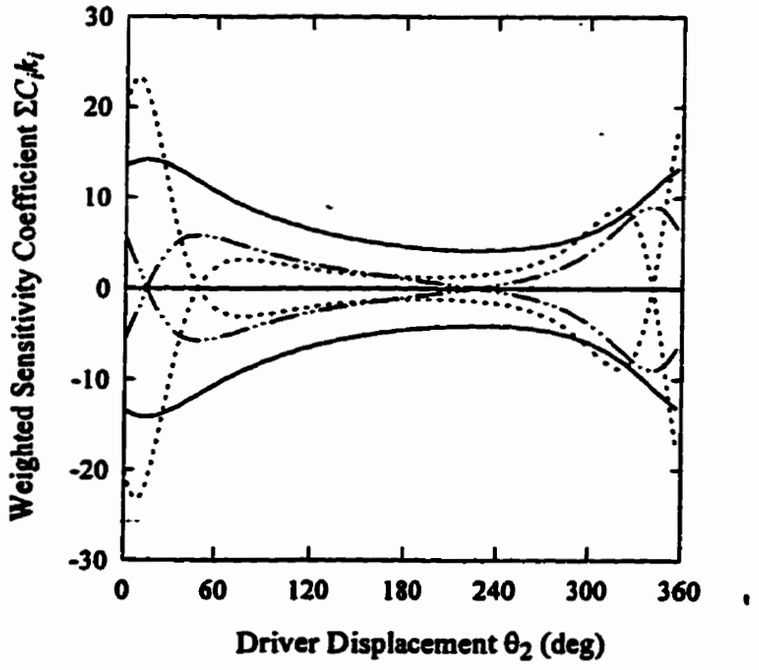

Figure 3.6: Maximum/minimum weighted sensitivity coefficient pairs for the 4-bar linkage (——— position, —·—·· velocity, ····· acceleration).

The results of the optimization are summarized in *Table* 3.4. As shown, the values of Δl_0 based on the position, velocity and acceleration requirements are given, together with their respective convergence errors in the objective function. The latter information is provided to give a measure of the accuracy of the values of Δl_0 obtained. Choosing the smallest value for the final design we see that the acceleration requirement governs, i.e. $\Delta l_0 = 2.1482 \times 10^{-3}$ must be used for computing the tolerance bands for all the links. This conclusion also confirms the observation in *Figure* 3.6.

Table 3.4: Optimization results for the 4-bar linkage.

	Δl_0 (10^{-3})	$f(\Delta l_0)(10^{-7})$	Δl_0 (Cleghorn et al.)
Position Requirement	3.5298	0.7929	3.67×10^{-3}
Velocity Requirement	5.5474	5.1159	-
Acceleration Requirement	2.1482	1.3927	-

It would be interesting to compare Δl_0 with that of Cleghorn et al. (1993). As listed in *Table* 3.4, the difference between the two position-based predictions of Δl_0 is approximately 3.8%, with ours being the smaller of the two. This implies that if our Δl_0 is adopted, it would lead to tighter input tolerance bands which are undesirable as they result in a more expensive design. However, upon a closer examination of the output motion plot in *Figure* 3.7, our design is more accurate than Cleghorn et al. (1993), as it satisfies the maximum/minimum allowable output bands more closely. Observe that even though our position and velocity-based output motions have slightly exceeded the maximum/minimum allowable output bands, they are nevertheless, smaller than the position-based output motion of Cleghorn et al.. To correct for the small inaccuracy in our output motion, the 4-bar linkage can be re-synthesized using the

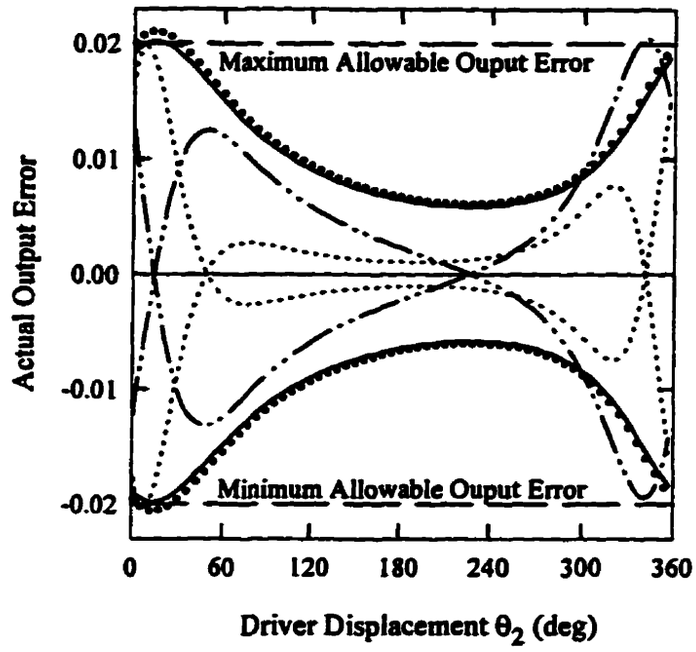

Figure 3.7: Preliminary output motion characteristics
(——— position, —··—·· velocity, ····· acceleration, ••• Cleghorn et al. 1993).

value of the governing $\Delta l_0 = 2.1482 \times 10^{-3}$ which is derived from the acceleration requirement. In this way, the link lengths of the 4-bar linkage are re-adjusted accordingly. The final output motion characteristics based on the re-designed link lengths are sketched in *Figure* 3.8. Observe that throughout the complete cycle of rotation, the final output motions synthesized in accordance to the position, velocity and acceleration requirements do not exceed the maximum/minimum allowable output bands. The final design is therefore, a valid and an acceptable mechanism. The final designed link lengths together with their respective tolerance bands are summarized in *Table* 3.5. Note that the signs of the tolerance bands are chosen in accordance to the respective signs of the sensitivity coefficients as discussed in the previous section.

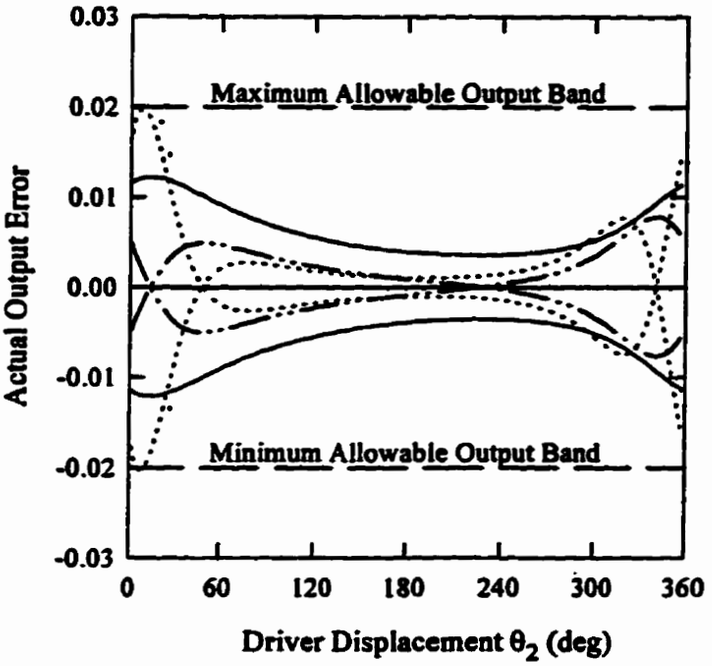

Figure 3.8: Final output motion characteristics for the 4-bar linkage (——— position, —·—·— velocity, ····· acceleration).

Table 3.5: Tolerance bands for final design for the 4-bar linkage.

Nominal Length	$\Delta l_i \left(10^{-3}\right)$
l_1=1.00000	∓2.1482
l_2=0.40000	±0.8593
l_3=1.20000	±2.5778
l_4=1.03923	∓2.2324

3.6.2 Six Bar Linkage

A 2-loop, 6-bar linkage together with its nominal dimensions are depicted in *Figure* 3.9. The weighting factors are $k_1 = 0.25, k_2 = 0.75,\ k_3 = 0.50,\ k_4 = 0.50,\ k_5 = 0.625,\ k_6 = 1.00,\ k_7 = 0.75$ for the links, and $k_8 = k_9 = 1.00,\ k_{10} = k_{11} = 0.0,\ k_{12} = k_{13} = 1.50$ for the fixed joints. Adopting the same numerical value for the maximum allowable output bands corresponding to the position, velocity and acceleration requirements, we have,

$$\begin{aligned} \left|(\Delta\psi_5)_{max}\right| &= 0.05 \text{ rad}, \\ \left|(\Delta\dot{\psi}_5)_{max}\right| &= 0.05 \text{ rad/s}, \\ \left|(\Delta\ddot{\psi}_5)_{max}\right| &= 0.05 \text{ rad/s}^2. \end{aligned} \tag{3.23}$$

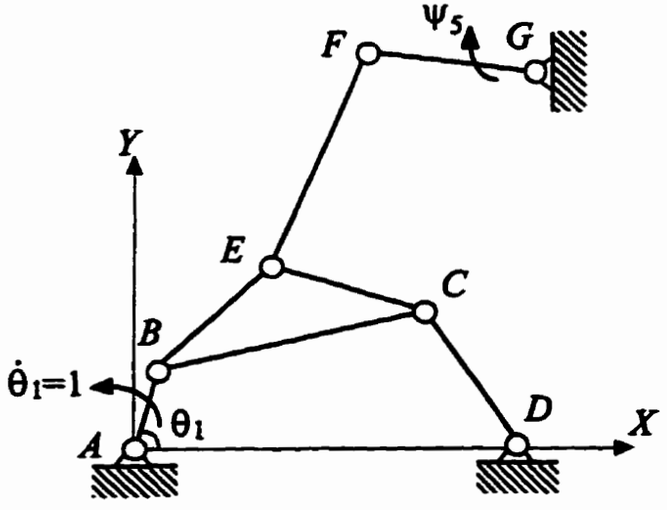

Nominal Dimensions

$l_1 = L_{AB} = 0.400$
$l_2 = L_{BC} = 1.200$
$l_3 = L_{BE} = 0.800$
$l_4 = L_{EC} = 0.800$
$l_5 = L_{CD} = 1.000$
$l_6 = L_{EF} = 1.600$
$l_7 = L_{FG} = 1.200$
$(x_A, y_A) = (0.0, 0.0)$
$(x_D, y_D) = (1.0, 0.0)$
$(x_G, y_G) = (1.0, 1.5)$

Figure 3.9: A six-bar linkage.

It is required to synthesize the optimum tolerance band Δl_0 corresponding to specified values of $\langle \Delta x_{A0}, \Delta y_{A0}, \Delta x_{G0}, \Delta y_{G0} \rangle^T = 0.001,\ 0.003, \cdots,\ 0.009$. Weighted sensitivity coefficients from the maximum and minimum error combinations are depicted in *Figure* 3.10. As shown, the maximum/minimum weighted sensitivity coefficient pair calculated from the acceleration

requirement is the largest and thus, would be expected to govern in the final design selection. The results of the optimization are summarized in *Table* 3.6. As shown, the values of Δl_0 based on the position, velocity and acceleration requirements are given, together with their respective convergence errors in the objective function. The latter information is provided to give a measure of the accuracy of the values of Δl_0 obtained. Note that $\Delta l_0, f(\Delta l_0)$ values for the three cases of $\Delta x = \Delta y = 0.005$, 0.007 and 0.009 are not listed in *Table* 3.6 due to the negative contributions by Δl_0. This situation arises because the input error from $\Delta x_{A0}, \Delta y_{A0}, \Delta x_{G0}, \Delta y_{G0}$ is already larger than the maximum allowable output error from ΔW_9. That is, $\left|\left(C_{9,10}k_{10}\Delta x_{D0} + C_{9,11}k_{11}\Delta y_{D0} + C_{9,12}k_{12}\Delta x_{G0} + C_{9,13}k_{13}\Delta y_{G0}\right)_{\max}\right| > \left|\left(\Delta W_9\right)_{\max}\right|$.

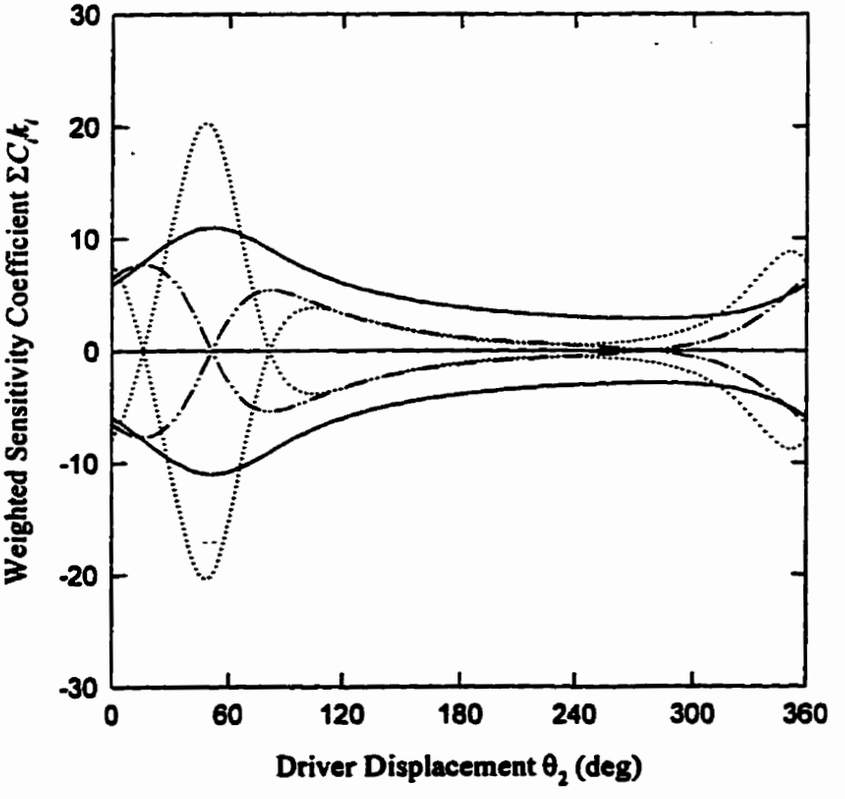

Figure 3.10: Maximum/minimum weighted sensitivity coefficient pairs for the 6-bar linkage (——— position, —·:—·:· velocity, ····· acceleration).

Table 3.6: Optimization results for the 6-bar linkage.

	Position		Velocity		Acceleration	
$\Delta x_{A0}, \Delta y_{A0}$ $\Delta x_{G0}, \Delta y_{G0}$	Δl_0 (10^{-3})	$f(\Delta l_0)$ (10^{-6})	Δl_0 (10^{-3})	$f(\Delta l_0)$ (10^{-6})	Δl_0 (10^{-3})	$f(\Delta l_0)$ (10^{-6})
0.001	7.7652	0.1510	8.8133	0.1002	3.4818	0.00240
0.003	5.7003	1.2698	8.0257	0.1494	1.4713	1.0776
0.005	3.55847	4.8462	7.1737	1.4436	-	-
0.007	1.3421	8.0696	5.9499	3.1107	-	-
0.009	-	-	4.0936	5.1841	-	-

Choosing the smallest value of Δl_0 for the final design we see that the acceleration requirement governs and thus, its value must be used for computing the tolerance bands for all the links. *Table* 3.7 shows the final design values for the various link lengths, together with their respective tolerance bands for the specified $\langle \Delta x_{A0}, \Delta y_{A0}, \Delta x_{G0}, \Delta y_{G0} \rangle^T = 0.001,\ 0.003$. For brevity, results for only 2 of the 5 specified values of $\langle \Delta x_{A0}, \Delta y_{A0}, \Delta x_{G0}, \Delta y_{G0} \rangle^T$ are listed. Note that the signs of the tolerance bands are chosen in accordance to the respective signs of the sensitivity coefficients. On the basis of the designed link lengths, the final output motion characteristics computed from the governing acceleration requirement are plotted in *Figure* 3.11. Observe that they all conform to within the maximum/minimum output tolerance bands and this implies that final mechanism is a valid and an acceptable design.

3.7 CONCLUSIONS

An error sensitivity analysis and the subsequent optimum dimensional tolerancing of planar

Table 3.7: Tolerance bands for final design for the 6-bar linkage.

Nominal Link Length	$\Delta l_i \left(10^{-3}\right)$	
	$\Delta x = \Delta y = 0.001$	$\Delta x = \Delta y = 0.003$
l_1=0.40	±0.8705	±0.3678
l_2=1.20	∓2.6114	∓1.1035
l_3=0.80	±1.7409	±0.7357
l_4=0.80	±1.7409	±0.7357
l_5=1.00	±2.1761	±0.9196
l_6=1.60	±3.4818	±1.4713
l_7=1.20	∓2.6114	∓1.1035

mechanisms are presented here. The approach consists of modeling the planar mechanism as consisting of an assemblage of drivers and dyad groups. Position, velocity and acceleration sensitivity coefficients are derived for drivers and dyad groups. A method for the direct identification of the most sensitive error combination without requiring to consider *all* the 2^m possibilities is suggested. This will significantly reduce the computational effort associated with the synthesis of optimum dimensional tolerancing in mechanisms. The modular approach suggested here permits the creation of a general multi-purpose program for error sensitivity analysis and tolerance synthesis of complex planar dyad linkages. A 4-bar and a 6-bar linkages are analyzed. The former serves to demonstrate and assess the accuracy of the method while the latter serves as an application of the technique. From the error sensitivity

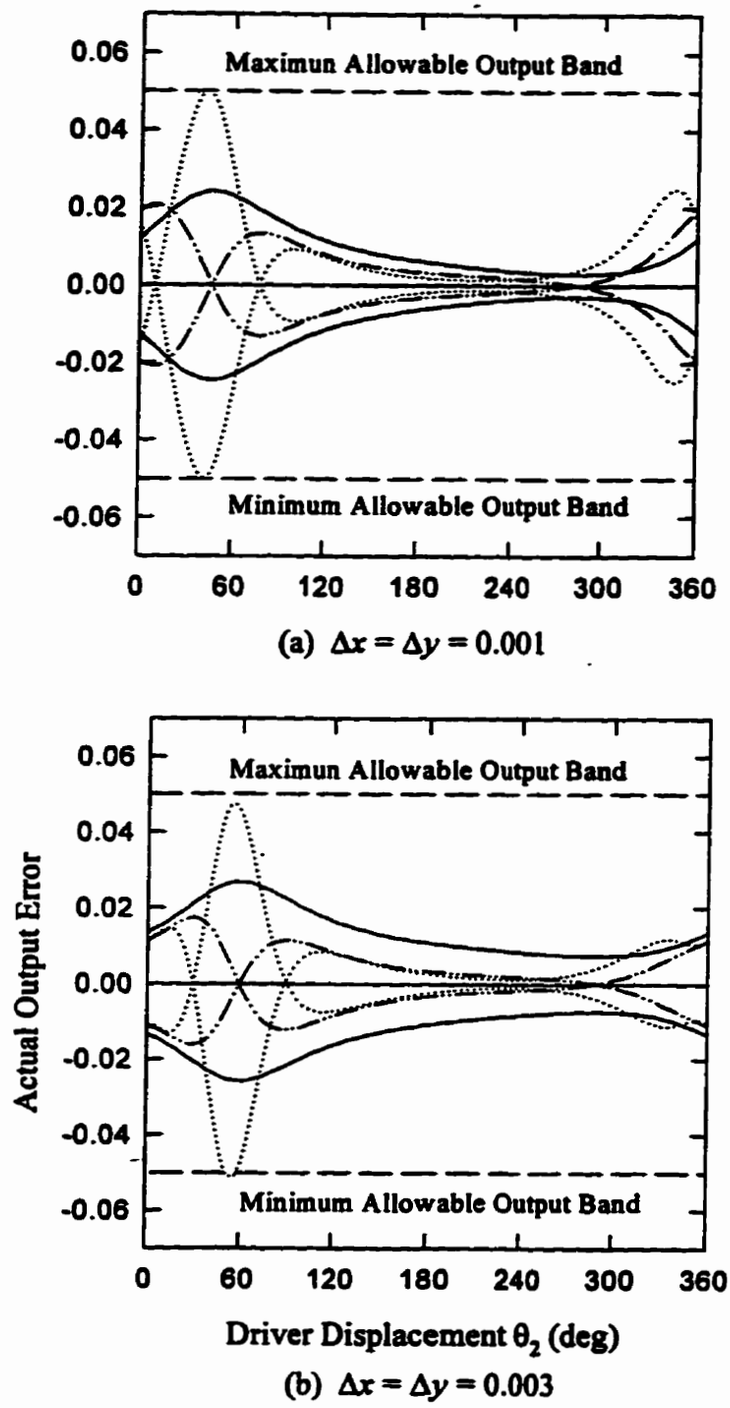

Figure 3.11: Final motion characteristics for the 6-bar linkage (——— position, —··—·· velocity, ····· acceleration).

analysis of the 2 linkage examples employed here, it is found that the acceleration requirement governs. Hence, in the synthesis of the optimum dimensional tolerancing of the final design, the acceleration-based Δl_0 should be used in the computation of the revised link lengths. Using these results, the position-based, velocity-based and acceleration-based final output motion characteristics of the two mechanisms all conform to within the prescribed maximum/minimum allowable output bands. This implies that the two final mechanisms are valid and acceptable designs.

CHAPTER 4

The Treatment of Planar Non-Dyad Mechanisms for Higher Order Mechanical Error Sensitivity Analysis and Optimum Dimensional Tolerancing

4.1 INTRODUCTION

In this chapter, a method is proposed for carrying out a higher-order error sensitivity analysis and optimum dimensional tolerancing of planar *non*-dyad mechanisms. Unlike the method described in *Chapter* 3 which is applicable to dyad mechanisms only, the method presented here is valid for both dyad and non-dyad mechanisms, and thus, constitutes a more general approach for carrying out the mechanical error sensitivity analysis and the synthesis of dimensional tolerance bands. As reported in *Chapter* 3, the methods of Fenton et al. (1989) and Cleghorn et al. (1993) can be employed for these purposes, but they are applicable to only to dyad mechanisms. To the best of our knowledge, no methods have been proposed for the treatment of non-dyad mechanisms.

Our method is made feasible by a unique analytical procedure for the determination of the position, velocity and acceleration sensitivity coefficients. They are computed via a kinematic analysis of the original and as well as, a supplemental mechanism. The latter is derived from the original mechanism by setting the virtual velocity term to either 0 or ± 1, depending on the particular sensitivity coefficient that is being evaluated. We called this procedure the *Method of Virtual Velocity*. Once the sensitivity coefficients have been determined, the

process of synthesizing for optimum dimensional tolerancing can be easily carried out following the method described in *Chapter* 3. It should also be pointed out that to carry out a kinematic analysis of non-dyad mechanisms for both the original and the supplemental linkages, the method of *Chapter* 2 and codified into the computer program **NDPLAn** can be employed.

4.2 THE METHOD OF VIRTUAL VELOCITY

The output variable U describing the displacement of a general linkage characterized by m-input variables θ_j $(j=1, ..., m)$ and n-dimensional parameters q_i $(i=1, ..., n)$ can be written as,

$$U = U\left(\theta_1,\cdots, \theta_j,\cdots, \theta_m, q_1,\cdots, q_i,\cdots, q_n\right). \tag{4.1}$$

Assuming the input variables are prescribed exactly, the output position, velocity and acceleration errors due to dimensional errors in the linkage can be approximated by the first order terms of a Taylor series expansion as follows:

$$\Delta U = \sum_{i=1}^{n} \frac{\partial U}{\partial q_i}\Delta q_i = \sum_{i=1}^{n} C_{p_i}\Delta q_i\,, \tag{4.2}$$

$$\Delta \dot{U} = \frac{d(\Delta U)}{dt} = \sum_{i=1}^{n}\left[\sum_{j=1}^{m}\frac{\partial^2 U}{\partial\theta_j\partial q_i}\dot{\theta}_j\right]\Delta q_i = \sum_{i=1}^{n} C_{v_i}\Delta q_i\,, \tag{4.3}$$

$$\Delta \ddot{U} = \frac{d(\Delta \dot{U})}{dt} = \sum_{i=1}^{n}\left[\sum_{k=1}^{m}\sum_{j=1}^{m}\frac{\partial^3 U}{\partial\theta_j\partial\theta_k\partial q_i}\dot{\theta}_j\dot{\theta}_k + \sum_{j=1}^{m}\frac{\partial^2 U}{\partial\dot{\theta}_j\partial q_i}\ddot{\theta}_j\right]\Delta q_i = \sum_{i=1}^{n} C_{a_i}\Delta q_i\,, \tag{4.4}$$

where C_{p_i}, C_{v_i} and C_{a_i} are termed respectively as the position, velocity and acceleration sensitivity coefficients corresponding to the dimensional error Δq_i. They capture the

sensitivity of the output parameters due to small changes in the dimensional parameters. After computing these sensitivity coefficients, the dimensional errors corresponding to position, velocity and acceleration terms can be evaluated. For the basic mechanism components identified in *Chapter* 2, the dyad groups in *Chapter* 3 and all simple dyad linkages, the determination of C_{p_i}, C_{v_i} and C_{a_i} is rather straightforward and efficient. This is not true for complex non-dyad linkages as the computation of the sensitivity coefficients can be very challenging even when numerical methods are employed. Hence, it is necessary to develop an effective approach to evaluate these coefficients. This will be addressed next where a unique analytical procedure is introduced.

4.2.1 Determination of the Position Sensitivity Coefficient

To determine the position sensitivity coefficient, the dimensional parameter q_i is assumed to be a function of time t, i.e., $q_i = q_i(t)$, and thus, differentiating *Equation* (4.1) with respect to time t yields the velocity relationship,

$$\dot{U} = \sum_{j=1}^{m} \frac{\partial U}{\partial \theta_j} \dot{\theta}_j + \frac{\partial U}{\partial q_i} \dot{q}_i . \tag{4.5}$$

Setting $\dot{\theta}_j = 0$ $(j = 1,2,\cdots,m)$ and the virtual velocity $\dot{q}_i = 1$, we obtain the partial velocity term $\partial U / \partial q_i$ for the evaluation of the position sensitivity coefficient C_{p_i}:

$$C_{p_i} = \frac{\partial U}{\partial q_i} \equiv \dot{U}^{(1)} . \tag{4.6}$$

4.2.2 Determination of the Velocity Sensitivity Coefficient

The velocity sensitivity coefficient C_{v_i} can be found by differentiating *Equation* (4.5) once more with respect to time t. Setting $\ddot{q}_i = 0$ leads to the acceleration relationship,

$$\ddot{U} = \sum_{j=1}^{m}\left(\sum_{k=1}^{m}\frac{\partial^2 U}{\partial\theta_j\partial\theta_k}\dot{\theta}_j\dot{\theta}_k + \frac{\partial U}{\partial\theta_j}\ddot{\theta}_j\right) + 2\sum_{j=1}^{m}\frac{\partial^2 U}{\partial\theta_j\partial q_i}\dot{\theta}_j\dot{q}_i + \frac{\partial^2 U}{\partial q_i^2}\dot{q}_i^2 . \tag{4.7}$$

Setting $\dot{\theta}_j = \ddot{\theta}_j = 0$ $(j = 1,2,\cdots,m)$ and $\dot{q}_i = 1$ yields the first partial acceleration term:

$$\ddot{U}^{(1)} = \frac{\partial^2 U}{\partial q_i^2}. \tag{4.8}$$

Using the known values of $\dot{\theta}_j$ and $\ddot{\theta}_j$ $(j = 1,2,\cdots,m)$ and setting $\dot{q}_i = 0$, we can compute the second partial acceleration term:

$$\ddot{U}^{(2)} = \sum_{j=1}^{m}\left(\sum_{k=1}^{m}\frac{\partial^2 U}{\partial\theta_j\partial\theta_k}\dot{\theta}_j\dot{\theta}_k + \frac{\partial U}{\partial\theta_j}\ddot{\theta}_j\right). \tag{4.9}$$

From the given values of $\dot{\theta}_j$ and $\ddot{\theta}_j$ $(j = 1,2,\cdots;m)$ and setting $\dot{q}_i = 1$, together with *Equations* (4.8) and (4.9), the third partial acceleration term is obtained:

$$\ddot{U}^{(3)} = \ddot{U}^{(2)} + 2\sum_{j=1}^{m}\frac{\partial^2 U}{\partial\theta_j\partial q_i}\dot{\theta}_j + \ddot{U}^{(1)}. \tag{4.10}$$

The velocity sensitivity coefficient is then determined from

$$C_{v_i} = \sum_{j=1}^{m}\frac{\partial^2 U}{\partial\theta_j\partial q_i}\dot{\theta}_j = \frac{\ddot{U}^{(3)} - \ddot{U}^{(2)} - \ddot{U}^{(1)}}{2}. \tag{4.11}$$

4.2.3 Determination of the Acceleration Sensitivity Coefficient

The acceleration sensitivity coefficient C_{a_i} is determined by differentiating *Equation* (4.7)

with respect to time t. Setting $\dddot{\theta}_j = 0$ $(j = 1,2,\cdots,m)$ and $\ddot{q}_i = 0$, the following jerk relationship is obtained,

$$\begin{aligned}\dddot{U} = &\sum_{j=1}^{m}\left[\sum_{k=1}^{m}\left(\sum_{h=1}^{m}\frac{\partial^3 U}{\partial\theta_h\partial\theta_k\partial\theta_j}\dot{\theta}_h\dot{\theta}_k\dot{\theta}_j + 3\frac{\partial^2 U}{\partial\theta_k\partial\theta_j}\dot{\theta}_k\dot{\theta}_j\right) + 3\frac{\partial^3 U}{\partial\theta_j\partial q_i^2}\dot{\theta}_j\dot{q}_i^2\right] \\ &+3\sum_{j=1}^{m}\left(\sum_{k=1}^{m}\frac{\partial^3 U}{\partial\theta_k\partial\theta_j\partial q_i}\dot{\theta}_k\dot{\theta}_j\dot{q}_i + \frac{\partial^2 U}{\partial\theta_j\partial q_i}\ddot{\theta}_j\dot{q}_i\right) + \frac{\partial^3 U}{\partial q_i^3}\dot{q}_i^3.\end{aligned} \tag{4.12}$$

Setting $\dot{\theta}_j = \ddot{\theta}_j = 0$ $(j = 1,2,\cdots,m)$ and $\dot{q}_i = 1$, we get the first partial jerk term:

$$\dddot{U}^{(1)} = \frac{\partial^3 U}{\partial q_i^3}. \tag{4.13}$$

From the prescribed values of $\dot{\theta}_j$ and $\ddot{\theta}_j$ $(j = 1,2,\cdots,m)$ and setting $\dot{q}_i = -1$, we get the second partial jerk term:

$$\begin{aligned}\dddot{U}^{(2)} = &\sum_{j=1}^{m}\left[\sum_{k=1}^{m}\left(\sum_{h=1}^{m}\frac{\partial^3 U}{\partial\theta_h\partial\theta_k\partial\theta_j}\dot{\theta}_h\dot{\theta}_k\dot{\theta}_j + 3\frac{\partial^2 U}{\partial\theta_k\partial\theta_j}\dot{\theta}_k\dot{\theta}_j\right) + 3\frac{\partial^3 U}{\partial\theta_j\partial q_i^2}\dot{\theta}_j\right] \\ &-3\sum_{j=1}^{m}\left(\sum_{k=1}^{m}\frac{\partial^3 U}{\partial\theta_k\partial\theta_j\partial q_i}\dot{\theta}_k\dot{\theta}_j + \frac{\partial^2 U}{\partial\theta_j\partial q_i}\ddot{\theta}_j\right) - \dddot{U}^{(1)}.\end{aligned} \tag{4.14}$$

Using the given values of $\dot{\theta}_j$ and $\ddot{\theta}_j$ $(j = 1,2,\cdots,m)$ and setting $\dot{q}_i = 1$ we have the third partial jerk term:

$$\begin{aligned}\dddot{U}^{(3)} = &\sum_{j=1}^{m}\left[\sum_{k=1}^{m}\left(\sum_{h=1}^{m}\frac{\partial^3 U}{\partial\theta_h\partial\theta_k\partial\theta_j}\dot{\theta}_h\dot{\theta}_k\dot{\theta}_j + 3\frac{\partial^2 U}{\partial\theta_k\partial\theta_j}\dot{\theta}_k\dot{\theta}_j\right) + 3\frac{\partial^3 U}{\partial\theta_j\partial q_i^2}\dot{\theta}_j\right] \\ &+3\sum_{j=1}^{m}\left(\sum_{k=1}^{m}\frac{\partial^3 U}{\partial\theta_k\partial\theta_j\partial q_i}\dot{\theta}_k\dot{\theta}_j + \frac{\partial^2 U}{\partial\theta_j\partial q_i}\ddot{\theta}_j\right) + \dddot{U}^{(1)}.\end{aligned} \tag{4.15}$$

Subtracting *Equation* (4.14) from *Equation* (4.15), yields the acceleration sensitivity coefficient,

$$C_{a_i} = \sum_{j=1}^{m}\left(\sum_{k=1}^{m}\frac{\partial^3 U}{\partial\theta_k\partial\theta_j\partial q_i}\dot{\theta}_k\dot{\theta}_j + \frac{\partial^2 U}{\partial\theta_j\partial q_i}\ddot{\theta}_j\right) = \frac{\dddot{U}^{(3)} - \dddot{U}^{(2)} - 2\dddot{U}^{(1)}}{6}. \qquad (4.16)$$

To summarize the steps involved in the computation of these 3 kinematic sensitivity coefficients, a kinematic analysis of the planar mechanism with m-dof (degrees of freedom) is first performed for positions, velocities and accelerations. Next, the various partial terms associated with velocity, acceleration and jerk are obtained via a kinematic analysis of a supplemental mechanism with $(m+1)$-dof. The supplemental mechanism is derived from the original m-dof mechanism by an appropriate setting of the virtual velocity $\dot{q}_i = 1, -1$ or 0, depending on the particular sensitivity coefficient that is being evaluated. This unique procedure of assigning the velocity of the dimensional parameter $\dot{q}_i = 1, -1$ or 0 is termed the *Method of Virtual Velocity*. It is applicable to both dyad and non-dyad planar mechanisms, and hence, constitutes a more general (and powerful) technique than the analytical method of *Chapter* 3, which is applicable only to dyad mechanisms. If the mechanism being analyzed is a dyad linkage, the method of virtual velocity is relatively simple and yields identical results to that of *Chapter* 3. If the mechanism is a non-dyad linkage, the process is more complicated as the kinematic analysis will now involve transforming the non-dyad mechanism into a series of dyad mechanisms. By disconnecting appropriate links/pairs and prescribing dyad drivers for the transformed dyad mechanisms, the affected geometric conditions are iteratively recovered, and thereby, restoring the original non-dyad mechanism from the series of transformed dyad mechanisms. These steps have been described in details in *Chapter* 2. Once the sensitivity coefficients corresponding to the dimensional error Δq_i have been determined, an error sensitivity analysis for the synthesis of optimum dimensional tolerancing of planar non-dyad mechanisms can then be performed in a similar manner as outlined in *Chapter* 3.

4.3 COMPUTATION OF SENSITIVITY COEFFICIENTS FOR SINGLE LINKS AND DYAD MECHANISMS

To illustrate the preceding mathematical derivations for the determination of the position, velocity and acceleration sensitivity coefficients, the following basic linkages are analyzed: the RR and PR single links, and the RRR dyad link. Their supplemental linkages with an extra-dof due to the application of a virtual velocity are also presented for each of the case considered. The results of the sensitivity coefficients computed using this method of virtual velocity are then compared with similar solutions obtained via the totally independent approach described in *Chapter* 3. Once the two sets of results have been confirmed to be identical, the solutions of the RRR dyad linkage are employed to generate the mathematical equations for the evaluation of the position, velocity and acceleration sensitivity coefficients of an 8-bar dyad mechanism.

4.3.1 Computation of Sensitivity Coefficients for the RR and PR Driver Links

The method of virtual velocity is applied to calculate the 3 kinematic sensitivity coefficients of the RR driver link due to the following dimensional errors: $\Delta q_i = \{\Delta l \quad \Delta x_A \quad \Delta y_A\}^T$. The supplemental RR link with the appropriate virtual velocity clearly marked is also presented. The results are summarized in *Table* 4.1 (a), (b) and (c) corresponding to errors Δl, Δx_A, Δy_A respectively. The final expressions of the 3 sensitivity coefficients of the original linkage, together with the various partial terms pertaining to velocity, acceleration and jerk of the supplemental linkage, are tabulated as shown. In *Table* 4.2, similar results but of the PR driver link are presented. Note that for brevity, the sensitivity coefficients due only to the dimensional error $\Delta\alpha_1$ are presented. Observe that for both the RR and the PR drivers, the results computed using the method of virtual velocity are identical to those listed in *Table* 3.1 which have been obtained via a completely different procedure.

Table 4.1 (a): Sensitivity coefficients for the RR driver and its supplemental link for Δl.

Dimensional Error Δq_i	Sensitivity Coefficients $C_{p_i}, C_{v_i}, C_{a_i}$	RR Driver	Supplemental RR Driver	
		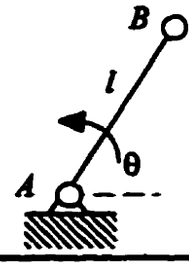	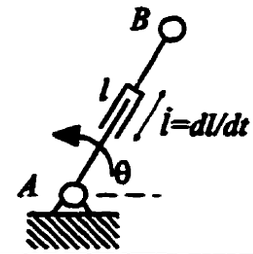	
Δl	$C_{pl}^{(x)}$	$\partial x_B/\partial l = \cos\theta$	$\dot\theta = 0,\ \dot l = 1$	$\dot x_B^{(1)} = \cos\theta$
	$C_{pl}^{(y)}$	$\partial y_B/\partial l = \sin\theta$		$\dot y_B^{(1)} = \sin\theta$
	$C_{vl}^{(x)}$	$\partial \dot x_B/\partial l = -\sin\theta\dot\theta$	$\dot\theta = \ddot\theta = 0,\ \dot l = 1$	$\ddot x_B^{(1)} = 0,\ \ddot y_B^{(1)} = 0$
			$\dot\theta, \ddot\theta$ given, $\dot l = 0$	$\ddot x_B^{(2)} = -l\cos\theta\dot\theta^2 - l\sin\theta\ddot\theta$ $\ddot y_B^{(2)} = -l\sin\theta\dot\theta^2 + l\cos\theta\ddot\theta$
			$\dot\theta, \ddot\theta$ given, $\dot l = 1$	$\ddot x_B^{(3)} = -2\sin\theta\dot\theta - l\cos\theta\dot\theta^2 - l\sin\theta\ddot\theta$ $\ddot y_B^{(3)} = 2\cos\theta\dot\theta - l\sin\theta\dot\theta^2 + l\cos\theta\ddot\theta$
	$C_{vl}^{(y)}$	$\partial \dot y_B/\partial l = \cos\theta\dot\theta$	$\ddot x_B = \left(\ddot x_B^{(3)} - \ddot x_B^{(2)} - \ddot x_B^{(1)}\right)/2 = -\sin\theta\dot\theta$ $\ddot y_B = \left(\ddot y_B^{(3)} - \ddot y_B^{(2)} - \ddot y_B^{(1)}\right)/2 = \cos\theta\dot\theta$	
	$C_{al}^{(x)}$	$\partial \ddot x_B/\partial l = -\cos\theta\dot\theta^2 - \sin\theta\ddot\theta$	$\dot\theta = \ddot\theta = 0,\ \dot l = 1$	$\dddot x_B^{(1)} = 0, \dddot y_B^{(1)} = 0$
			$\dot\theta, \ddot\theta$ given, $\dot l = -1$	$\dddot x_B^{(2)} = 3\cos\theta\dot\theta^2 + 3\sin\theta\ddot\theta + l(\sin\theta\dot\theta^3 - 3\cos\theta\dot\theta\ddot\theta)$ $\dddot y_B^{(2)} = 3\sin\theta\dot\theta^2 - 3\cos\theta\ddot\theta - l(\cos\theta\dot\theta^3 + 3\sin\theta\dot\theta\ddot\theta)$
			$\dot\theta, \ddot\theta$ given, $\dot l = 1$	$\dddot x_B^{(3)} = -3\cos\theta\dot\theta^2 - 3\sin\theta\ddot\theta + l(\sin\theta\dot\theta^3 - 3\cos\theta\dot\theta\ddot\theta)$ $\dddot y_B^{(3)} = -3\sin\theta\dot\theta^2 + 3\cos\theta\ddot\theta - l(\cos\theta\dot\theta^3 + 3\sin\theta\dot\theta\ddot\theta)$
	$C_{al}^{(y)}$	$\partial \ddot y_B/\partial l = -\sin\theta\dot\theta^2 + \cos\theta\ddot\theta$	$\dddot x_B = \left(\dddot x_B^{(3)} - \dddot x_B^{(2)} - 2\dddot x_B^{(1)}\right)/6 = -\cos\theta\dot\theta^2 - \sin\theta\ddot\theta$ $\dddot y_B = \left(\dddot y_B^{(3)} - \dddot y_B^{(2)} - \dddot y_B^{(1)}\right)/6 = -\sin\theta\dot\theta^2 + \cos\theta\ddot\theta$	

Table 4.1 (b): Sensitivity coefficients for the RR driver and its supplemental link for Δx_A.

Dimensional Error Δq_i	Sensitivity Coefficients $C_{p_i}, C_{v_i}, C_{a_i}$	RR Driver	Supplemental RR Driver
		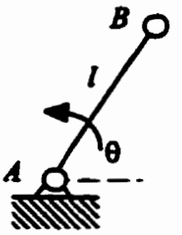	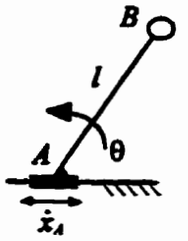
			$\dot{\theta}=0,\ \dot{x}_A=1$
Δx_A	$C_{px_A}^{(x)}$	$\partial x_B/\partial x_A=1$	$\dot{x}_B=1$
	$C_{px_A}^{(y)}$	$\partial y_B/\partial x_A=0$	$\dot{y}_B=0$
	$C_{vx_A}^{(x)}$	$\partial \dot{x}_B/\partial x_A=0$	$\ddot{x}_B=0$
	$C_{vx_A}^{(y)}$	$\partial \dot{y}_B/\partial x_A=0$	$\ddot{y}_B=0$
	$C_{ax_A}^{(x)}$	$\partial \ddot{x}_B/\partial x_A=0$	$\dddot{x}_B=0$
	$C_{ax_A}^{(y)}$	$\partial \ddot{y}_B/\partial x_A=0$	$\dddot{y}_B=0$

Table 4.1 (c): Sensitivity coefficients for the RR driver and its supplemental link for Δy_A.

Dimensional Error Δq_i	Sensitivity Coefficients $C_{p_i}, C_{v_i}, C_{a_i}$	RR Driver	Supplemental RR Driver
		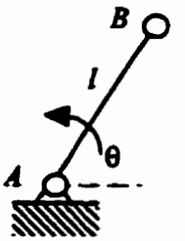	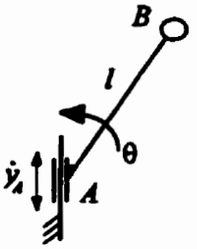
			$\dot{\theta}=0,\ \dot{y}_A=1$
Δy_A	$C_{py_A}^{(x)}$	$\partial x_B/\partial y_A=0$	$\dot{x}_B=0$
	$C_{py_A}^{(y)}$	$\partial y_B/\partial y_A=1$	$\dot{y}_B=1$
	$C_{vy_A}^{(x)}$	$\partial \dot{x}_B/\partial y_A=0$	$\ddot{x}_B=0$
	$C_{vy_A}^{(y)}$	$\partial \dot{y}_B/\partial y_A=0$	$\ddot{y}_B=0$
	$C_{ay_A}^{(x)}$	$\partial \ddot{x}_B/\partial y_A=0$	$\dddot{x}_B=0$
	$C_{ay_A}^{(y)}$	$\partial \ddot{y}_B/\partial y_A=0$	$\dddot{y}_B=0$

Table 4.2: Sensitivity coefficients for the PR driver and its supplemental link for $\Delta\alpha_1$.

Dimensional Error Δq_i	Sensitivity Coefficients $C_{p_i}, C_{v_i}, C_{a_i}$	PR Driver	Supplemental PR Driver	
		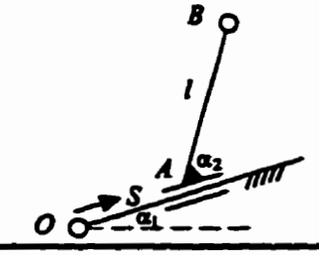	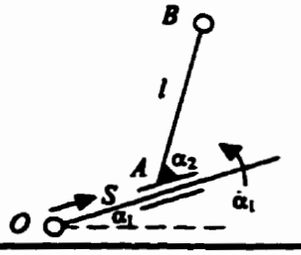	
$\Delta\alpha_1$	$C_{p\alpha_1}^{(x)}$	$\frac{\partial x_B}{\partial \alpha_1} = -s\sin\alpha_1 - l\sin(\alpha_1+\alpha_2)$	$\dot{s}=0,\ \dot{\alpha}_1=1$	$\dot{x}_B^{(1)} = -s\sin\alpha_1 - l\sin(\alpha_1+\alpha_2)$
	$C_{p\alpha_1}^{(y)}$	$\frac{\partial y_B}{\partial \alpha_1} = s\cos\alpha_1 + l\cos(\alpha_1+\alpha_2)$	$\dot{s}=0,\ \dot{\alpha}_1=1$	$\dot{y}_B^{(1)} = s\cos\alpha_1 + l\cos(\alpha_1+\alpha_2)$
	$C_{v\alpha_1}^{(x)}$	$\frac{\partial \dot{x}_B}{\partial \alpha_1} = -\dot{s}\sin\alpha_1$	$\dot{s}=\ddot{s}=0,\ \dot{\alpha}_1=1$	$\ddot{x}_B^{(1)} = -s\cos\alpha_1 - l\cos(\alpha_1+\alpha_2)$ $\ddot{y}_B^{(1)} = -s\sin\alpha_1 - l\sin(\alpha_1+\alpha_2)$
			$\dot{s},\ddot{s}$ given $\dot{\alpha}_1=0$	$\ddot{x}_B^{(2)} = \ddot{s}\cos\alpha_1$ $\ddot{y}_B^{(2)} = \ddot{s}\sin\alpha_1$
			$\dot{s},\ddot{s}$ given $\dot{\alpha}_1=1$	$\dddot{x}_B^{(3)} = \ddot{s}\cos\alpha_1 - 2\dot{s}\sin\alpha_1 - s\cos\alpha_1 - l\cos(\alpha_1+\alpha_2)$ $\dddot{y}_B^{(3)} = \ddot{s}\sin\alpha_1 + 2\dot{s}\cos\alpha_1 - s\sin\alpha_1 - l\sin(\alpha_1+\alpha_2)$
	$C_{v\alpha_1}^{(y)}$	$\frac{\partial \dot{y}_B}{\partial \alpha_1} = \dot{s}\cos\alpha_1$	$\ddot{x}_{\alpha_1} = \left(\dddot{x}_{\alpha_1}^{(3)} - \ddot{x}_{\alpha_1}^{(2)} - \ddot{x}_{\alpha_1}^{(1)}\right)/2 = -\dot{s}\sin\alpha_1$ $\ddot{y}_{\alpha_1} = \left(\dddot{y}_{\alpha_1}^{(3)} - \ddot{y}_{\alpha_1}^{(2)} - \ddot{y}_{\alpha_1}^{(1)}\right)/2 = \dot{s}\cos\alpha_1$	
	$C_{a\alpha_1}^{(x)}$	$\frac{\partial \ddot{x}_B}{\partial \alpha_1} = -\ddot{s}\sin\alpha_1$	$\dot{s}=\ddot{s}=0,\ \dot{\alpha}_1=1$	$\dddot{x}_B^{(1)} = s\sin\alpha_1 + l\sin(\alpha_1+\alpha_2)$ $\dddot{y}_B^{(1)} = -s\cos\alpha_1 - l\cos(\alpha_1+\alpha_2)$
			$\dot{s},\ddot{s}$ given $\dot{\alpha}_1=-1$	$\ddot{\ddot{x}}_B^{(2)} = 3\ddot{s}\sin\alpha_1 - 3\dot{s}\cos\alpha_1 - s\sin\alpha_1 - l\sin(\alpha_1+\alpha_2)$ $\ddot{\ddot{y}}_B^{(2)} = -3\ddot{s}\cos\alpha_1 - 3\dot{s}\sin\alpha_1 + s\cos\alpha_1 + l\cos(\alpha_1+\alpha_2)$
			$\dot{s},\ddot{s}$ given $\dot{\alpha}_1=1$	$\ddot{\ddot{x}}_B^{(3)} = -3\ddot{s}\sin\alpha_1 - 3\dot{s}\cos\alpha_1 + s\sin\alpha_1 + l\sin(\alpha_1+\alpha_2)$ $\ddot{\ddot{y}}_B^{(3)} = 3\ddot{s}\cos\alpha_1 - 3\dot{s}\sin\alpha_1 - s\cos\alpha_1 - l\cos(\alpha_1+\alpha_2)$
	$C_{a\alpha_1}^{(y)}$	$\frac{\partial \ddot{y}_B}{\partial \alpha_1} = \ddot{s}\cos\alpha_1$	$\dddot{x}_{\alpha_1} = \left(\ddot{\ddot{x}}_{\alpha_1}^{(3)} - \dddot{x}_{\alpha_1}^{(2)} - 2\dddot{x}_{\alpha_1}^{(1)}\right)/6 = -\ddot{s}\sin\alpha_1$ $\dddot{y}_{\alpha_1} = \left(\ddot{\ddot{y}}_{\alpha_1}^{(3)} - \dddot{y}_{\alpha_1}^{(2)} - 2\dddot{y}_{\alpha_1}^{(1)}\right)/6 = \ddot{s}\cos\alpha_1$	

4.3.2 Computation of Sensitivity Coefficients for Dyad Links

Table 4.3: Dimensional errors for the RRR dyad and its supplemental dyad links.

(a) Original RRR Dyad	(b) Supplemental RRR Dyad	(c) Supplemental RRR Dyad	(d) Supplemental RRR Dyad
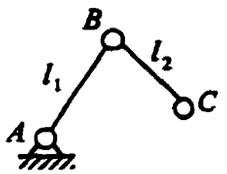	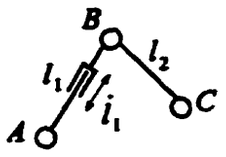	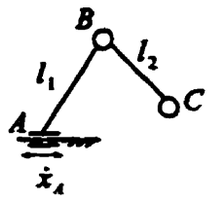	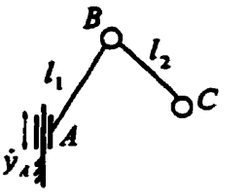
	Dimensional Error Δl_1	Dimensional Error Δx_A	Dimensional Error Δy_A

An RRR dyad and its supplemental dyad links are sketched in *Table* 4.3. If the 3 kinematic sensitivity coefficients of node B due to the dimensional error Δl_1 are desired, a fictitious slide along the direction of Δl_1 is introduced in link l_1 as shown in *Table* 4.3 (b), so that the partial terms associated with the velocity, acceleration and jerk at B can be computed. Likewise, the sensitivity coefficients of node B due to the dimensional errors Δx_A and Δy_A can be evaluated by introducing at the fixed joint A, a fictitious slide along the horizontal and vertical directions respectively as depicted in *Table* 4.3 (c) and *Table* 4.3 (d), and computing their partial terms. For the purpose of illustration, the process of calculating the position sensitivity coefficients of node B is outlined here. From geometrical considerations, we have:

$$\begin{aligned}(x_A - x_B)^2 + (y_A - y_B)^2 &= l_1^2, \\ (x_C - x_B)^2 + (y_C - y_B)^2 &= l_2^2.\end{aligned} \tag{4.17}$$

Differentiating *Equation* (4.17) with respective to time and putting $\dot{\theta} = 0$, we get 3 groups of equations corresponding to the 3 unity settings of the virtual velocities i.e. $\dot{l}_1 = 1, \dot{x}_A = 1, \dot{y}_A = 1$ for the 3 dimensional errors $\Delta l, \Delta x_A, \Delta y_A$. That is,

Dimensional Error $\Delta l \left(\dot{l}_1 = 1, \dot{x}_A = 0, \dot{y}_A = 0\right)$

$$\begin{aligned}(x_A - x_B)(0 - \dot{x}_B) + (y_A - y_B)(0 - \dot{y}_B) &= l_1, \\ (x_C - x_B)(0 - \dot{x}_B) + (y_C - y_B)(0 - \dot{y}_B) &= 0,\end{aligned} \tag{4.18}$$

$$C_{pl}^{(x)} = \dot{x}_B = \frac{1}{D}\begin{vmatrix} l_1 & (y_B - y_A) \\ 0 & (y_B - y_C) \end{vmatrix}, \quad C_{pl}^{(y)} = \dot{y}_B = \frac{1}{D}\begin{vmatrix} (x_B - x_A) & l_1 \\ (x_B - x_C) & 0 \end{vmatrix}, \tag{4.19}$$

Dimensional Error $\Delta x_A \left(\dot{l}_1 = 0, \dot{x}_A = 1, \dot{y}_A = 0\right)$

$$\begin{aligned}(x_A - x_B)(1 - \dot{x}_B) + (y_A - y_B)(0 - \dot{y}_B) &= 0, \\ (x_C - x_B)(0 - \dot{x}_B) + (y_C - y_B)(0 - \dot{y}_B) &= 0,\end{aligned} \tag{4.20}$$

$$C_{px_A}^{(x)} = \dot{x}_B = \frac{1}{D}\begin{vmatrix} (x_B - x_A) & (y_B - y_A) \\ 0 & (y_B - y_C) \end{vmatrix}, \quad C_{px_A}^{(y)} = \dot{y}_B = \frac{1}{D}\begin{vmatrix} (x_B - x_A) & (x_B - x_A) \\ (x_B - x_C) & 0 \end{vmatrix}, \tag{4.21}$$

Dimensional Error $\Delta y_A \left(\dot{l}_1 = 0, \dot{x}_A = 0, \dot{y}_A = 1\right)$

$$\begin{aligned}(x_A - x_B)(0 - \dot{x}_B) + (y_A - y_B)(1 - \dot{y}_B) &= 0, \\ (x_C - x_B)(0 - \dot{x}_B) + (y_C - y_B)(0 - \dot{y}_B) &= 0,\end{aligned} \tag{4.22}$$

$$C_{py_A}^{(x)} = \dot{x}_B = \frac{1}{D}\begin{vmatrix} (y_B - y_A) & (y_B - y_A) \\ 0 & (y_B - y_C) \end{vmatrix}, \quad C_{py_A}^{(y)} = \dot{y}_B = \frac{1}{D}\begin{vmatrix} (x_B - x_A) & (y_B - y_A) \\ (x_B - x_C) & 0 \end{vmatrix}, \tag{4.23}$$

where

$$D = \begin{vmatrix} (x_B - x_A) & (y_B - y_A) \\ (x_B - x_C) & (y_B - y_C) \end{vmatrix}. \tag{4.24}$$

The position sensitivity coefficients of node B due to dimensional errors $\Delta l, \Delta x_A, \Delta y_A$ can be computed via *Equations* (4.19), (4.21) and (4.23). Observe that they are identical to the expressions derived in *Chapter* 3 (viz. *Equations* (3.5a), (3.6a) and (3.7a)) based on a different formulation. Further time differentiation yields the velocity and acceleration sensitivity coefficients. The results should be identical to those presented in *Chapter* 3 (*Equations* (3.5b, c), (3.6b, c) and (3.7b, c)) and thus, are not repeated here.

4.3.3 Computation of Sensitivity Coefficients for Dyad Mechanisms

The next step is to demonstrate the procedure for a "full-blown" planar mechanism and the dyad mechanism is illustrated first. Consider the 1-dof planar dyad mechanism sketched in *Figure* 4.1 (a). It is composed of 3 RRR dyads with link ① being the driver. To calculate the sensitivity coefficients with respect to the position, velocity and acceleration due to say, Δl_1, for all the joints, a fictitious slide in direction of the dimensional error is inserted in link ① as depicted in *Figure* 4.1 (b). The partial terms are then evaluated by setting the virtual velocity $\dot{l}_1 = 0$ or ± 1; and using *Equations* (4.6), (4.11) and (4.16), the 3 kinematic sensitivity coefficients are readily computed.

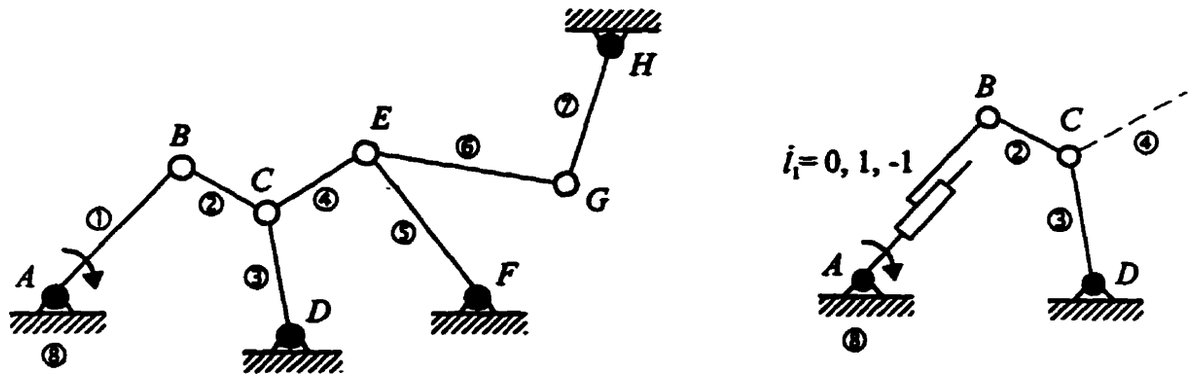

(a) original mechanism (b) supplemental mechanism

Figure 4.1: An eight-bar dyad mechanism.

4.4 COMPUTATION OF SENSITIVITY COEFFICIENTS FOR NON-DYAD MECHANISMS

To demonstrate the process of computing the kinematic sensitivity coefficients for a complex non-dyad mechanism, the 1-dof, 22-bar linkage of *Chapter* 2 is adopted again. As illustrated in *Figure* 4.2, the driver is link ①. It is required to compute the position, velocity and acceleration sensitivity coefficients of any moving joint J ($J = 1, \cdots, 31$; other than the numbers representing the *fixed* joints) due to the dimensional error Δl_{3-5} in the ternary link ③. Clearly, this is not as easy a task as in all the previous examples considered up to now.

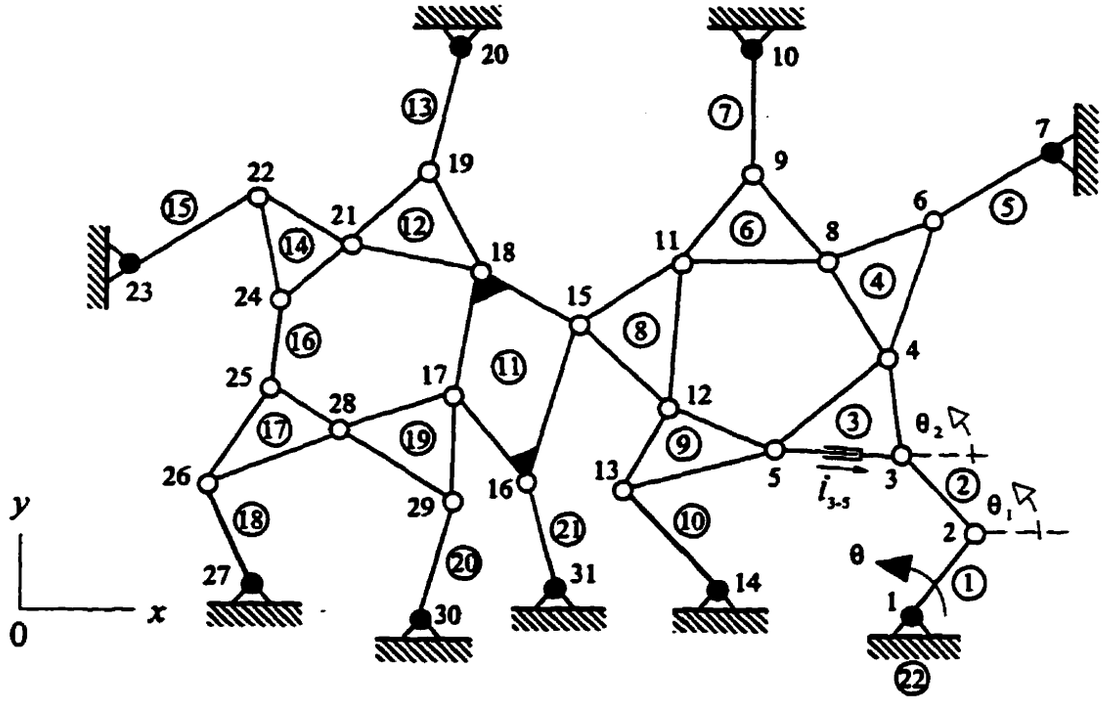

Figure 4.2: A 22-bar non-dyad linkage.

A supplemental 2-dof linkage is created from the original mechanism by inserting a fictitious slider in the ternary link ③ as depicted. Next, velocity, acceleration and jerk analyses are performed on the supplemental linkage using the virtual input $\dot{l}_{3-5} = 0$ or ± 1. Unfortunately,

the supplemental linkage is a non-dyad linkage and its kinematic analysis requires special handling. The novel method that employs disconnected links/pairs with prescribed dyad drivers and coded into the computer program **NDPLAn** described in *Chapter* 2, is suitable for usage here. Adopting this approach, the supplemental non-dyad linkage is transformed into a dyad mechanism by disconnecting links ⑩ and ⑱ and prescribing 2 dyad drivers θ_1 and θ_2 for the 2-dof supplemental linkage. The coordinates of joints 13 and 14 (of link ⑩), and joints 26 and 27 (of link ⑱) must satisfy the link-length condition:

$$\begin{aligned}(x_{13}-x_{14})^2+(y_{13}-y_{14})^2 &= l_{13\text{-}14}^2,\\ (x_{26}-x_{27})^2+(y_{26}-y_{27})^2 &= l_{26\text{-}27}^2.\end{aligned} \tag{4.25}$$

The velocity, acceleration and jerk of the pairs 13 and 14, and 26 and 27, can be derived by differentiating *Equation* (4.25) to yield the following 3 sets of equations representing:

Link-Velocity Condition

$$\begin{aligned}(x_{13}-x_{14})(\dot{x}_{13}-\dot{x}_{14})+(y_{13}-y_{14})(\dot{y}_{13}-\dot{y}_{14}) &= 0,\\ (x_{26}-x_{27})(\dot{x}_{26}-\dot{x}_{27})+(y_{26}-y_{27})(\dot{y}_{26}-\dot{y}_{27}) &= 0.\end{aligned} \tag{4.26}$$

Link-Acceleration Condition

$$\begin{aligned}(\dot{x}_{13}-\dot{x}_{14})^2+(x_{13}-x_{14})(\ddot{x}_{13}-\ddot{x}_{14})+(\dot{y}_{13}-\dot{y}_{14})^2+(y_{13}-y_{14})(\ddot{y}_{13}-\ddot{y}_{14}) &= 0,\\ (\dot{x}_{26}-\dot{x}_{27})^2+(x_{26}-x_{27})(\ddot{x}_{26}-\ddot{x}_{27})+(\dot{y}_{26}-\dot{y}_{27})^2+(y_{26}-y_{27})(\ddot{y}_{26}-\ddot{y}_{27}) &= 0.\end{aligned} \tag{4.27}$$

Link-Jerk Condition

$$\begin{aligned}(x_{13}-x_{14})(\dddot{x}_{13}-\dddot{x}_{14})+3(\dot{x}_{13}-\dot{x}_{14})(\ddot{x}_{13}-\ddot{x}_{14})&\\ +(y_{13}-y_{14})(\dddot{y}_{13}-\dddot{y}_{14})+3(\dot{y}_{13}-\dot{y}_{14})(\ddot{y}_{13}-\ddot{y}_{14}) &= 0,\\ (x_{26}-x_{27})(\dddot{x}_{26}-\dddot{x}_{27})+3(\dot{x}_{26}-\dot{x}_{27})(\ddot{x}_{26}-\ddot{x}_{27})&\\ +(y_{26}-y_{27})(\dddot{y}_{26}-\dddot{y}_{27})+3(\dot{y}_{26}-\dot{y}_{27})(\ddot{y}_{26}-\ddot{y}_{27}) &= 0.\end{aligned} \tag{4.28}$$

The partial terms pertaining to the velocity, acceleration and jerk of joint J of transformed dyad linkage with prescribed inputs θ_1 and θ_2 can be obtained via the principle of superposition and the results are,

Velocity Partial Terms

$$\begin{aligned} \dot{x}_J &= \dot{x}_{1J} + \dot{x}_{2J}\dot{\theta}_1 + \dot{x}_{3J}\dot{\theta}_2, \\ \dot{y}_J &= \dot{y}_{1J} + \dot{y}_{2J}\dot{\theta}_1 + \dot{y}_{3J}\dot{\theta}_2. \end{aligned} \tag{4.29}$$

Acceleration Partial Terms

$$\begin{aligned} \ddot{x}_J^{(1)} &= \ddot{x}_{1J}^{(1)} + \dot{x}_{2J}\ddot{\theta}_1^{(1)} + \dot{x}_{3J}\ddot{\theta}_2^{(1)}, \\ \ddot{y}_J^{(1)} &= \ddot{y}_{1J}^{(1)} + \dot{y}_{2J}\ddot{\theta}_1^{(1)} + \dot{y}_{3J}\ddot{\theta}_2^{(1)}, \end{aligned} \tag{4.30}$$

$$\begin{aligned} \ddot{x}_J^{(2)} &= \ddot{x}_{1J}^{(2)} + \dot{x}_{2J}\ddot{\theta}_1^{(2)} + \dot{x}_{3J}\ddot{\theta}_2^{(2)}, \\ \ddot{y}_J^{(2)} &= \ddot{y}_{1J}^{(2)} + \dot{y}_{2J}\ddot{\theta}_1^{(2)} + \dot{y}_{3J}\ddot{\theta}_2^{(2)}, \end{aligned} \tag{4.31}$$

$$\begin{aligned} \ddot{x}_J^{(3)} &= \ddot{x}_{1J}^{(3)} + \dot{x}_{2J}\ddot{\theta}_1^{(3)} + \dot{x}_{3J}\ddot{\theta}_2^{(3)}, \\ \ddot{y}_J^{(3)} &= \ddot{y}_{1J}^{(3)} + \dot{y}_{2J}\ddot{\theta}_1^{(3)} + \dot{y}_{3J}\ddot{\theta}_2^{(3)}. \end{aligned} \tag{4.32}$$

Jerk Partial Terms

$$\begin{aligned} \dddot{x}_J^{(1)} &= \dddot{x}_{1J}^{(1)} + \dot{x}_{2J}\dddot{\theta}_1^{(1)} + \dot{x}_{3J}\dddot{\theta}_2^{(1)}, \\ \dddot{y}_J^{(1)} &= \dddot{y}_{1J}^{(1)} + \dot{y}_{2J}\dddot{\theta}_1^{(1)} + \dot{y}_{3J}\dddot{\theta}_2^{(1)}, \end{aligned} \tag{4.33}$$

$$\begin{aligned} \dddot{x}_J^{(2)} &= \dddot{x}_{1J}^{(2)} + \dot{x}_{2J}\dddot{\theta}_1^{(2)} + \dot{x}_{3J}\dddot{\theta}_2^{(2)}, \\ \dddot{y}_J^{(2)} &= \dddot{y}_{1J}^{(2)} + \dot{y}_{2J}\dddot{\theta}_1^{(2)} + \dot{y}_{3J}\dddot{\theta}_2^{(2)}, \end{aligned} \tag{4.34}$$

$$\begin{aligned} \dddot{x}_J^{(3)} &= \dddot{x}_{1J}^{(3)} + \dot{x}_{2J}\dddot{\theta}_1^{(3)} + \dot{x}_{3J}\dddot{\theta}_2^{(3)}, \\ \dddot{y}_J^{(3)} &= \dddot{y}_{1J}^{(3)} + \dot{y}_{2J}\dddot{\theta}_1^{(3)} + \dot{y}_{3J}\dddot{\theta}_2^{(3)}. \end{aligned} \tag{4.35}$$

in which

$\dot{x}_{1J}, \dot{y}_{1J}$ - velocity components evaluated by setting $\dot{\theta} = \dot{\theta}_1 = \dot{\theta}_2 = 0$ and $\dot{l}_{3-5} = 1$;

$\dot{x}_{2J}, \dot{y}_{2J}$ - velocity components evaluated by setting $\dot{\theta} = \dot{\theta}_2 = \dot{l}_{3-5} = 0$ and $\dot{\theta}_1 = 1$;

$\dot{x}_{3J}, \dot{y}_{3J}$ - velocity components evaluated by setting $\dot{\theta} = \dot{\theta}_1 = \dot{l}_{3-5} = 0$ and $\dot{\theta}_2 = 1$;

$\ddot{x}_{1J}^{(1)}, \ddot{y}_{1J}^{(1)}$ - acceleration components evaluated by setting $\dot{\theta} = \ddot{\theta} = \dot{\theta}_1^{(1)} = \ddot{\theta}_1^{(1)} = \dot{\theta}_2^{(1)} = \ddot{\theta}_2^{(1)} = 0$ and $\dot{l}_{3-5} = 1$;

$\ddot{x}_{1J}^{(2)}, \ddot{y}_{1J}^{(2)}$ - acceleration components evaluated using given values of $\dot{\theta}$ and $\ddot{\theta}$, and setting $\dot{\theta}_1^{(2)} = \ddot{\theta}_1^{(2)} = \dot{\theta}_2^{(2)} = \ddot{\theta}_2^{(2)} = \dot{l}_{3-5} = 0$;

$\ddot{x}_{1J}^{(3)}, \ddot{y}_{1J}^{(3)}$ - acceleration components evaluated using given values of $\dot{\theta}$ and $\ddot{\theta}$, and setting $\dot{\theta}_1^{(3)} = \ddot{\theta}_1^{(3)} = \dot{\theta}_2^{(3)} = \ddot{\theta}_2^{(3)} = 0$, and $\dot{l}_{3-5} = 1$;

$\dddot{x}_{1J}^{(1)}, \dddot{y}_{1J}^{(1)}$ - jerk components evaluated by setting $\dot{\theta} = \ddot{\theta} = \dddot{\theta} = \dot{\theta}_1^{(1)} = \ddot{\theta}_1^{(1)} = \dddot{\theta}_1^{(1)} = 0$, $\dot{\theta}_2^{(1)} = \ddot{\theta}_2^{(1)} = \dddot{\theta}_2^{(1)} = 0$, and $\dot{l}_{3-5} = 1$;

$\dddot{x}_{1J}^{(2)}, \dddot{y}_{1J}^{(2)}$ - jerk components evaluated using given values of $\dot{\theta}$ and $\ddot{\theta}$, and setting $\dddot{\theta} = \dot{\theta}_1^{(2)} = \ddot{\theta}_1^{(2)} = \dddot{\theta}_1^{(2)} = \dot{\theta}_2^{(2)} = \ddot{\theta}_2^{(2)} = \dddot{\theta}_2^{(2)} = 0$, and $\dot{l}_{3-5} = -1$;

$\dddot{x}_{1J}^{(3)}, \dddot{y}_{1J}^{(3)}$ - Jerk components evaluated using given values of $\dot{\theta}$ and $\ddot{\theta}$, and setting $\dddot{\theta} = \dot{\theta}_1^{(3)} = \ddot{\theta}_1^{(3)} = \dddot{\theta}_1^{(3)} = \dot{\theta}_2^{(3)} = \ddot{\theta}_2^{(3)} = \dddot{\theta}_2^{(3)} = 0$, and $\dot{l}_{3-5} = 1$.

Note that the superscripts (1), (2) and (3) in the adopted notations refer respectively to the first, second and third partial terms of the corresponding kinematic term. Assuming the joint positions of the 2 disconnected links have already been solved (via *Equations* (4.25)), *Equation* (4.29) can be substituted repeatedly for J=13, 14, 26 and 27 into the link-velocity condition in *Equation* (4.26), to obtain the 2 linear equations for the determination of the unknowns $\dot{\theta}_1$ and $\dot{\theta}_2$ of the supplemental linkage. Similarly, *Equations* (4.30)-(4.32) can be substituted repeatedly for J=13, 14 26 and 27 into the link-acceleration condition given by *Equation* (4.27), to arrive at the 2 linear equations for solving $\ddot{\theta}_1^{(1)}, \ddot{\theta}_2^{(1)}, \ddot{\theta}_1^{(2)}, \ddot{\theta}_2^{(2)}, \ddot{\theta}_1^{(3)}, \ddot{\theta}_2^{(3)}$ of the supplemental linkage. The remaining unknowns $\dddot{\theta}_1^{(1)}, \dddot{\theta}_2^{(1)}, \dddot{\theta}_1^{(2)}, \dddot{\theta}_2^{(2)}, \dddot{\theta}_1^{(3)}, \dddot{\theta}_2^{(3)}$ may likewise,

be found via *Equations* (4.33)-(4.35) for J=13, 14 26 and 27 and the link-jerk condition of *Equation* (4.28). Once all the unknown terms have been evaluated, they can be substituted into *Equations* (4.29)-(4.35), to enable the kinematic partial terms of any joint to be determined. Finally, the position, velocity and acceleration sensitivity coefficients of any moving joint J due to dimensional error Δl_{3-5} can be readily computed using *Equations* (4.6), (4.11) and (4.16), respectively. The results are,

Position Sensitivity Coefficients

$$\begin{aligned} C_{p_J}^{(x)} &= \dot{x}_J, \\ C_{p_J}^{(y)} &= \dot{y}_J. \end{aligned} \tag{4.36}$$

Velocity Sensitivity Coefficients

$$\begin{aligned} C_{v_J}^{(x)} &= \frac{\ddot{x}_J^{(3)} - \ddot{x}_J^{(2)} - \ddot{x}_J^{(1)}}{2}, \\ C_{v_J}^{(y)} &= \frac{\ddot{y}_J^{(3)} - \ddot{y}_J^{(2)} - \ddot{y}_J^{(1)}}{2}. \end{aligned} \tag{4.37}$$

Acceleration Sensitivity Coefficients

$$\begin{aligned} C_{a_J}^{(x)} &= \frac{\dddot{x}_J^{(3)} - \dddot{x}_J^{(2)} - 2\dddot{x}_J^{(1)}}{6}, \\ C_{a_J}^{(y)} &= \frac{\dddot{y}_J^{(3)} - \dddot{y}_J^{(2)} - 2\dddot{y}_J^{(1)}}{6}. \end{aligned} \tag{4.38}$$

Obviously, the preceding method can be applied to compute the kinematic sensitivity coefficient of any complex planar mechanisms, dyad or non-dyad, by repeating the process for each of the dimensional error under consideration. Once all sensitivity coefficients have been determined, synthesizing for optimum dimensional tolerancing can be performed in the manner outlined in *Chapter* 3.

4.5 CALCULATIONS OF OUTPUT ERRORS OF A MECHANISM DUE TO ITS INPUT PARAMETERS ERRORS

Having obtained all the kinematic sensitivity coefficients of a mechanism arising from a single or any combinations of dimensional errors, the position, velocity or acceleration output errors of the mechanism can be evaluated. To facilitate the process, these output errors are grouped into 2 types: $\Delta P, \Delta V, \Delta A$ for linear kinematic quantities and $\Delta\theta, \Delta\dot{\theta}, \Delta\ddot{\theta}$ for angular kinematic quantities. They are given by as follows:

$$\Delta P = \begin{Bmatrix} \Delta P_{1x} \\ \Delta P_{1y} \\ \vdots \\ \Delta P_{nx} \\ \Delta P_{ny} \end{Bmatrix} = \begin{bmatrix} c_{p_{1x,1}} & \cdots & c_{p_{1x,n}} \\ c_{p_{1y,1}} & & c_{p_{1y,n}} \\ \vdots & \ddots & \vdots \\ c_{p_{nx,1}} & & c_{p_{nx,n}} \\ c_{p_{ny,1}} & \cdots & c_{p_{ny,n}} \end{bmatrix} \begin{Bmatrix} \Delta q_1 \\ \Delta q_2 \\ \vdots \\ \Delta q_n \end{Bmatrix}, \tag{4.39}$$

$$\Delta V = \begin{Bmatrix} \Delta V_{1x} \\ \Delta V_{1y} \\ \vdots \\ \Delta V_{nx} \\ \Delta V_{ny} \end{Bmatrix} = \begin{bmatrix} c_{v_{1x,1}} & \cdots & c_{v_{1x,n}} \\ c_{v_{1y,1}} & & c_{v_{1y,n}} \\ \vdots & \ddots & \vdots \\ c_{v_{nx,1}} & & c_{v_{nx,n}} \\ c_{v_{ny,1}} & \cdots & c_{v_{ny,n}} \end{bmatrix} \begin{Bmatrix} \Delta q_1 \\ \Delta q_2 \\ \vdots \\ \Delta q_n \end{Bmatrix}, \tag{4.40}$$

$$\Delta A = \begin{Bmatrix} \Delta A_{1x} \\ \Delta A_{1y} \\ \vdots \\ \Delta A_{nx} \\ \Delta A_{ny} \end{Bmatrix} = \begin{bmatrix} c_{a_{1x,1}} & \cdots & c_{a_{1x,n}} \\ c_{a_{1y,1}} & & c_{a_{1y,n}} \\ \vdots & \ddots & \vdots \\ c_{a_{nx,1}} & & c_{a_{nx,n}} \\ c_{a_{ny,1}} & \cdots & c_{a_{ny,n}} \end{bmatrix} \begin{Bmatrix} \Delta q_1 \\ \Delta q_2 \\ \vdots \\ \Delta q_n \end{Bmatrix}, \tag{4.41}$$

$$\Delta\psi = \begin{Bmatrix} \Delta\psi_1 \\ \vdots \\ \Delta\psi_n \end{Bmatrix} = \begin{bmatrix} c_{p_{1,1}} & \cdots & c_{p_{1,n}} \\ \vdots & \ddots & \vdots \\ c_{p_{n,1}} & \cdots & c_{p_{n,n}} \end{bmatrix} \begin{Bmatrix} \Delta q_1 \\ \vdots \\ \Delta q_n \end{Bmatrix}, \tag{4.42}$$

$$\Delta\dot{\psi} = \begin{Bmatrix} \Delta\dot{\psi}_1 \\ \vdots \\ \Delta\dot{\psi}_n \end{Bmatrix} = \begin{bmatrix} c_{v_{1,1}} & \cdots & c_{v_{1,n}} \\ \vdots & \ddots & \vdots \\ c_{v_{n,1}} & \cdots & c_{v_{n,n}} \end{bmatrix} \begin{Bmatrix} \Delta q_1 \\ \vdots \\ \Delta q_n \end{Bmatrix}, \tag{4.43}$$

$$\Delta\ddot{\psi} = \begin{Bmatrix} \Delta\ddot{\psi}_1 \\ \vdots \\ \Delta\ddot{\psi}_n \end{Bmatrix} = \begin{bmatrix} c_{a_{1,1}} & \cdots & c_{a_{1,n}} \\ \vdots & \ddots & \vdots \\ c_{a_{n,1}} & \cdots & c_{a_{n,n}} \end{bmatrix} \begin{Bmatrix} \Delta q_1 \\ \vdots \\ \Delta q_n \end{Bmatrix}. \tag{4.44}$$

4.6 COMPARISON CHECK OF THE COMPUTED OUTPUT ERRORS

In order to assess the accuracy of the proposed method for computing the kinematic sensitivity coefficients and thus, the computed output errors, the 22-bar non-dyad mechanism in *Figure* 4.2 is used again. A link-length error of +0.005 mm is specified on each side of ternary link ③ and the resulting actual dimensions are summarized in *Table* 4.4. Note that for performing the test, we have assumed only a positive dimensional error.

Table 4.4: A prescribed dimensional error +0.005 mm in ternary link ③.

Link ③	Nominal Dimension	Actual Dimension
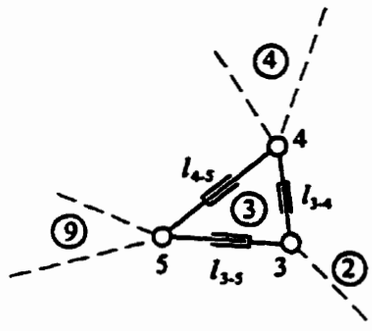	$l_{3-4} = 25.4951$	$l_{3-4} = 25.5001$
	$l_{3-5} = 25.4951$	$l_{3-5} = 25.5001$
	$l_{4-5} = 28.2843$	$l_{4-5} = 28.2893$

The test consists of two independent parts. In the first part, the method of virtual velocity is employed to calculate the kinematic sensitivity coefficients based on the nominal dimensions of the mechanism and the prescribed dimensional error. From these coefficients, the output position, velocity and acceleration error bands are computed using *Equations* (4.39)-(4.41) for a joint, and *Equations* (4.42)-(4.44) for a link. In the second part, the kinematic analysis program **NDPLAn** (in *Chapter* 2) is used to calculate the position, velocity and acceleration values based on the *actual* (i.e. nominal plus error) link dimensions as input parameters. The results of these two parts are then compared to see if good agreement between them is obtained. *Figures* 4.3-4.6 depict the position, velocity and acceleration of joint 15, and the angular velocity and angular acceleration of links ③, ⑪ and ⑯. Observe that the results from these two independent checks agree almost perfectly, and thus, confirm the accuracy of the proposed method for computing the kinematic sensitivity coefficients. In the next section, we will discuss how to employ the technique to synthesize for optimum dimensional tolerancing of complex planar mechanisms.

4.7 SYNTHESIS FOR OPTIMUM DIMENSIONAL TOLERANCES

To carry out the process of optimization, the flowchart sketched in *Figure* 3.5 of the previous chapter can be re-used. This implies that the framework for this section can be taken from *Section* 3.5. Since the bulk of the materials has already been presented in that section, it is unnecessary to repeat it in here again. However, it is strongly encouraged that the reader be re-acquainted with that section. Specifically, the reader should be familiar with the concepts and notations employed not only in the main *Section* 3.5, but also, as used in its sub-*Sections* 3.5.1 and 3.5.2 on the *identification of the most sensitive error combination* and the procedure for *optimum dimensional tolerancing*, respectively. It should also be pointed out that in the implementation of the search algorithm used for non-dyad mechanisms, it was found that a more robust algorithm compared to the one perfected for dyad mechanisms of the previous

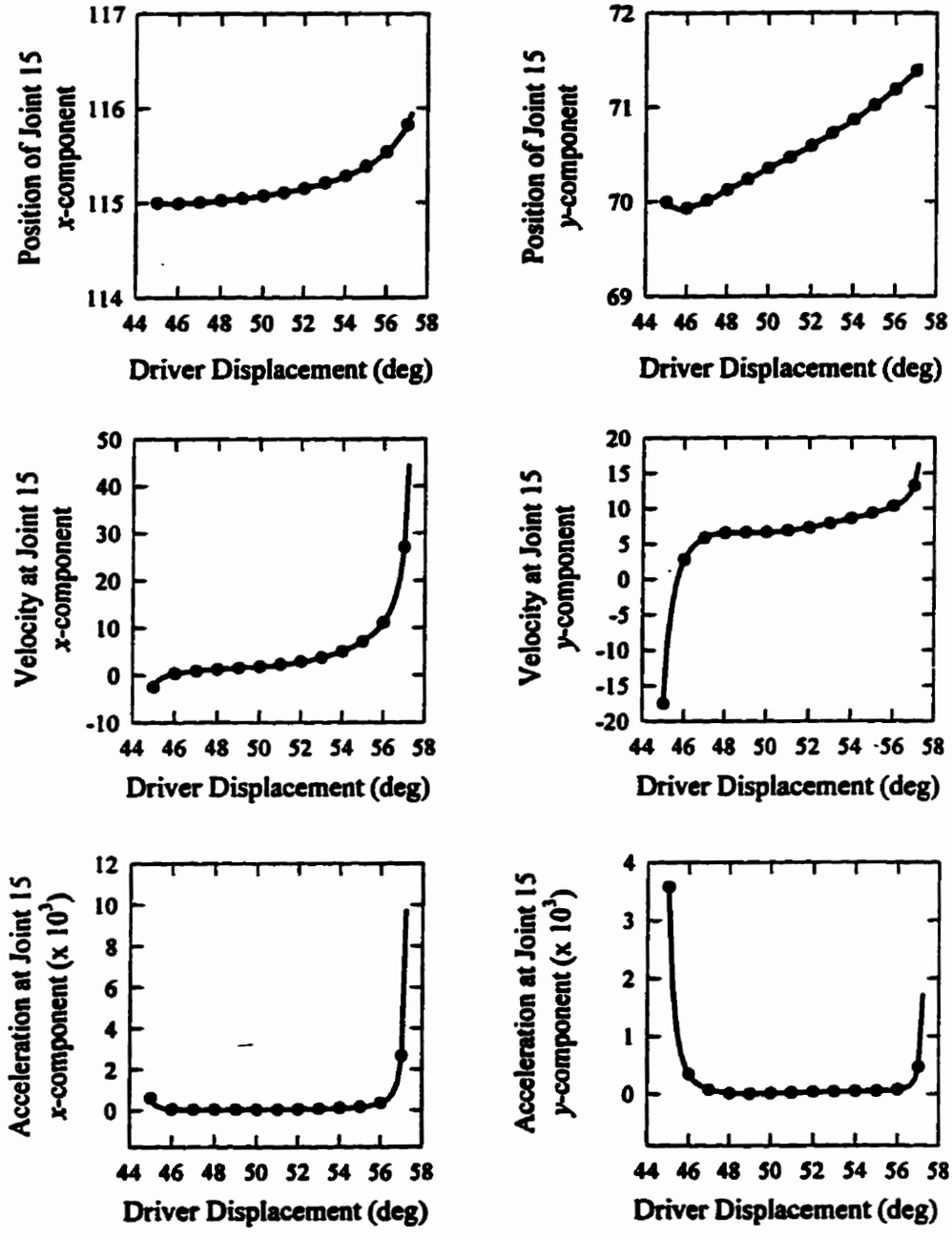

Figure 4.3: Comparison of position, velocity and acceleration at joint 15 (——— Error Analysis, ●●● NDPLAn).

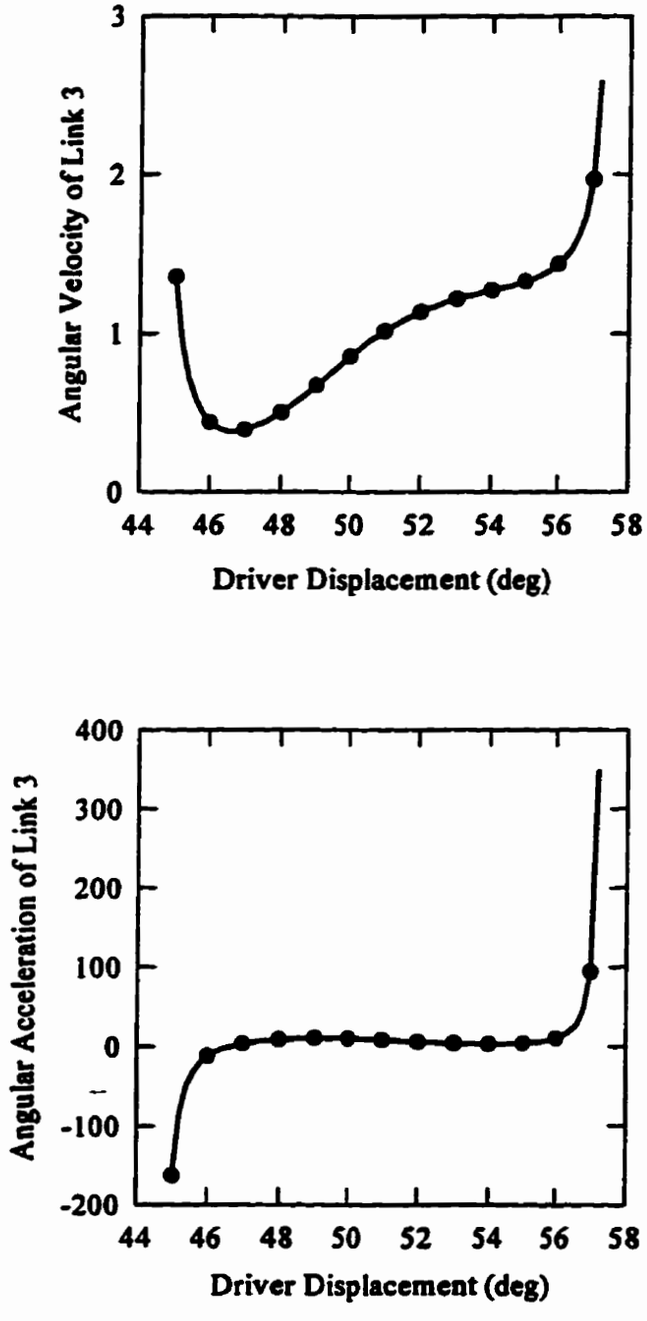

Figure 4.4: Comparison of angular velocity and angular acceleration for link ③ (—— Error Analysis, ●●● NDPLAn).

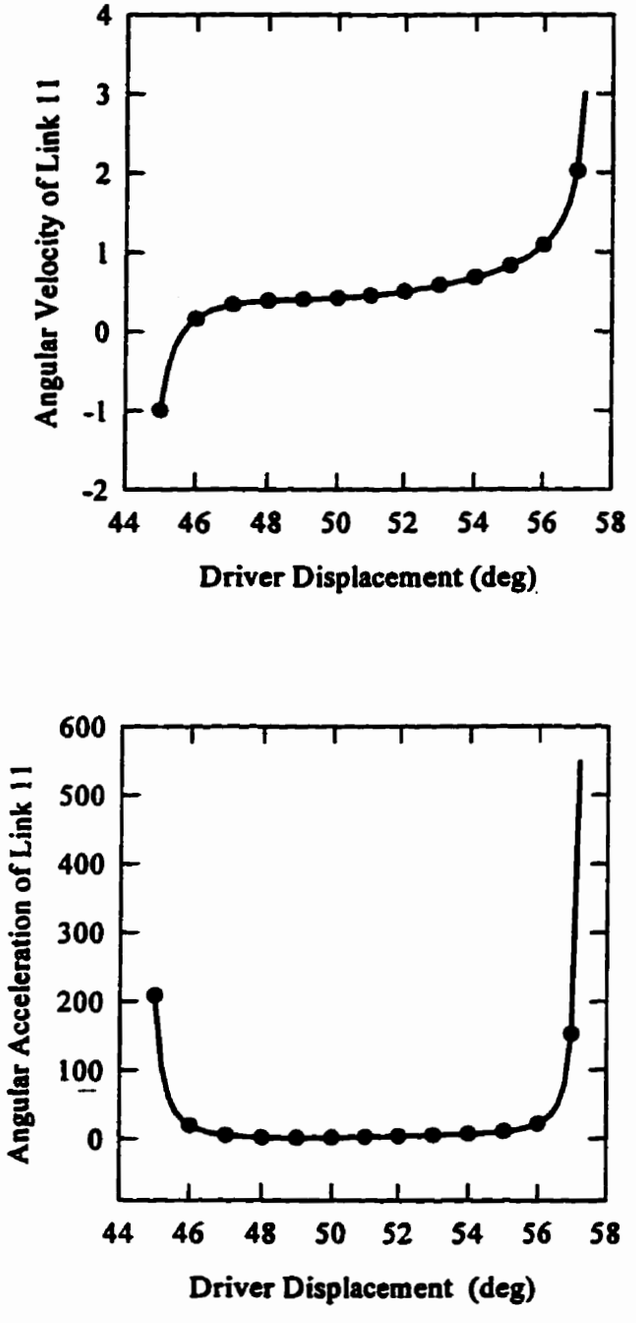

Figure 4.5: Comparison of angular velocity and angular acceleration of link ⑪ (——Error Analysis, ●●● NDPLAn).

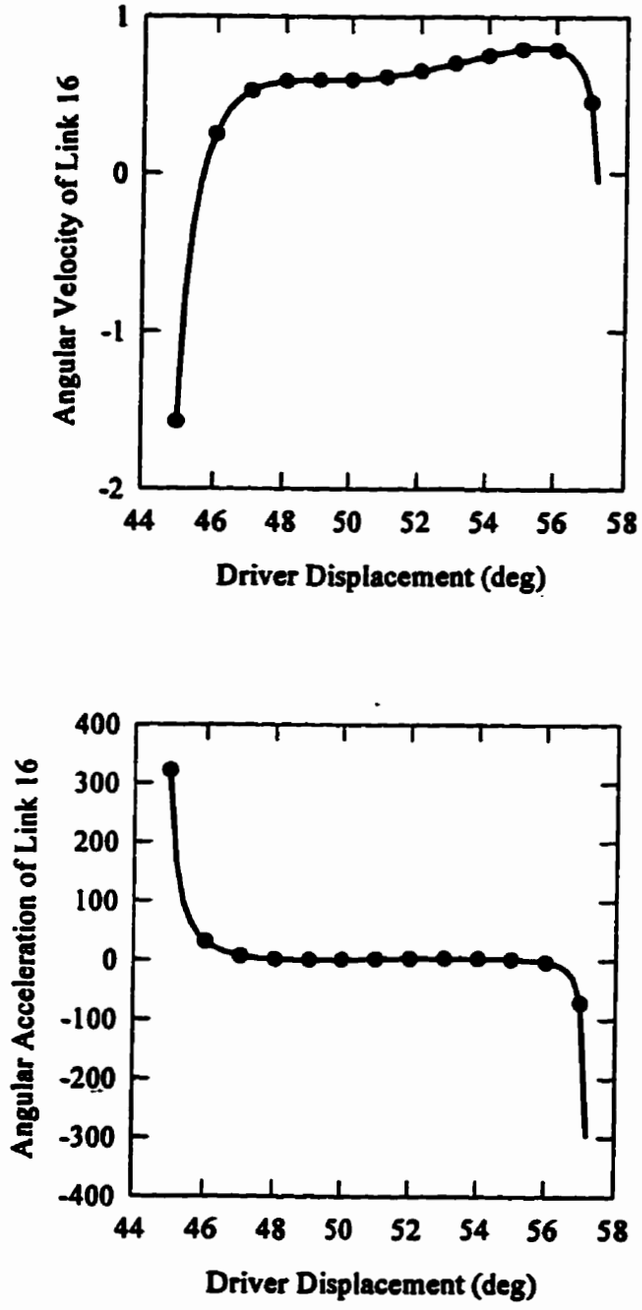

Figure 4.6: Comparison of angular velocity and angular acceleration of link ⑯ (——Error Analysis, ●●● NDPLAn).

chapter is required, and consequently, an improved algorithm for the quadratic polynomial approach has been developed for this section. The improved algorithm ensures that the value of objective function not only converges properly but also, rapidly. The flowchart of the improved algorithm, consisting of 3 parts: (a), (b) and (c), is drawn in *Figure* 4.7. Part (a) depicts the search for extremum values, Part (b) characterizes the approximate extremum values using an interpolation technique, and Part (c) modifies the value of objective function and the length of search step. The entire cycle of iteration is repeated until the value of objective function satisfies the prescribed tolerance ε .

4.8 A NUMERICAL EXAMPLE

To illustrate the process of synthesizing for optimum dimensional tolerancing, the 2-loop, 6-bar non-dyad linkage introduced in *Chapter* 2 is re-used here. The mechanism and its MN incidence matrix are given in *Figure* 4.8. The latter information is required since we will be using the method of disconnected link and prescribed dyad drivers (see *Chapter* 2) to solve for the kinematics of the original and supplemental non-dyad mechanisms. In the synthesis of the final design, the tolerance bands for input parameters based on the specified output error limits are determined and from these results, the smallest one chosen. Since the proposed method is capable of handling higher-order error sensitivity analysis, the tolerance bands will be computed based on the position, velocity and acceleration requirements. Noting that tolerance bands are always specified with binary signs, we will use the direct approach developed in *Section* 3.5.1, to identify the most sensitive error combinations instead of carrying out a very computationally demanding task of checking all 2^{13} combinations at every motion increment of the 6-bar linkage. Recall that in this direct approach, no computations are required. Also, we will adopt the standard practice of grouping tolerance bands of similar types together and prescribe within each group, tolerance values that are proportional to a suitably selected but still to be solved error parameter. The chosen objective function employed for the optimization is given by the sum-square of the actual maximum and minimum output errors based on the most sensitive error combinations (see *Equation* (3.21)).

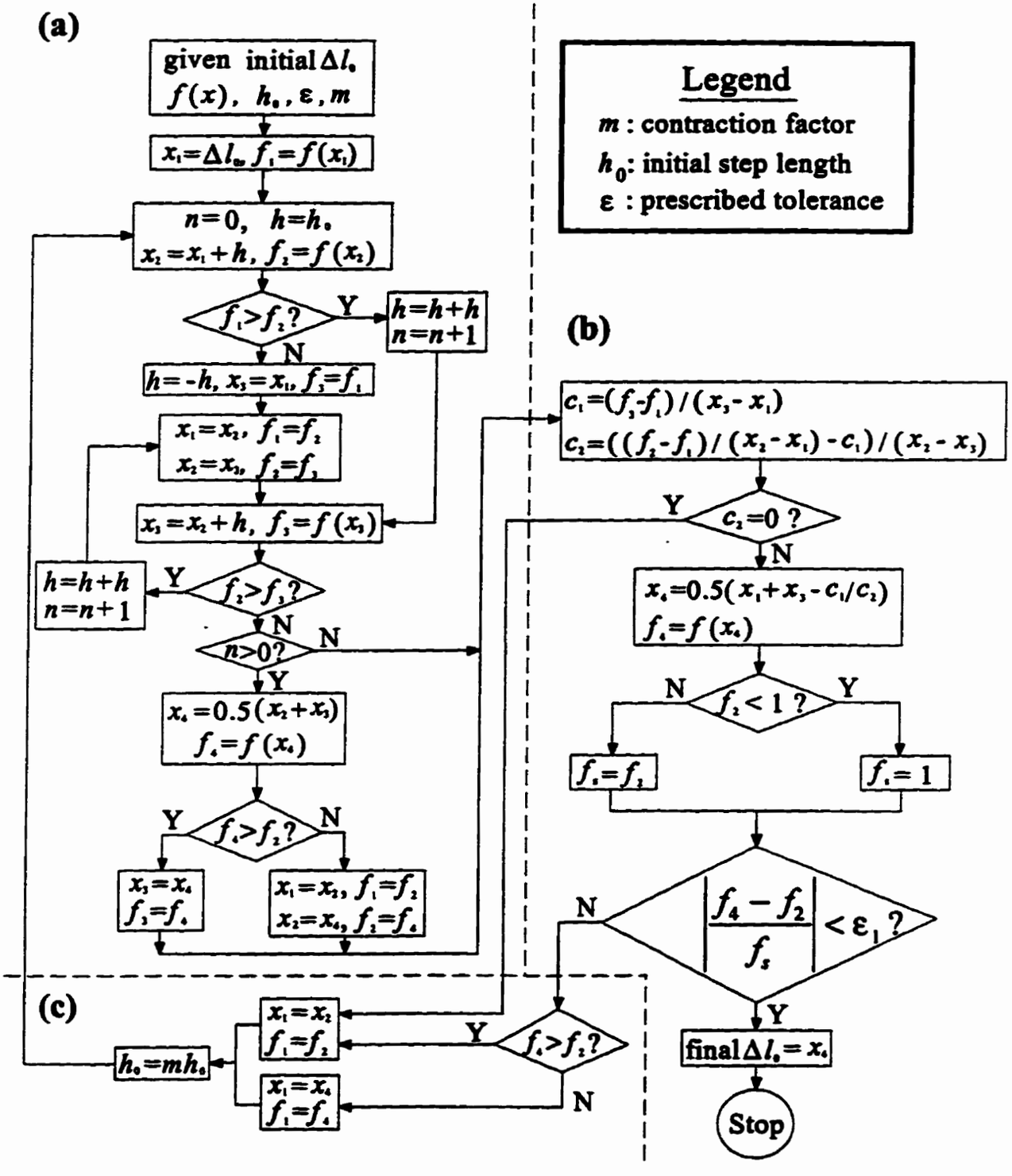

Figure 4.7: Flowchart for the improved quadratic polynomial approach.

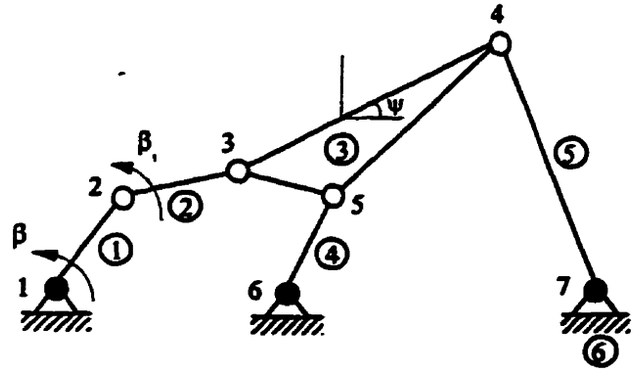

MN MATRIX

$$\begin{bmatrix} 1 & 1 & 0 & 0 & 0 & 0 & 0 \\ 0 & 1 & 1 & 0 & 0 & 0 & 0 \\ 0 & 0 & 1 & 1 & 1 & 0 & 0 \\ 0 & 0 & 0 & 0 & 1 & 1 & 0 \\ 0 & 0 & 0 & 1 & 0 & 0 & 1 \\ 1 & 0 & 0 & 0 & 0 & 1 & 1 \end{bmatrix}$$

Figure 4.8: A 6-bar non-dyad mechanism with its MN incidence matrix.

The link lengths and the joint coordinates are tabulated in *Table* 4.5. Based on this information and normalizing with respect to l_{3-4}, the following weighting factors $k_1,\cdots,k_{13}$ where $k_1 = l_{1-2}/l_{3-4} = 0.25$, $k_2 = l_{2-3}/l_{3-4} = 0.375$, $k_3 = l_{3-4}/l_{3-4} = 1$, $k_4 = l_{3-5}/l_{3-4} = 0.3125$, $k_5 = l_{4-5}/l_{3-4} = 0.75$, $k_6 = l_{5-6}/l_{3-4} = 0.25$, $k_7 = l_{4-7}/l_{3-4} = 0.625$, for the links; and $k_8 = k_9 = 0$, $k_{10} = k_{11} = 1$, and $k_{12} = k_{13} = 2$ for the fixed joints; are computed for use in performing the synthesis of the dimensional tolerance bands.

Table 4.5: Link lengths and joint positions for the 6-bar non-dyad mechanism.

Known Joint Positions

Joint	x	y
1	1.0	0.0
6	2.0	0.0
7	3.0	0.0

Link Lengths

①: L_{1-2}	0.4	③: L_{3-5}	0.5	⑤: L_{4-7}	1.0
②: L_{2-3}	0.6	③: L_{4-5}	1.2	⑥: L_{1-6}	1.0
③: L_{3-4}	1.6	④: L_{5-6}	0.4	⑥: L_{6-7}	1.0

The position, velocity and acceleration requirements are prescribed by assuming the same numerical value for all maximum allowable output error bands, as the driver-link turns from 60^0 at its starting position to 210^0 at its final position. That is,

$$\begin{aligned} \left|(\Delta\psi_3)_{max}\right| &= 0.02 \text{ rad}, \\ \left|(\Delta\dot{\psi}_3)_{max}\right| &= 0.02 \text{ rad/s}, \\ \left|(\Delta\ddot{\psi}_3)_{max}\right| &= 0.02 \text{ rad/s}^2. \end{aligned} \tag{4.45}$$

It is required to synthesize the optimum tolerance band Δl_0 corresponding to specified values of $\langle \Delta x_0, \Delta y_0 \rangle^T = 0.00025,\ 0.00050,\ 0.00075,\ 0.001$. All output angular position, velocity and acceleration sensitivity coefficients of link ③, corresponding to a dimensional error in each of the link (or edge for link ③) and in each of the fixed joint (both x and y directions), for a total of 13 inputs are plotted in *Figure* 4.9. Multiplying these coefficients with their respective weighting factors $k_1, \cdots, k_{13}$, the weighted sensitivity coefficients from the maximum and minimum error combinations are determined and the results graphed in *Figure* 4.10. It is obvious from this plot that the maximum/minimum weighted sensitivity coefficient pair calculated based on the acceleration requirement is the largest and thus, would be expected to govern in the final design selection.

The results of the dimensional optimization are summarized in *Table* 4.6. As listed, the values of Δl_0 determined from the position, velocity and acceleration requirements are given. As a gauge of the accuracy of the computed values of Δl_0, their respective convergence errors in the objective function $f(\Delta l_0)$ are also provided. Note that the missing $\Delta l_0, f(\Delta l_0)$ values for $\langle \Delta x_0, \Delta y_0 \rangle^T = 0.00075$ and 0.001 are due to the negative contributions of Δl_0. This situation arises for these two cases because the input error from Δx_1, Δy_1, Δx_4, Δy_4, Δx_7 and Δy_7 is already larger than the maximum allowable output error from $\Delta W_9 \left(\equiv \left|(\Delta\ddot{\psi}_3)_{max}\right|\right)$. That is,

$$\left|(C_{9,8}k_8\Delta x_0 + C_{9,9}k_9\Delta y_0 + C_{9,10}k_{10}\Delta x_0 + C_{9,11}k_{11}\Delta y_0 + C_{9,12}k_{12}\Delta x_0 + C_{9,13}k_{13}\Delta y_0)_{max}\right| > \left|(\Delta\ddot{\psi}_3)_{max}\right|.$$

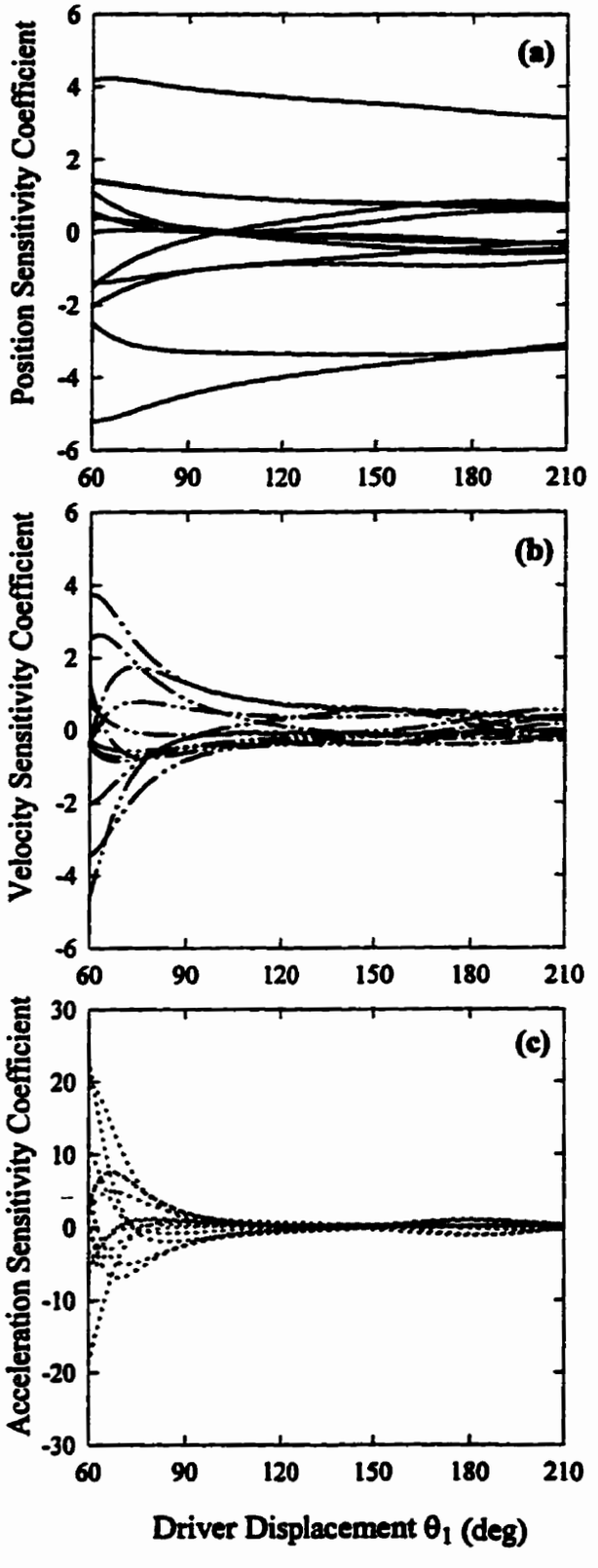

Figure 4.9: Angular kinematic sensitivity coefficients of link ③ for the 6-bar non-dyad linkage.

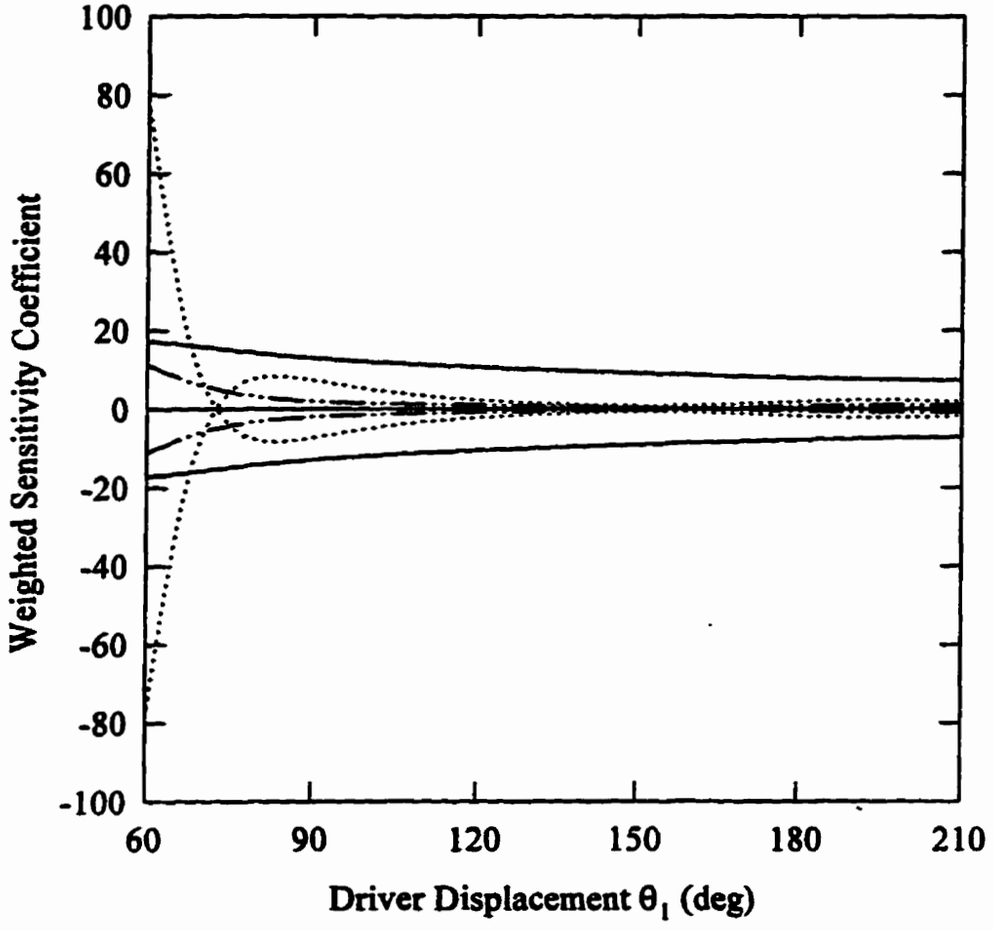

Figure 4.10: Maximum/minimum weighted sensitivity coefficient pairs for the 6-bar non-dyad linkage (——— position, —··—··— velocity, ····· acceleration).

Choosing the smallest value of Δl_0 for use in the final design, it is clear from *Table* 4.6 that the value based on the acceleration requirement governs and therefore, must be used for computing the tolerance bands of all the links in the mechanism. *Table* 4.7 depicts the final design lengths of the various links, together with their respective tolerance bands for the two cases of $\langle \Delta x_0, \Delta y_0 \rangle^T = 0.00025$ and 0.00050. Note that the actual signs of the tolerance bands are chosen in accordance to the respective signs of the sensitivity coefficients.

Table 4.6: Optimization results for the 6-bar non-dyad linkage.

$\Delta x_0, \Delta y_0$	Position		Velocity		Acceleration	
	Δl_0 (10^{-3})	$f(\Delta l_0)$ (10^{-6})	Δl_0 (10^{-3})	$f(\Delta l_0)$ (10^{-6})	Δl_0 (10^{-3})	$f(\Delta l_0)$ (10^{-6})
0.00025	3.5865	1.0812	3.2557	0.1687	0.2494	0.6466
0.00050	3.2571	0.8465	3.0141	0.2627	0.1080	0.2542
0.00075	2.9752	0.9829	2.7694	0.3440	-	-
0.00100	2.6750	0.8025	2.5381	0.3794	-	-

Table 4.7: Tolerance bands for the final design of the 6-bar non-dyad linkage.

Nominal Link Length	$\Delta l_i \left(10^{-3}\right)$	
	$\Delta x_0 = \Delta y_0 = 0.00025$	$\Delta x_0 = \Delta y_0 = 0.00050$
$l_1 = 0.40$	±0.0624	±0.0270
$l_2 = 0.60$	±0.0935	±0.0405
$l_3 = 1.60$	∓0.2494	∓0.1080
$l_4 = 0.50$	±0.0780	±0.0338
$l_5 = 1.20$	±0.1871	±0.0810
$l_6 = 0.40$	±0.0624	±0.0270
$l_7 = 1.00$	∓0.1559	∓0.0675

Using the designed link lengths, the final output motion characteristics computed based on the governing acceleration requirement are plotted in *Figure* 4.11. Observe that they all conform to within the prescribed maximum/minimum output tolerance bands. The final design is therefore, a valid and an acceptable mechanism.

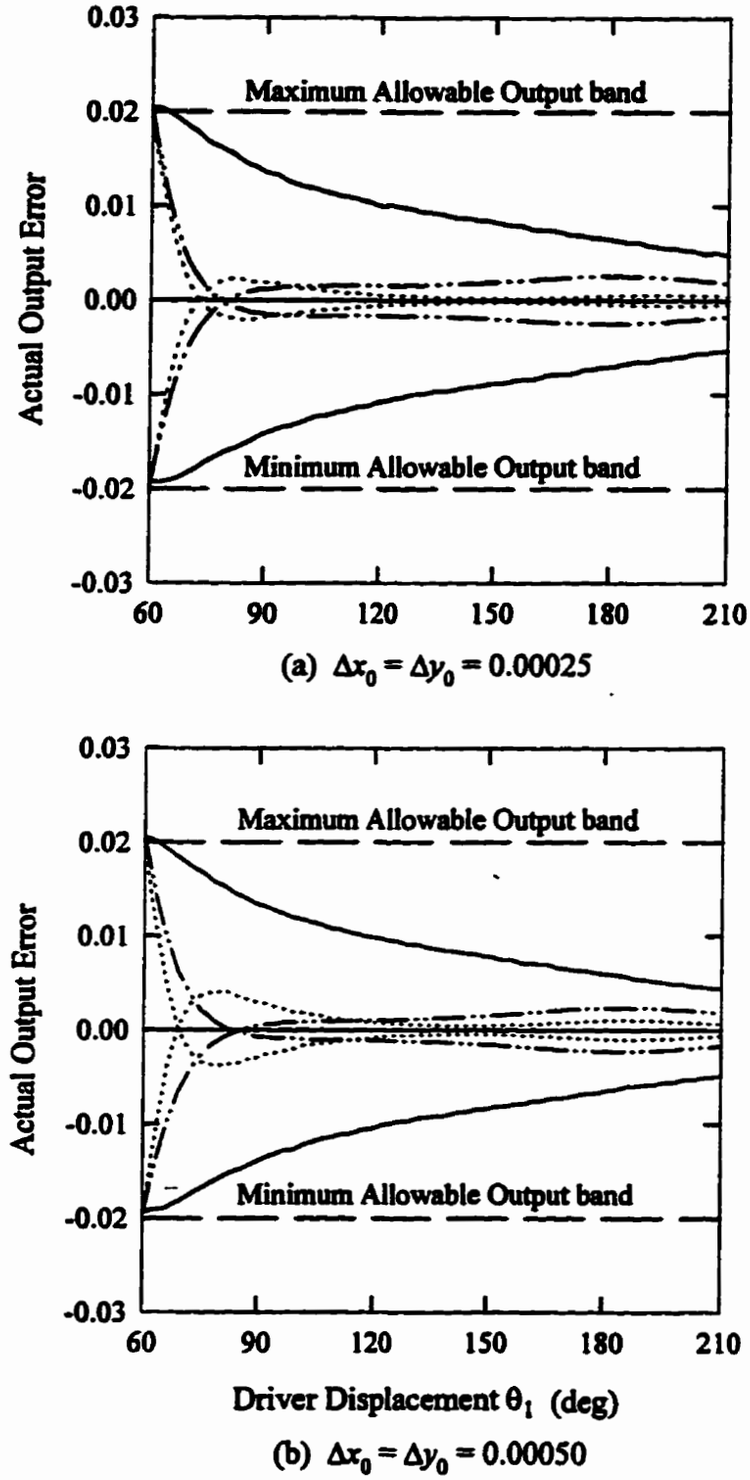

Figure 4.11: Final motion characteristics for the 6-bar non-dyad linkage (——— position, —·—·— velocity, ····· acceleration).

4.9 CONCLUSIONS

A mechanical error sensitivity analysis and the synthesis of dimensional tolerance bands of planar non-dyad mechanisms are presented here. The method is valid for both dyad and non-dyad mechanisms, and thus, constitutes a general approach for linkage modeling. A unique analytical procedure named as the method of virtual velocity is developed for the determination of the position, velocity and acceleration sensitivity coefficients. The technique consists of a kinematic analysis of the original and its supplemental mechanism. The latter is derived from the original mechanism by setting the virtual velocity term to either 0 or ± 1, depending on the particular sensitivity coefficient that is being evaluated. After computing these sensitivity coefficients, the task of synthesizing for optimum dimensional tolerancing can be easily carried out. As an example, a 6-bar, non-dyad linkage is re-designed for optimum dimensional tolerancing. It is found from the error sensitivity analysis that the acceleration-based Δl_0 should be used in the synthesis of the tolerance bands of the final design. Using this result, the position-based, velocity-based and acceleration-based output motion characteristics of the designed mechanism are generated and found to conform to within the prescribed maximum/minimum allowable output bands. The final design is therefore, a valid and an acceptable mechanism.

CHAPTER 5

Conclusions

5.1 REMARKS

Several new approaches for kinematic analysis and the synthesis for optimum dimensional tolerancing of any complex dyad or non-dyad planar mechanisms have been developed in this thesis. The research achievements are as follows.

(1) A fully automated computer program **NDPLAn** has been developed for performing the kinematic analysis of dyad and non-dyad mechanisms. The novel method involves transforming the non-dyad mechanism into a series of dyad mechanisms by disconnecting appropriate link and/or joints, and prescribing dyad drivers for the transformed linkage. An iterative technique is then employed to recover the disconnected links by restoring the affected geometric conditions back to their original values. Several examples are used to verify and demonstrate the accuracy of the method.

(2) An approach for performing a mechanical error sensitivity analysis and the subsequent use of the results for carrying out the synthesis of optimum dimensional tolerancing of

dyad mechanisms has been developed. The method includes an analytical determination of the position, velocity and acceleration sensitivity coefficients. To illustrate the procedure, two examples are presented.

(3) A new and unique method has been devised for the direct identification of the most sensitive error combination from all the 2^m possibilities where m is the number of input parameters. The fact that our technique does not require any computations is a significant contribution as the task of identifying the most sensitive error combination can easily be very computationally intensive. For example, a mechanism with $m = 12$ input parameters produces 4,096 combinations and if the mechanism is analyzed at 30^0 interval, there will be a total of just under 50,000 computations for one 360^0 rotation!

(4) A completely different method [from (2)] has been developed for carrying out a mechanical error sensitivity analysis and synthesis of optimum dimensional tolerancing for *non-dyad* mechanisms. The procedure includes a unique analytical determination of the position, velocity and acceleration sensitivity coefficients via the method of virtual velocity. An example is presented to demonstrate the technique.

5.2 FUTURE WORK

The following future work can be considered as an extension of the current research.

(1) It would be nice to develop a Windows version of **NDPLAn** so that the computer program can be more user-friendly.

(2) Only dimensional tolerancing is considered in this study. It would be very useful to consider the effects of clearances in estimating the mechanical errors.

(3) The proposed method of error sensitivity analysis assumes only rigid links. In the real world, one has to deal with flexible links.

(4) The proposed method is restricted to kinematic errors in the output displacements, velocities and accelerations. Kinetic quantities such as forces and torques are ignored in the modeling.

REFERENCES

Artobolovski, I., 1977, *Theory des Mecanismes et des Machines*, MIR Edition, Moscow.

Barker, C., 1985, "SYNTRA - an interactive program to design Grashof planar four-bar mechanisms," *Engineering Software 4: Proc. 4th Int. Conf.*, Kensington Exhibition Center, London, England, 15-77.

Baumgarton, J.R. and Van Der Werff, K., 1985, "A probabilistic study relating to tolerancing and path generation error," *Mech. Mach. Theory*, **20**, 71-76.

Bottema, O. and Roth, B., 1979, *Theoretical Kinematics*, North Holland (reprinted by Dover Publications, New York (1990)).

Brat, V. and Lederer, P., 1973, "KIDYAN: computer-aided kinematic and dynamic analysis of planar mechanisms," *Mech. Mach. Theory*, **8**, 457-467.

Breteler, A.J.K., 1979, "Parial derivatives in kinematic optimization," *Proc. 5th World Congress Theory of Machines and Mechanisms*, ASME, New York.

Bruevich, N.G., 1946, *Precision of Mechanisms*, (in Russian), Moscow.

Chace, M.A., 1964, "Development and application of vector mathematics for kinematic analysis of 3-dimensional mechanisms," Ph.D. Dissertation, University of Michigan.

Chakraborty, J., 1975, "Synthesis of mechanical error in linkages", *Mech. Mach. Theory*, **10**, 155-165.

Chatterjee, G. B. and Mallik, A.K., 1987, "Mechanical error of a four-bar linkage coupler curve," *Mech. Mach. Theory*, **22**, 85-87.

Cleghorn, W.L., Fenton, R.G. and Fu, J., 1993, "Optimum tolerancing of planar mechanisms based on an error sensitivity analysis," *ASME J. Mech. Design*, **115**, 306-313.

Crossley, F.R.E., 1965, "The permutations of kinematic chains of eight members or less from the graph-theoretic viewpoint," *Proc. 2nd Southeastern Conf.*, **2**, Atlanta, GA, Pergamon Press, Oxford, 467-486.

Davies, T.H., 1968, "An extension of Manolescu's classification of planar kinematic chains and mechanisms of mobility $M \geq 1$, using graph theory," *J. Mech.*, **3**, 87-100.

Dhande, S.G. and Chakraborty J., 1973, "Analysis and synthesis of mechanical error in linkages - a stochastic approach," *ASME J. Eng. Ind.*, **95B**, 672-676.

Dhande, S.G. and Chakraborty, J., 1978, "Mechanical error analysis of spatial linkages," *ASME J. Mech. Design*, **100**, 732-738.

Dubowsky, S., Maatuk, J. and Perreira, N.D., 1974, "A parameter identification study of kinematic errors in planar mechanisms," ASME Paper No. 74-DET-52.

Dhande, S.G. and Chakraborty, J., 1975, "Mechanical error analysis of cam-follower systems - a stochastic approach", *Proc. 4th World Congress on Theory of Machines and Mechanisms*, University of Newcastle Upon Tyne, England, **4**, 957-962.

Erdman, A.G. and Gustafson, J.E., 1977, "LINCAGES: linkage interactive computer analysis and graphically enhanced synthesis packages," *ASME Paper 77-DET-5*.

Erdman, A.G. and Sandor, G.N., 1984, *Mechanism design: analysis and synthesis*, **1**, Prentice-Hall, New York.

Erdman, A.G., 1995, "Computer-aided mechanism design: now and the future," *ASME J. Mech. Design*, **117**, 93-100.

Fan, M.Y. and Zhang, Y., 1982, *Fundamentals of Optimization*, Tsinghua University, China.

Fenton, R.G., Cleghorn, W.L. and Fu, J., 1989, "Allocation of dimensional tolerances for multiple loop planar mechanisms," *ASME J. Mech., Trans. Auto. Design*, **111**, 465-470.

Fichter, E., Smith, G., Todd, P. and Wagner, F., 1992, *The Atlas of Linkage Design and Analysis: Vol. 1, the Four-Bar Linkage*, Saltire Software Inc., Beaverton, OR.

Fu, J. F., Cleghorn, W. L. and Fenton, R. G., 1988a, "Synthesis of the dimensional tolerance of a slider-crank mechanism," *Proc. 10th Oklahoma State University Applied Mechanism Conf.*, **2**, New Orleans, LA.

Fu, J. F., Fenton, R. G. and Cleghorn, W. L., 1988b, "Synthesis of the dimensional tolerance of a four-bar mechanism," *Trans. CSME*, **12**, 9-14.

Fu, J. F., Fenton, R. G. and Cleghorn, W. L., 1988, "Kinematic analysis of complex planar mechanisms using symbolic language," *Proc. ASME Design Technology Conf., Montreal*, **1**, 223-228.

Galleti, C.U., 1986, "A note on modular approaches to planar linkage kinematic analysis," *Mech. Mach. Theory*, **21**, 385-391.

Garret, R.E. and Hall, A.S., 1969, "Effects of tolerance and clearance in linkage design," *ASME J. Eng. Ind.*, **91**, 198-202.

Hall, A.S. and Tao, D.C., 1954, "Linkage design – a note on one method," *Trans. ASME*, 633-637.

Han, Ray P.S. and Tsuyuki, R., 1993, "Kinematic simulations of planar mechanisms," *J. Adv. Eng. Software & Workstations*, **16**, 209-217.

Hartenberg, R.S. and Denavit, J., 1964, *Kinematic Synthesis of Linkages*, McGraw Hill, New York.

Haug, E.J., Wehage, R.A. and Barman, N.C., 1982, "Dynamic analysis and design of

constrained mechanical systems," *ASME J. Mech, Design*, **104**, 778-784.

Ho, C., Erdman, A.G. and Riley, D.R., 1994, "Minnsketch©: a graphic kinematic and dynamic analysis tool for planar mechanism design," *Proc. ASME Des. Tech. Conf., Mech. Elem. & Mach. Dyn.*, **DE-Vol. 71**, 401-412.

Ho, J.R., Han, R.P.S. and Zhang, Q., 1996, "Automatic generation of dyad mechanisms for computer-aided kinematic analysis of complex non-dyad planar mechanisms," *Mech. Mach. Theory*, submitted.

Huang, Z., 1981, "The method of successive approximation of link length for the position problem of complex planar mechanisms," *Chinese J. Mech. Eng.*, **17**, 68-76.

Jone, J. R. and Rooney, G. T., 1970, "Motion analysis of rigid-link mechanisms by gradient optimization on an analogue computer", *J Mech.*, **5**, 191-201.

Kinzel, G.L. and Chang, C., 1984, "The analysis of planar linkages using a modular approach," *Mech. Mach. Theory*, **19**, 165-172.

Kolhatkar, S.A. and Yajnik, K.S., 1970, "The effect of play in joints of a function-generating mechanism," *J. Mech.*, **5**, 521-532.

Lakshiminaragana, K. and Narayanamurthi, R.G., 1971, "On the analysis of the effects of tolerance in linkages," *J. Mech.*, **6**, 59-67.

Mallik, A.K. and Dhande S.G., 1987, "Analysis and synthesis of mechanical error in path-generating linkage using a stochastic approach," *Mech. Mach. Theory*, **22**, 115-123.

Molian, S., 1984, "Software for mechanism design," *Proc. Mech. Conf.*, **2**, Granfield.

Mruthyunjaya, T.S. and Raghavan, M.R., 1984, "Computer-aided analysis of the structure of kinematic chains," *Mech. Mach. Theory*, **19**, 357-368.

Orlandea, N., 1973, "Development and application of node analogous sparcity-oriented

methods for simulation of mechanical dynamic systems," Ph.D. Dissertation, University of Michigan.

Paul, B., 1960, "A unified criterion for the degree of constraint of plane kinematic chains," *ASME J. Appl. Mech.*, **27**, 196-200.

Paul, B., 1977, "Dynamic analysis of machinery via program DYMAC," *SAE Paper 770049*, Warrendale, PA.

Raicu, A., 1974, "Matrices associated with kinematic chains with 3 to 5 members," *Mech. Mach. Theory*, **9**, 123-129.

Rooney, G.T. and Jones, J.R., 1975, "Curve following in kinematic analysis," *Proc. 4th World Congress TMM*, I. Mech. Eng., London.

Rubel, A.J. and Kaufman, R.E., 1977, "KINSYN III: a new human-engineered system for interactive computer-aided design of planar linkages," *ASME J. Eng. Ind.*, **99**, 440-448.

Shigley, J.E., 1969, *Kinematic Analysis of Mechanism*, McGraw-Hill, New York.

Shigley, J.E. and Uicker, J.J., 1980, *Theory of Machines and Mechanisms*, McGraw-Hill, New York.

Sheth, P.N. and Uicker, J.J., 1972, "IMP, a computer-aided design analysis system for mechanism and linkage," *ASME J. Eng. Ind.*, **93**, 454-464.

Smith, J.A., 1975, "Kinematic analysis of mechanisms by the complex conjugate exponential method," *ASME J. Eng. Ind.*, **97**, 795-800.

Smith, M.R. and Ye, Z., 1984, "Simplified data structure for analyzing mechanisms using character handling techniques," *CAD*, **16**, 197-202.

Suh, C.H. and Radcliffe, C.W., 1978, *Kinematics and Mechanisms Design*. Wiley, New York.

Svoboda, A., 1948, *Computing Mechanisms and Linkages*, McGraw-Hill, N.Y., 199-222.

Tuttle, S.B., 1960, "Error analysis," *Machine Design*, **32**, 153-158.

Vadnagarwala, M., 1988, "KADAM 2, a comprehensive package for analysis of planar mechanisms," M.S. Project, University of Minnesota.

William, R., 1986, "MICRO-MECH, a mechanical analysis system for microcomputers," Users Guide.

Wu, R. and Zhang, Q., 1988, "Kinematic analysis of planar multi-link complex mechanism via the method of disconnecting certain links and joints," *ASME Proc. Trends and Dev. Mech., Mach. & Rob.*, 245-248.

Zhao, H., 1980, "Kinematic analysis of multi-link and multi-degree-of-freedom mechanisms," *J. Shanxi Inst.. Mech. Eng.*, 3.

APPENDIX

1. User Manual for NDPLAn Program

1.1 Purpose

This program written in **FORTRAN** can be used to perform kinematic analysis for position, velocity, acceleration and error of dyad and non-dyad planar mechanisms.

1.2 Input Parameters Definitions:

All the instructions have been arranged to display on the screen for the user to choose the values of input parameters. For the purpose of clarification, here are further explanations of the input parameters definitions.

1.2.1 MIN=1 displacement analysis only
MIN=2 displacement and velocity analyses
MIN=3 displacement, velocity and acceleration analyses

1.2.2 M : number of links
N : number of joints
I : link number
J : joint number

1.2.3 If input MN matrix by using file, the user must set up a file named as 'mndata*' ('*' is any integer number) which includes all data of the MN matrix.

1.2.4 INPUT L(J1-J2)=? Y/N: if the value of length is known before starting the calculation, input Y, otherwise input N.

1.2.5 J1, J2, J3, MODEL

- J* : the joint number of the current link which has three or more sides.

MODEL= 1 : all joints are arranged in the anti-clockwise direction

MODEL= 0 : all joints are arranged in the straight line

MODEL=-1 : all joints are arranged in the clockwise direction

1.2.6 PX(J), PY(J)

PX(J) : the *x* coordinate of joint J.

PY(J) : the *y* coordinate of joint J.

1.2.7 THETA(J1-J2) : degree of angle measured from the horizontal position to the driver in the anti-clockwise direction, where J1 is the starting joint and J2 is the ending joint .

S(J1-J2) : linear distance measured from the initial starting position of slider to its current position, where J1 is the starting joint and J2 is the ending joint.

1.2.8 How many times to calculate : the number of calculations in whole complete cycle

1.2.9 DTHETA: interval of rotation for rotation driver

DS : interval of sliding for slider driver

1.2.10 H: length of step for the iteration

E: tolerance for the iteration

1.2.11 VI(I) : angular velocity of rotation driver

AI(I) : angular acceleration of rotation driver

VS(I) : linear velocity of slider driver

AS(I) : linear acceleration of slider driver

1.3 Output Definitions:

3.1 Output File Name : DATA.*

(1) The number of the file data.* depends how many input parameters the mechanism has.

(2) '*' is the digital number which matches the corresponding number of input parameters.

(3) It includes the solution of displacement, velocity and acceleration sensitivity coefficients for all links and joints of mechanism due to certain input parameter unit error in the complete cycle.

3.2 Output File Name : PVA

It includes the solution of displacement, velocity and acceleration for all links and joints of mechanism by using input parameter nominal values in a complete cycle.

3.3 Output File Name : EIJ

It includes the solution of displacement, velocity and acceleration output error for all links and joints of mechanism due to the actual input parameter error in a complete cycle.

3.4 Output File Name : EPVA

It includes the solution of displacement, velocity and acceleration for all links and joints of mechanism by using input parameter actual values in a complete cycle

2. User Manual for NDPLAs Program

2.1 Function

This program written using **FORTRAN** can be used to solve optimum dimensional tolerancing of dyad and non-dyad planar mechanisms.

2.2 Input Parameters Definitions:

All the instructions have been arranged to display on the screen for the user to choose the values of the input parameters. For the purpose of clarification, here are further explanations of the input parameter definitions except for those which have already been described Section 1.2.

2.2.1 EIJ=1 : calculate the maximum allowable output error bands of a joint
EIJ=2 : calculate the maximum allowable output error bands of a link

2.2.2 JEJ : joint number
IEI : link number

2.2.3 EN01: starting position of the synthesis calculation period
EN02: ending position of the synthesis calculation period

2.2.4 HOW MANY INPUT PARAMETERS GROUPS? : input 1 for linear or angular quantities only, otherwise input 2 .

2.2.5 HO : length of step for the iteration
E : tolerance for the iteration

2.3 Output Definitions

All final design solutions will be shown on the screen.